
# Predicting Mechanical Properties of Polymer Films after Extrusion Coating using Supervised Machine Learning Algorithms

Sara Khayyami

2019

DIVISION OF PRODUCTION AND MATERIALS ENGINEERING
LUND INSTITUTE OF TECHNOLOGY, LUND UNIVERSITY

Supervisor:
Professor Jinming Zhou at Production and Materials Engineering
Examiner:
Professor Jan-Eric Ståhl

Industrial Supervisor:

Jan Wahlberg, Technology Specialist at Tetra Pak®

Co Industrial Supervisors:

Nils Toft, Technology Specialist at Tetra Pak®

Linda Hartman, Statistical Engineering Expert at Tetra Pak®

Maria Eriksson, Technology Specialist Rheology at Tetra Pak®

Author:
Sara Khayyami
Lund, Sweden 2019


Faculty of Engineering, Lund University
Box 118
SE-221 00 Lund
Sweden
Printed in Sweden
Media-Tryck
Lund University

## Abstract

Tetra Pak is a world leader in providing innovative packaging solutions and processing technologies and has been so for a very long time. It is well – known that the material used for packaging purposes gets subjected to high temperature and pressure during folding and filling which could compromise the integrity of the material. The polymer layer in the packaging material acts as a barrier, and thus a break in the polymer layer will influence the barrier properties. The process by which the polymer layer is applied on to the paperboard is called extrusion coating. The barrier properties of the polymer are affected by the process conditions in the extruder. It is therefore important to understand how the processing affects the mechanical properties of the polymer and hence the barrier properties.

In this thesis, polyethylene films are created by varying the process settings, line speed and melt temperature, in the extruder. The mechanical properties are measured by the use of tensile tests and the effect from processing on the mechanical properties are investigated. A model for predicting the mechanical properties of polymer films is built using the collected data. The primary tool for data processing used in this thesis is Python, and the predictive model is built using machine learning algorithms. In the data, there is clear and visible effect from line speed on the mechanical properties but effect from melt temperature is not as strong. The predictive capacity of the simplest model based on linear regression has been found to predict with highest accuracy. Predictive models built on random forest regression has also been found to predict fairly well. The complex models are overall sensitive and require more data than was collected in this study to provide reliable predictions.



*Key words: Machine Learning, Predicting Polymer Properties, Mechanical Properties, Stress – Strain, Processed Polymer, Extrusion Coating*

# Acknowledgements

This master thesis project was carried out at the department of Materials & Package (M&P) at Tetra Pak in Lund during the spring of 2019. The thesis was a continuation of my work as a Technical Talent at Tetra Pak. During my time at the company I have gained a lot of practical experience. It has been incredibly fun to work in projects so close to reality and to be a part of an extremely experienced team.

First and foremost I would like to thank my Tetra Pak supervisor Jan Wahlberg for all the guidance and support. Thank you for directing me towards this project and thank you for listening to everything I have had to say and pushing me to be creative and work independently. Through this thesis I have evolved enormously as a person. I would also like to thank my co – supervisors Nils Toft and Maria Eriksson for all the knowledge and support that you have been providing me with. Also thanks to my third co – supervisor Linda Hartman who has taught me a lot about statistics and provided me with a lot of support. I am grateful for all the help that I have been given and consider you as a big part of the thesis.

A very special thank you to Berit Stålbom who has been my manager during my years at the company. Thanks to you I have been given the opportunity to work at Tetra Pak which I am forever grateful for. You have constantly kept me at the edge of my comfort zone and provided with an enormous support.

I would also like to express my gratitude to the rest of the Materials & Package team who has provided me with support and knowledge. I would also like to thank Anders Ljung and Filip Markeling in Industrial Base Performance (IBP) for helping me gather material for my thesis. Last but not least I would like to thank my supervisor and examiner from Production and Materials Engineering; Jinming Zhou and Jan-Eric Ståhl. Many more have been a part of this thesis and I am thankful for all the help that I have gained from you. I hope that this project has awakened the interest in using machine learning in material science and that it can be used for further studies in the area.

# Abbreviations

PE – Polyethylene

LDPE – Low-density polyethylene

HDPE – High-density polyethylene

LLDPE – Linear low-density polyethylene

LCB – Long chain branching

SCB – Short chain branching

MW – Molecular weight

MWD – Molecular weight distribution

UTS – Ultimate tensile strength

DSC – Differential scanning calorimetry

RMSE – Root Mean Squared Error

# Table of Contents

# 1. Introduction

## 1.1 Background

Tetra Pak is a global leading company in providing innovative packaging solutions and processing technologies that can be used for a broad range of products. The company was founded 1951 by Ruben Rausing based on the development of the tetrahedron shaped package. The idea behind this unique package was to form a tube from a roll of plastic-coated paper, fill it with beverage and seal it below the level of the liquid. Nowadays, a package can come in a different size and shape depending on the area of application. The packaging material consists of different layers which serve different functions. The material used in the different layers depend on the content and if the product has to be chilled or stored in room temperature and also if it needs to be distributed to another country. [1] A typical carton package, which is used to preserve both beverage and food, has several layers which serve different functions and they are presented in *figure 1:1*. Together, these layers give full protection of the content.

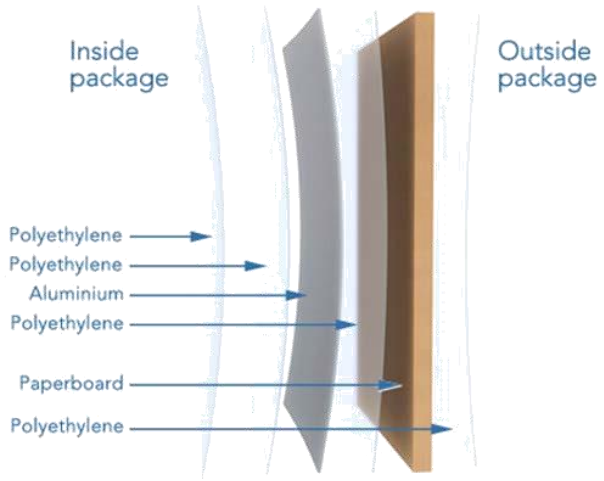


*Figure 1:1. Packaging material for Tetra Pak carton packages. [2]*

In a typical carton package, paperboard is the main constituent. The purpose of the paperboard is to make the package stable and strong while providing smoothness to the printing surface. The paper is then coated with different layers and grades of polyethylene in order to protect against moisture, improve performance and appearance, see *figure 1:1*. The outside polymer, called décor, ensures moisture protection and helps flap sealing. The laminate polymer provides adhesion since it enables the board to stick to the aluminium foil. The foil in turn protects the product by blocking out oxygen and light in order to maintain the nutritional value and flavours of the food in the package. The foil also minimizes product loss. The inside polymer seals the package and protects the product. The mechanical properties of the polymer layer influence the properties of the packaging material as the polymer acts as a barrier, and thus a break in the polymer layer will influence the barrier properties. The process by which the polymer layers are applied on to the paperboard is called extrusion coating which will be the focus of this thesis. [2]

When application of the layers has been made on to the paperboard, it is folded in the filling machine and filled with food or beverage. During the folding and filling process, the material is subjected to high pressure and temperature which can compromise the integrity of the material. It is therefore of great importance that the material can withstand these conditions. Polyethylene is an important constituent in the packaging material as previously discussed. It is well-known that the mechanical properties and hence the barrier properties of the polymer change during the extrusion coating process. Some of the studied extrusion parameters that contribute to this change in material properties are line speed, air gap, and melt temperature but to what extent and how the material changes is unknown.

It is therefore of great interest to investigate how the mechanical properties of the polymer film alters when changing the settings of the process. There is also an interest in investigating if the resultant mechanical properties of the polymer film can be predicted by creating a model using supervised machine learning algorithms. If successful, one could speed up the development process instead of running full scale tests which are time-consuming and expensive.

## 1.2 Problem formulation

The purpose of this master thesis is to understand how and to what extent the extrusion-process influences the mechanical properties of polyethylene. The collected data will be used in an attempt to create a model using supervised machine learning algorithms to investigate if the mechanical properties after extrusion coating can be predicted by only knowing the processing conditions.

## 1.3 Objective

Performing full scale tests are both time-consuming and expensive. The interest in creating models using machine learning algorithms to predict material properties is therefore rapidly growing. Polyethylene is one of the most commonly used polymers in the packaging material and will therefore be the focus of this thesis. In order to create this kind of model, knowledge regarding the extrusion coating process is needed. The parameters that influence the mechanical properties of the polymer film have to be determined by performing a literature study. Data has to be gathered from extrusion coating experiments where a thorough investigation of the process influence on the mechanical properties of polyethylene will be made. Knowledge regarding how the processing conditions in the extruder affects the crystallisation of the polymer will also be gained through differential scanning calorimetry measurements. Further morphological studies will not be conducted since it is not a part of the scope.

## 1.4 Delimitations

There are several different types of polyethylene grades that can be used in the packaging material but due to time limitations only one grade of polyethylene will be investigated. Furthermore, tensile testing is usually performed in both cross direction and machine

direction though in this thesis tests are focused on machine direction. The experiments in the extruder are also performed in such way that only two processing condition will be varied, line speed and melt temperature. This depend on the complexity of the extruder; all the processing settings are connected so changing one leads to the alteration of another parameter. Due to the cost of running experiments in the coating line, a limited amount of data points can be collected which compromises the performance of the predictive model.

## 1.5 Disposition

The disposition of the master thesis is as follows:

- *Introduction* – A short introduction to the master thesis and questions the thesis should answer. It also provides a brief explanation to how this subject can be of importance to Tetra Pak.

- *Fundamentals of polymers and processing* – This part of the thesis is focused on the fundamentals of polymers. It also covers the basics behind extrusion coating and how this process affects the properties of polymers.

- *Characterization of structural, mechanical and thermal properties* – Explains briefly how rheology and differential scanning calorimetry measurements are made. This section also provides information regarding tensile testing which provides mechanical information.

- *Machine Learning* – Provides with a brief explanation of the concept of machine learning with focus on its application in material science.

- *Method* – Provides with a brief explanation of the techniques used in the experimental part.

- *Experiments and results* – In this section, the procedure of each experiment is described. Each experimental part is followed by the results from those measurement.

- *Modelling with Machine Learning* – This section contains an analysis of variance, description of which methods were used during modelling and the issues that I encountered during the development phase of it. The evaluation of the predictive models is also a part of this section.

- *Discussion* – The effect of different process setting on the mechanical properties are discussed in this section. It also involves a discussion regarding if and how the degree of crystallization is affected by the process which has been measured with differential scanning calorimetry. A discussion regarding the evaluation of the models is also included in this part.

- *Conclusion* – The conclusion tries to answer the questions described in the introduction.

- *Future work* – This section of the thesis contains information regarding future work; what could be improved and how the model can be expanded in order to be valid for other grades of polyethylene. It also contains information regarding further analysis that could be made on the material.

# 2. Fundamentals of Polymers and Processing

## 2.1 Polymers

Polymeric materials are conventionally referred to as plastics. A polymer molecule is formed by combining a large number of chemical entities, often referred to as the repeating unit or monomer. The main building block of a polymer is Carbon, but other elements can also be present such as nitrogen in Nylon. The combination of many repeating units leads to the formation of chain molecules. The length of the chains and degree of branching determines how the polymer molecule will behave when subjected to thermal or mechanical energy. Polymers therefore have a wide range of physical and mechanical properties which depend on the morphology of the polymer in use. [3]

### 2.1.1 Morphology of polyethylene

Polymeric materials can be divided into three categories: thermoplastics, thermosets and elastomers. [3] Polyethylene belongs to the first category, thermoplastics. Thermoplastics are usually semicrystalline, a combination of crystalline and amorphous regions. [4] The crystalline regions of these polymers form regular birefringent structures with circular symmetry called spherulites. The spherulite growth proceeds from a small crystal nucleus that develops into a fibril. With time, a bundle of fibrils will be produced and eventually fill out into the characteristic spherical structure. Each fibril consists of ordered regions called lamellae. The highly ordered lamellae plates are interrupted by amorphous regions that make up the disordered content of the semicrystalline polymer, see *figure 2:1*. [5]

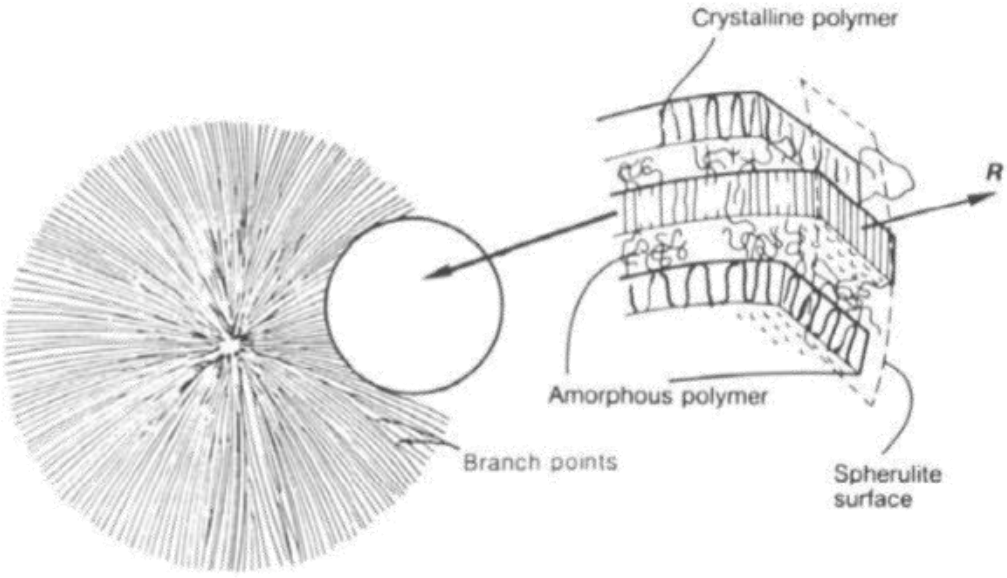


*Figure 2:1. A polymer crystalline spherulite. [6]*

Thermoplastic polymers can be softened and re-hardened indefinitely provided that they are reheated. When reheating the polymers, the temperature must stay below the degradation temperature, otherwise chain scission reactions and crosslinking may occur. [4]

Polyethylene (PE) is one of the most important polymers used in food packaging due to its sealing abilities among other things. The polymerization of polyethylene can be performed using different mechanisms which gives rise to the three general grades; high-density polyethylene (HDPE), low-density polyethylene (LDPE) and linear low-density polyethylene (LLDPE). The grades have different degree of branching compared to one another and hence crystallinity. [7] HDPE is a structurally regular chain material with very few branch points (less than seven branch points per 1000 carbon atoms). The polymer chains can thus pack efficiently which results in a highly crystalline material with corresponding high density. LDPE is, on the contrary, a highly branched polymer with 60 branch points per 1000 carbon which results in a much lower crystalline content and density.

The property gap existing between HDPE and LDPE is filled by LLDPE which has a controlled number of short-chain branches (SCB) and the density is an intermediate between HDPE and LDPE. The branching plays a significant role in determining the properties of the polymer and so the three grades of polyethylene are used in different applications depending on the usage of the product. As seen in *figure 2:2*, both HDPE and LLDPE have some degree of SCB while LDPE has a high degree of long-chain branches (LCB) and some degree of SCB. [8]

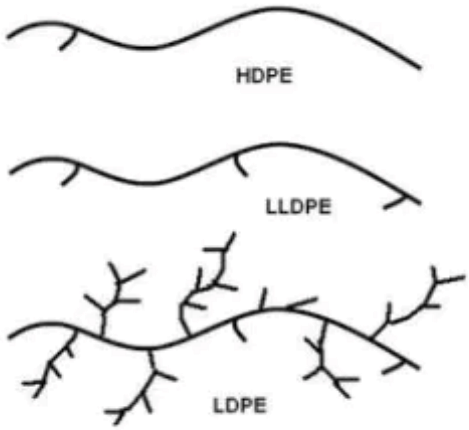


*Figure 2:2. Lateral branching of HDPE, LLDPE and LDPE. [9]*

Polyethylene will be of focus in this thesis since it is widely used by Tetra Pak in their packaging materials. This polymer provides overall great toughness, ability to deform without rupture, and can stretch up to several times its original length before breaking, depending on the grade. [7] The polymer has good chemical resistance which is important in food packaging. It can protect food products since it does not allow microorganisms to permeate or leach any harmful materials. [10]

### 2.1.2 Rheology of polymers

Rheology is defined as the study of flow and deformation of matter, while viscosity is defined as the ability of a fluid to resist a change in the molecular structure when subjected to shear stress. The flow properties of polymers are quite complex which makes them interesting to study. Polymers can be described as viscoelastic fluids which means that they exhibit both viscous and elastic characteristics, depending on how fast they flow or are deformed in the process. [11] The processing conditions thus have an impact on the flow properties of the polymer. There are various instruments available to measure the viscosity of polymer melts, and more generally their rheological behavior. [12]

The rheological behavior of polymer melts is strongly dependent on the molecular architecture and on the strain history of the process, the processing temperature and pressure. [11] The molecular structure can be described by the molecular weight (MW), molecular weight distribution (MWD) and branching (SCB and LCB). Each of these parameters can be measured by using a rheometer. The MWD and a fraction of the SCB are related to the elasticity of the polymer and can be estimated from the shear storage modulus, $G'$. The zero-shear viscosity, $\eta_0$, can be used to determine the average MW and the activation energy, $E_0$, can be used to determine the amount of LCB in the polymer melt which also determines the elasticity of the polymer.

Polymers have a very complex and unique structure and the same grade can have large variations in the molecular structure depending on the manufacturer. There can also be variations in the structure between different batches produced by the same manufacturer.

Polymers of the same grade thus process differently and so the process reacts sensitively to small variations in the polymer. This means that the rheology of the polymer melt is sensitive to small changes in the structure. Due to the sensitivity, rheology is the most suitable method to characterize polymers. The molecular structure thus, together with how the material has been processed, determine the material properties of the final product. [12]

### 2.1.3 Mechanics of polymers

The mechanical properties of polymers depend on the molecular architecture and on the manufacturing process, as mentioned earlier. A typical stress – strain curve gives information regarding polymer deformation, how much it can be elongated before breaking, during certain circumstances. [13] Young's modulus, or modulus of elasticity, yield strength and tensile strength are measurements used to describe the mechanical performance of polymeric materials and these are usually illustrated in a stress – strain curve, see *figure 2:3*. Young's modulus describes the elastic properties of a solid undergoing tension or compression in one direction at low strains. [14] It is a measurement on the stiffness of a material, how easily it can be bent or stretched. Young's modulus can be calculated from the linear region of the curve, *figure 2:3*. [15]

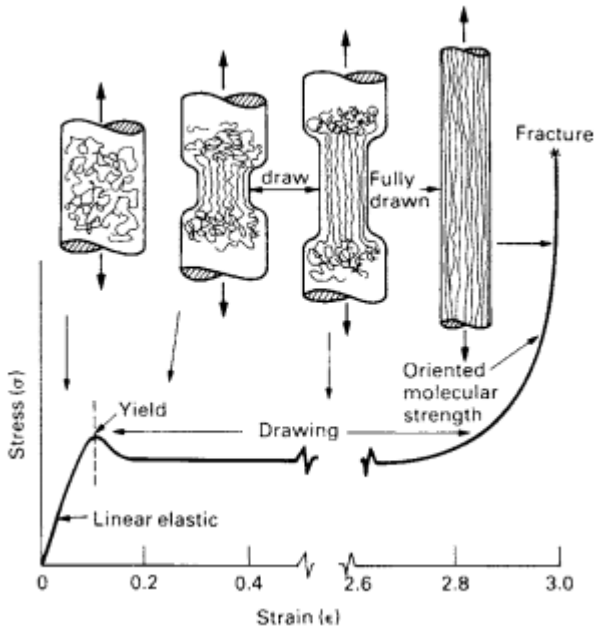


*Figure 2:3. Typical stress – strain curve of a polyethylene. [16]*

The yield strength of the polymer corresponds to the maximum stress that can be applied before it begins to change shape. In other words, where the elastic region ends, and the plastic deformation takes place. The tensile strength of a polymer is the stress corresponding to fracture and it can be higher or lower than the yield strength since it depends of the material properties. If the polymer is brittle then this usually breaks before it reaches its yield strength but if the polymer is ductile it flows plastically beyond the yield strength and thus forms a region called neck, see *figure 2:3*, where it then breaks. [15] Necking occurs in semi –

crystalline polymers with co-existing amorphous and crystalline phases. According to recent experiments, necking is believed to be related to the unfolding of crystalline blocks. [17]

The stress – strain curve of a polymer is strongly dependent on temperature and strain rate. An increase in temperature leads to a decrease of the Young's modulus and tensile strength however, ductility is enhanced, see *figure 2:4*. When the strain rate is increased the Young's modulus and yield strength also increase and the material appears stronger and stiffer while ductility decreases. If strain rate is high, the material will have a stress – strain curve that resembles the one for the lowest temperature, see *figure 2:4*. The stress – strain curve for the highest temperature is the corresponding for low strain rate. [18]

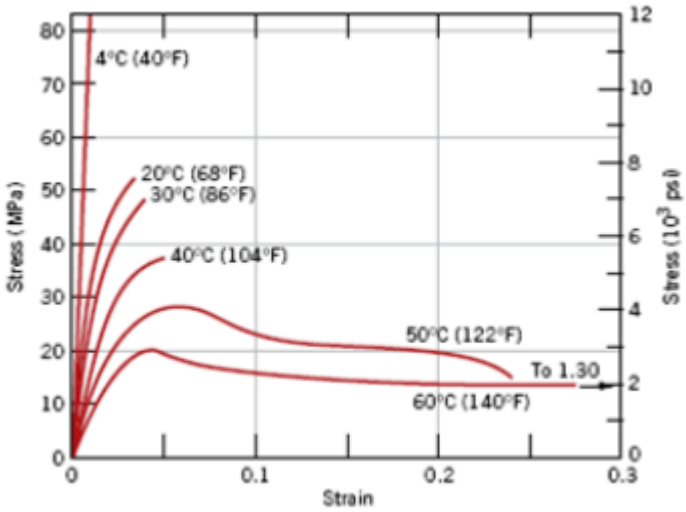


*Figure 2:4. The effect of heat on the mechanical properties of polymers. [19]*

## 2.2 Extrusion Coating

### 2.2.1 Usage in the packaging industry

Extrusion coating is a coating technique widely used in packaging material companies. In the process of extrusion coating, a molten plastic is applied to a substrate and afterwards, chilled to form an extremely thin, smooth layer of uniform thickness. The application of a molten plastic to a substrate is useful when the purpose is to laminate a plastic film or a metal foil since the molten plastic can act as an adhesive.

When packing dry products, materials such as paperboard are useful. However, since paperboard have no barrier properties and limited mechanical strength, it is not suitable for direct contact with moist and greasy foods. The reason to this is because the mechanical properties of paperboard are affected by moisture. The paperboard will also absorb some of the grease which will cause stains to appear. These effects will reduce the protective function of the package, and so the content will no longer be safe for consumption. [20] To overcome this issue, paperboard is coated in a laminator with different layers of polymers and in some cases foil, read section 1:1, to obtain a packaging material with attractive appearance, grease resistance, excellent mechanical properties and heat sealing properties. Other qualities such

as moisture protection, barrier to water vapour, oxygen, aroma etc., can also be achieved. [21]

### 2.2.2 Process of extrusion coating

In a full scale laminator the paperboard enters in the beginning of the laminator and passes three stations, each providing with one layer (laminate, inside or décor) that give rise to the resulting packaging material which exits at the end of the laminator. The order in which the layers are coated on the paperboard have not always been the same over the years. Nowadays, in Tetra Pak, the paperboard is first coated with the laminate layer followed by the inside layer and lastly the décor layer. Each station has an individual extruder with different process settings. This is due to the fact that each layer comprises different polymers which behave differently and have different prerequisites such as degradation temperature. The different layers in the packaging material also have different thicknesses which can only be produced by having different settings in the extruder.

The raw material, polymer granules, is fed into the hopper which then enters the feed throat of the extruder see *figure 2:5*. When the material has entered the feed throat, at the rear of the barrel, it is conveyed into the rotating screw, see *figure 2:5*, which is driven by an electrical motor. [22]

There are two types of extruders, single-screw (most common) and twin-screw extruders. The task of the rotating screw, regardless of being single or twin, is to generate enough pressure in order to push the polymer forward into the barrel. The barrel is heated to the desired melt temperature and together with shearing the polymer granules are converted to their molten state. At the end of the screw, the polymer is completely in its molten state. [23]

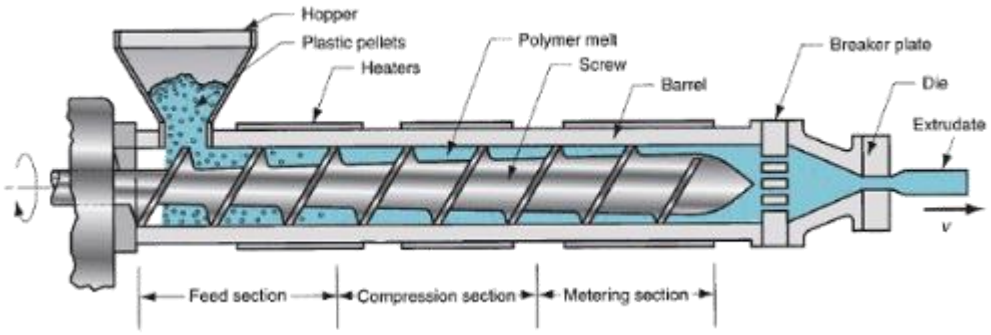


*Figure 2:5. Schematic representation of a single-screw extruder. [24]*

The extruder can be divided into three controlled heat zones that gradually increase the temperature of the barrel with the lowest temperature at the rear of the barrel. The division of the heat zones is made to allow the polymer to melt gradually as it is being pushed through the barrel and to prevent degradation in the polymer. After passing through the barrel, the molten plastic passes through a screen-pack and is then transported out by pressure flow for use in subsequent manufacturing process.

In the extruder, the molten plastic is transported through heated channels into a narrow slit die, see *figure 2:6*. The polymer melt passes through the die exit and enters the airgap where

it is immediately stretched into a film as it is drawn down into a nip and applied to the substrate. The temperature of the molten film as it reaches the nip is usually of interest since it has a large impact on the material properties. The film is pressed against chilled steel rolls that removes the heat from the molten film in order to solidify it and to control the finish of the plastic surface, see *figure 2:6*. The coated substrate is then transported into the next station where it is coated with the next layer. When the board has passed through all coating stations, it is rolled up into a large roll at the end of the laminator. [23, 25]

When the polymer flows from the barrel to the die, the melt is subjected to shear and extensional deformation. When exiting the die, the polymer deforms under non-isothermal conditions. These conditions in turn govern the orientation and morphology of the end product. [25]

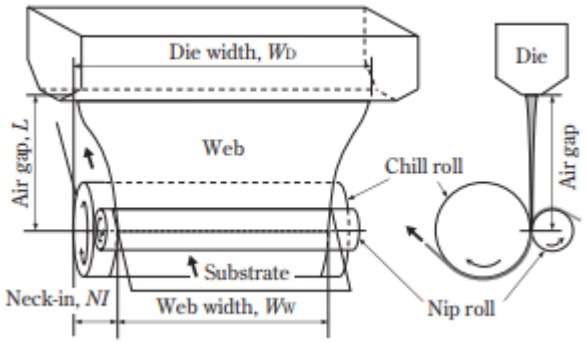


*Figure 2:6. Schematic representation of the extrusion coating process. [21]*

When performing extrusion coating, it is important to control some properties during the process. These properties include neck-in and the draw-down ability which are rheology-related phenomena. The neck-in phenomenon occurs in extrusion coating and means that the edge of the extruded web tends to shrink inwards towards the center of the web, see *figure 2:6*. The edges of the polymer film becomes thicker than in the central area, called edge-bead. The edge-bead must be cut off in the final products. However, not all polymers exhibit the same degree of neck-in since this phenomenon depends on the elasticity of the melt. The neck-in length thus varies depending on polymer grade. Neck-in is evidently an unwanted phenomenon that arises due to extrusion coating and so a low value is more desirable. A low neck-in value means that the polymer film has a wider field of application, decreasing the loss, and can coat a larger area of the paperboard. [21]

Draw-down is the ability of the polymer melt to be drawn into thin films without breaking. It is favored by a melt that is more viscous than elastic. If processing speed is gradually increased, the molten film will reach a point where it can no longer be stretched and instead breaks. So it is more favorable to have a high draw-down ability. The maximum draw-down speed at which the molten film is broken is dependent on molecular structure of the polymer, just as in neck-in. There is a strong correlation between draw-down and neck-in properties and so both criteria need to be met. [26]

### 2.2.3 Influence of extrusion coating on morphology and tensile properties of polyethylene

The molecular characteristics of polyethylene determine the rheological properties. As previously mentioned, these characteristics are MW, MWD and degree of branching and they control the mechanical properties of unprocessed polymers. However, if the polymer has been processed such as in extrusion coating, rheology is not the only contributing factor in determining the mechanical properties. The process technology and processing conditions also play an important role in determining the properties of the final film.

The processing can have an impact on the structural characteristics of the polymer such as the crystallinity, which is controlled by cooling conditions, and molecular orientation, as mentioned earlier in the text. The molecular orientation determines the deformability of the polymer film; if the film is highly oriented then de ultimate deformation is lower. This underlines the importance of the processing conditions for the mechanical properties of the polymer film.

Processing can also result in thermal and mechanical degradation, which are favored by high melt temperatures and long residence times. Processing can also induce cross-linking reactions in the polymer. The degradation in turn alters the mechanical performance of the final product.

The elongational strain rate depends on the process settings and can be derived as

$$\dot{\varepsilon} = \frac{v_1}{h} ln \frac{v_1}{v_o} \qquad (2:1)$$

where $h$ is the air gap between the die exit and the chill roll, $v_1$ is the line speed and $v_0$ is the extruder speed. This parameter also has an impact in determining the mechanical properties of the film. The elongational strain rate applies during the drawing phase (when polymer film exits the die and enters the chill rolls), as seen in *equation 2:5*, of the extrusion coating process. An increase in line speed thus leads to an increase in the elongational strain rate which is reflected in the mechanical properties by giving a lower ultimate strain. So the elongational strain rate is a parameter that determines the deformability of the final film, but it cannot be used to predict how the polymer will be changed. Breakage points are relevant for comparison of the polymers ultimate stress and strain which can be related to their ability as leakage barrier. As a conclusion, it can be said that the morphology of the solidified extrusion-coated polymer film depends on process induced properties and rheology. [25]

# 3. Characterization of Structural, Mechanical and Thermal Properties

## 3.1 Oscillatory Rheometer

Characterizing the mechanical behavior of viscoelastic materials such as polymers can be done using oscillatory rheology. It quantifies the viscous and elastic parts of the material at different time scales. Oscillatory rheology provides a useful tool for understanding structural and dynamic properties of such systems.

In an oscillatory rheometer, a sample is typically placed between two plates as shown in *figure 3:1* below.

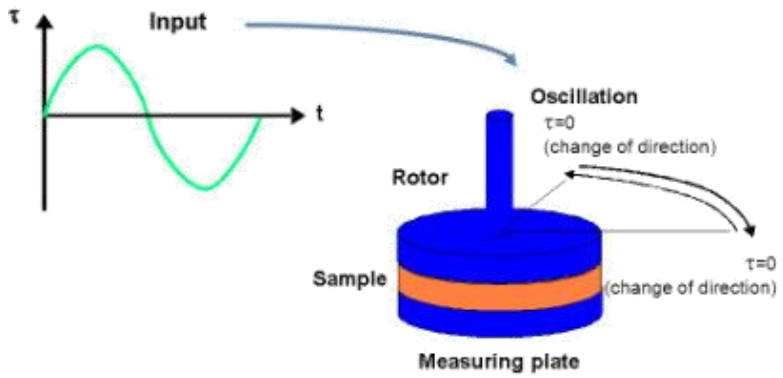


*Figure 3:1. Schematic illustration of a typical oscillatory rheometer setup. [27]*

A time-dependent strain is imposed on to the sample by letting the top plate remain stationary while the bottom is rotated by a motor. The time-dependent stress is simultaneously quantified by measuring the torque that the sample imposes on the top plate. The time-dependent stress gives information regarding the sample type, if it is elastic or viscous.

From the rheometer, the storage modulus, G', and loss modulus, G'', can be obtained. These measurements characterize the solid-like and fluid-like contributions of the viscoelastic system respectively at a given frequency. Other relevant measurements such as zero-shear viscosity and activation energy can also be obtained using an oscillatory rheometer. [28]

## 3.2 Tensile Testing

The tensile test is one of the most widely used testing standards for measuring the mechanical properties of a polymeric material when under tension load. The result of this kind of test is a graph of stress versus strain which includes the Young's modulus of elasticity and other tensile properties. In a tensile test, a sample of known dimensions is placed between two fixtures called "grips" which clamp the material. The material, which is gripped at one end while the other end is fixed, is subjected to an increasing weight. While increasing the weight, the change in length is measured until the material reaches its breaking point which determines the ultimate tensile strength of the material. With this, information is conducted regarding the strength of the sample and how much it can elongate. The strength of the sample can be expressed in terms of stress, force per unit area, and strain, change in length expressed in

percentage, see *figure 3:2*. Since the applied weight needed for rupture depends on the size of the sample, it is important that all samples have the same dimensions when comparisons between materials are to be made. The dimensions include, length and cross-sectional area. The thickness of the sample is also of great importance since it affects the result of the tensile test.

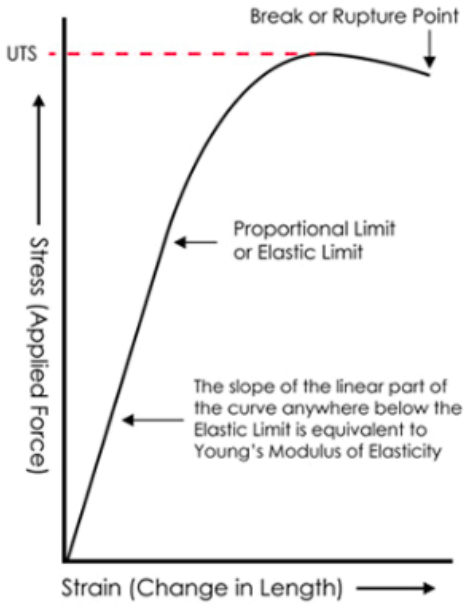


*Figure 3:2. The shape of the polymer during tensile testing. [29]*

The ultimate tensile strength, denoted UTS in *figure 3:2*, is the maximum stress that a material can withstand while being pulled before breaking. UTS is one of the most important material properties that can be determined. It is used for quality control to roughly determine the material type for unknown samples.

When polymers are subjected to tensile testing, they exhibit a linear relationship between the applied force and the elongation in the initial portion of the test. This linear region obeys the Hooke's Law which states that, for relatively small deformations, the size of the deformation is directly proportional to the deforming force. The slope of the linear region is called the Young's modulus which is a measure of the polymer's stiffness. [29]

In order to be able to directly compare different materials, the strength has to be independent of the size of the material. So, from the measured force, the engineering stress can be derived as

$$\sigma = \frac{F}{A_0} \qquad (2:2)$$

where F is the applied force and $A_0$ is the initial cross – sectional area of the specimen. When the material is subjected to the force, it deforms. If the amount it moves (displacement), $\Delta l$, is divided by the initial length, $l_0$, the engineering strain can be derived as [30]

$$\varepsilon = \frac{\Delta l}{l_0} \qquad (2:3)$$

For engineering stress and engineering strain, the initial dimensions of the specimen are employed, but these dimensions continuously change during the test. The cross – sectional area decreases during loading which will result in a higher stress than that presented in the engineering stress – strain curve. So, an engineering stress – strain curve does not give a true indication of the deformation characteristics. True stress and true strain are to be used instead for a more accurate definition of these characteristics by considering the actual (instantaneous) dimensions. The true stress can be derived as

$$\sigma' = \frac{F}{A} \qquad (2:4)$$

where F is the applied force divided by the actual area, A. True strain can be derived as

$$\varepsilon' = ln\frac{l}{l_o} \qquad (2:5)$$

where $l$ is the instantaneous length. [31]

## 3.3 Differential Scanning Calorimetry

A differential scanning calorimetry (DSC) is an important thermal analysis technique in material science. It is used to determine the energy absorbed or released by a sample as it is heated or cooled several times. From a DSC measurement the melting/recrystallization temperature, crystallization and glass transition temperature can be determined. [32] A schematic representation of the DCS can be seen in *figure 3:3* below.

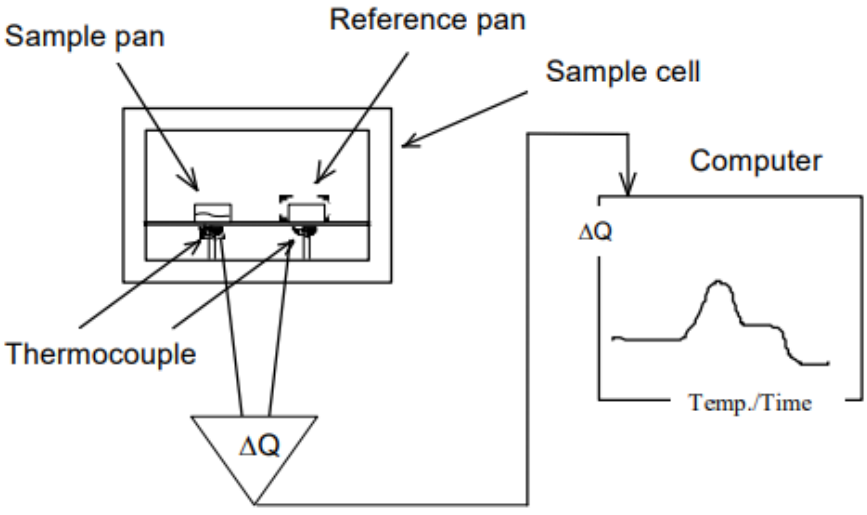


*Figure 3:3. A schematic representation of a DSC-instrument. [33]*

The DSC comprises the sample pan, reference pan and a heater. The heater supplies the sample and reference with heat at a defined rate to keep the temperature difference constant until the sample undergoes a transition and the heat capacity is changed. The difference in heat flow is recorded in the computer as a function of temperature or time. This will in turn create a thermogram which reveals when the melting/recrystallization, glass transition and crystallization have occurred. In this thesis, a DSC will be performed on PE that has been used in the extrusion coating process in order to get information regarding the crystallization in the

polymer samples. The first cycle of heating is of interest in this thesis since this is the one that can be related to the mechanical properties. The area under the first melting peak is usually measured since it contains the information regarding the crystallization. In this thesis, the crystallization of the polymer samples that have been processed with different process settings in the extruder will be compared. The purpose of this is to investigate if different process settings have an impact on the crystallization of the polymers. [34]

# 4. Machine Learning

## 4.1 Introduction to Machine Learning

Machine learning is a category of algorithms used by computer systems to become more accurate in predicting outcomes. One of the most common programming languages used for machine learning is Python, which will be applied in this thesis. Machine Learning is a branch of artificial intelligence where a machine is trained on how to learn from data, recognize patterns and draw conclusions without being explicitly programmed. In order to perform machine learning, a large and diverse amount of data is needed to find the patterns and learn. The process of machine learning can be described by *figure 4:1* below.

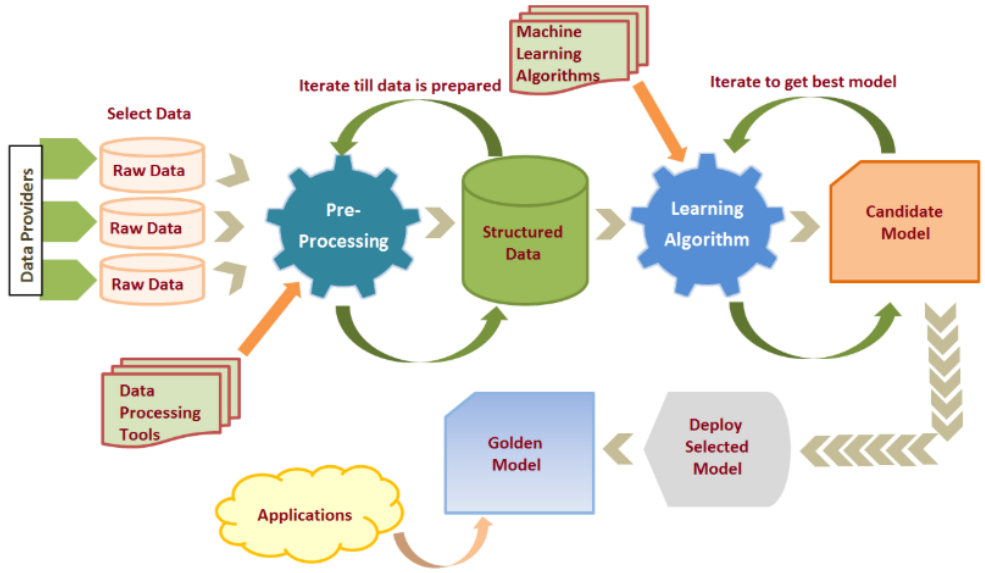


*Figure 4:1. A schematic representation of the machine learning process. [35]*

The two most common machine learning algorithms are unsupervised learning and supervised learning. Unsupervised learning algorithms train on a given input data, no corresponding output variables are given. The "right" answer has not been given to the system and so it must explore the input data that has been given and try to find useful relationships and patterns in it. This type of learning algorithm can be further grouped into clustering and association problems and is more advanced and less commonly used compared to supervised learning algorithms. [36]

Supervised learning algorithms train on already existing data where the "right" answer is present. This method is going to be adopted in this thesis. The learning algorithm will receive a set of training data used as input along with the corresponding response/output. The algorithm then learns by comparing its actual output/response with the correct (given) output/response to find errors which it will use to modify the model accordingly. Supervised learning uses patterns to predict values of the label on additional unlabelled data by using methods such as classification, regression, prediction and gradient boosting. The process of a supervised learning process where the algorithm learns from training dataset can be compared to a teacher supervising the learning process. The teacher knows the correct answers, the algorithm makes predictions of the training data while continuously being corrected by the teacher until it achieves an acceptable level of performance. The final goal is approximate the model so well that new input data can be used to predict output variables for that specific data.

The input data in this thesis will be the process-related factors and the rheological data. The rheological data will however be on unprocessed PE. Therefore, rheology will be performed on PE before being processed at three different temperatures, as a complement, in order to see how an increased temperature affects the storage modulus, zero shear viscosity and activation energy. Rheology will not be performed on the processed PE.

In industries, the interest of using machine learning has grown rapidly. Machine learning enables companies to analyse a large and complex amount of data quickly and more accurate. Building precise models with machine learning is beneficial for companies from a financial point of view. There is a greater chance of identifying opportunities or avoiding unknown risks. [36, 37]

### 4.1.1 Application of machine learning in material science

To experimentally determine mechanical properties of extruded polymers is a very costly and time-consuming process. Predicting material properties of polymers becomes more important each day. However, in order to predict these properties non-linear classification pattern recognition techniques need to be adopted due to the complexity of polymer behaviour. In supervised machine learning algorithms there are several pattern recognition methods available that are suitable for such purpose where Neural Networks (NN), Decision Tree, k-Nearest Neighbours (kNN) and Support Vector Machines (SVM) are the most commonly used.

In a study made by Alhindawi and Altarazi [38], supervised machine learning algorithms were used in predicting the tensile strength of extrusion-blown HDPE film while considering material characteristics (ingredients) and process parameters. The benefit of using such advanced computing algorithms is that it can reveal complicated relationships between process parameters and ingredients and tensile strength of HDPE film. The training set was used to train three supervised machine learning algorithms; Neural Networks, Decision Tree, k-Nearest Neighbours, see *figure 4:2*. These algorithms have the advantage that they are

suitable to be used when predicting qualities of products produced in a manufacturing process, extrusion blow moulding in this case, that includes a variety of input parameters.

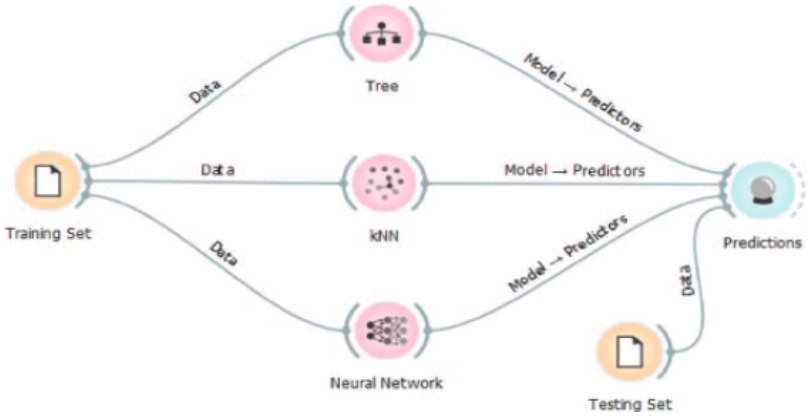


*Figure 4:2. Representation of the methodology used in the study made by Alhindawi and Altarazi. [38]*

When models have been trained, a testing set is fed into the trained models to evaluate the ability of the models to predict. The predicted output is compared with the true labels using Mean Absolute Error (MAE). MAE is used to evaluate all three models, and the most suitable one is chosen for the application. Supervised machine learning algorithms also allow the mapping of significant process and material related parameters. The model can also be useful when the purpose is to achieve a required tensile strength by implementing appropriate parameters. [38]

In another study made by Kopal et al., artificial neural network (ANN) was used to predict the engineering tensile stress – strain curves of a rubber blend with different contents of carbon black under uniaxial tensile loading. Modelling of this material is even more difficult compared to other traditional engineering materials since the structure of carbon black filled rubber blends are nonlinear and complex. Their behaviour cannot be described by models based on classic mathematical methods and so ANN must be used which is a supervised machine learning algorithm. ANN has the ability to learn from patterns presented in the form of input and corresponding output which are generated from experimental results. In this case the carbon black content and strain values were used as inputs and the corresponding experimental stress values were used as output values. The resulting model showed excellent consistency between experimental and simulated data. [39]

A similar study made by Srinivasu et al. was made but instead of predicting mechanical properties of carbon black filled rubber blends as Kopal studied, it was made on titanium alloy. The supervised machine learning algorithm ANN was also used in this study to predict entire stress – strain curves and the model was found to be successful in predicting new data. [40]

# 5. Method

The experimental stage in this thesis comprises production of material in the coating line and analysis of the produced material. The coating line was used to produce numerous PE films of the same grade. The films had been manufactured under different processing conditions: line speed and temperature on molten film which was regulated by adjusting the temperature in the heating zones in the extruder. Some problems were encountered during the initial experiments, when investigating whether the desired temperatures on the molten films could be obtained. The temperature on the molten film could not go beyond 315°C and 290°C which caused a relatively small process window for the melt temperature. The problems caused by a small temperature range is that it can get relatively hard to investigate the temperature-dependency on the mechanical properties of the polymer films with machine learning. Ideally the range would be wider.

The production of materials was made for two days. On the first day, 12 materials were produced and on the second day the measurements were repeated resulting in a total of 24 materials. The first 12 materials were made for each combination of line speed and temperature on molten film. The remaining 12 materials were produced by repeating the measurements made on the first day but in a different sequence to investigate the reproducibility of the experiment.

The polymer films were analyzed in order to investigate if the processing had any effect on the material properties of the polymer films. Thickness measurements were performed on the PE films to check for variations in each sample. The mean thickness of each film was calculated and used as input for the mechanical testing. Mechanical properties of the films were investigated through tensile testing. Stress – strain diagrams showing the mechanical properties of the polymer films were studied qualitatively for any irregularities indicating that the processing has had an impact on the mechanical properties. The degree of crystallinity of each material was calculated by performing a DSC were the first heating cycle was of interest since it contains the thermal history of the sample and thus information regarding the process influence.

Raw material, unprocessed PE, was taken from the same container as the extruder took material from during the coating experiment at different occasions. Rheology was performed on this to obtain the material ingredients. Plates were pressed from the raw material which were then used for rheology measurements. Rheology was performed three times with three different temperatures in order to be able to calculate the activation energy.

# 6. Experiments and Results

## 6.1 Material

The material studied in this thesis is a pure semi – crystalline polyethylene free from additives and special treatments. The density of the polymer is 920.5 kg/$m^3$ with a corresponding melt – flow index of 6.5 – 8.5 g/10min. All the experiments were conducted on the same grade of PE produced from the same batch in order to minimize sample variations.

## 6.2 Extrusion Coating

### 6.2.1 Design of experiment – DOE

A design of experiment consists mainly of three parts; screening, optimization and robustness testing. Performing these steps will ensure that the selected design of experiment contains a maximum amount of relevant information. In this thesis, the design of the experiment will be based on previous studies.

As can be seen in *table 6:1* and *6:2*, two parameters were varied in the extruder; temperature on molten film and line speed. Three temperatures were chosen in the experiment; one low, one high and one midpoint. The midpoint was repeated leading to a total of four temperatures. Having the correct temperature setting in the heating zones in the extruder enabled the desired temperature on the molten film to be achieved. Three line speeds were also chosen in the experiment; one low, one high and one midpoint. Hence, coating of the paperboard was made at four different temperatures and each temperature was coated three times at three different line speeds. This led to the production of 12 materials coated with different process settings. The experiments were recreated the day after, but at a different sequence. The experiments were repeated on the second day to investigate the reproducibility of the experiment. A total of 24 materials were produced, each having an individual test-ID (1 – 24) to be able to differentiate between these, see *table 6:1* and *6:2*. The selected design of the experiment was made in order to provide maximum amount of information.

*Table 6:1 The design of experiment and order on the first day.*

| Run # | Melt temperature $[°C]$ | Line speed $\left[\frac{m}{min}\right]$ | Test – ID |
|---|---|---|---|
| 1 | 280 | 200 | 1 |
| | | 400 | 2 |
| | | 600 | 3 |
| 2 | 300 | 200 | 4 |
| | | 400 | 5 |
| | | 600 | 6 |
| 3 | 330 | 200 | 7 |
| | | 400 | 8 |
| | | 600 | 9 |
| 4 | 300 | 200 | 10 |
| | | 400 | 11 |
| | | 600 | 12 |

*Table 6:2 The design of experiment and order on the second day.*

| Run # | Melt temperature $[°C]$ | Line speed $\left[\frac{m}{min}\right]$ | Test – ID |
|---|---|---|---|
| 1 | 300 | 200 | 13 |
| | | 400 | 14 |
| | | 600 | 15 |
| 2 | 330 | 200 | 16 |
| | | 400 | 17 |
| | | 600 | 18 |
| 3 | 300 | 200 | 19 |
| | | 400 | 20 |
| | | 600 | 21 |
| 4 | 280 | 200 | 22 |
| | | 400 | 23 |
| | | 600 | 24 |

### 6.2.2 Producing polymer films

The experiment was performed in the lab line in pilot plant at Tetra Pak AB at the décor station of the laminator. Before each test a setup roll was sent into the laminator. Purpose of the setup roll is to enable the laminator to adopt the proper settings so when it starts running the test roll everything should be working accordingly. The test roll consists of clay coated paperboard. One test roll per temperature meaning each roll provides with polymer films produced at three different line speeds at a given temperature. This resulted in eight setup rolls and eight test rolls for the trials in total, together on both days. The test plan was the same on the second day, only difference was the run order, see *table 6:1* and *6:2*, to investigate the reproducibility of the experiment.

During the first experiment, the temperature was set inside the extruder in order to reach the desired temperature on the molten film. When the temperature had been reached a setup roll was sent into the laminator which always began by running at the lowest line speed, 200 m/min. When the proper settings had been adopted, the test roll was inserted. Coating of the test roll was done at three different line speed in the order of 200, 400 and 600 m/min. Afterwards, the test roll was removed and marked with the correct label in order to keep track of all the materials. When the first run was performed, the next test in line was executed according to *table 6:1* and *6:2*. The procedure was repeated by first inserting another setup roll and afterwards the second test roll. Each time a new test roll started to run in the laminator, the time was recorded to be able to monitor afterwards if the laminator had adopted the correct settings for each run (according to the test plan) in CDAS. The coated test rolls were cut into smaller rolls and a total of 24 materials, paperboard coated with polymer film at different processing conditions, were produced.

To enable smooth removal of the thin polymer films without destroying them, Nitto single coated tape was applied to all eight test rolls before the experiment was conducted. The tape is used for packaging purposes and consists of a flat black kraft paper coated with a pressure sensitive modified acrylic adhesive, see *figure 6:1* below. The tape has a siliconized backing which allows an easy unwind.

As previously stated, one test roll was coated at three line speeds at a fixed temperature, providing with three materials. In order to ensure that enough material was to be produced, 12 sheets of tape with the size 40 x 60 cm respectively was applied to each test roll. One test roll is around 6000 meters and so the first four tapes were applied to the paperboard 500 meters in to the roll with a little distance in between the four tapes. The next four tapes were attached to the test roll after approximately 2000 meters in counting from the previous tapes. The last four tapes were applied to the test roll after 2500 meters in counting from the previous tapes, see *figure 6:1*.

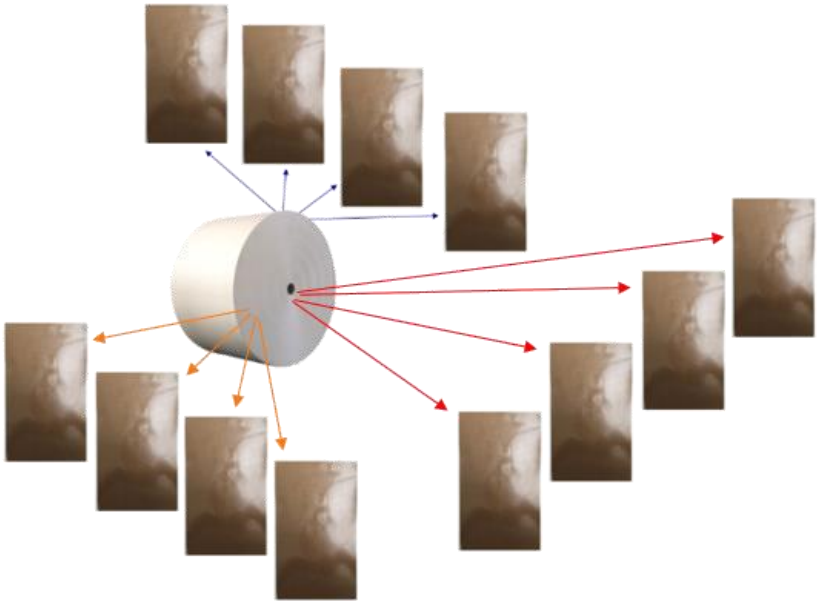

*Figure 6:1 Displays the position of the tapes on the test roll after coating. The blue arrows indicate the position of the tapes coated at the highest line speed. The orange arrows indicate the position of the tapes coated at the medium line speed. The red arrows indicate the position of the tapes coated at the lowest line speed.*

On the first four tapes, material was produced at the given temperature and the lowest line speed. Directly after the coating of the first tapes, the settings were altered to reach the next speed according to the test plan. The operator's hade 2000 meters of paperboard which corresponded to approximately 10 minutes until the correct settings had to be reached for the second coating to occur. Immediately after the second coating, the settings were altered a third time by the operator´s whom had 2500 meters of paperboard which also corresponded to approximately 10 minutes, due to faster line speed, until correct settings had to be reached for the third and last coating to occur. A more elaborated description of the process settings can be found in section 6.2.3.

### 6.2.3 Process settings

Before the real tests were conducted, experiments on the extruder were made in order to investigate if the desired temperatures (*table 6:1 and 6:2*) on the molten film could be obtained. Pellets of PE were fed into the extruder which was first set to reach the lowest temperature and line speed. As the molten polymer left the die and entered the airgap, the temperature was recorded using Raytek thermal camera. While the line speed was increased, the extruder speed was slightly increased which as well resulted in a small increase in melt temperature. This was performed on the other two temperatures as well, see *figure 6:2* below where all three temperature profiles are illustrated. The result from the Raytek measurements indicated that the desired temperatures on the molten film set in the design of experiment

could not be obtained by the extruder. The actual temperatures on the molten films can be found in Appendix A *table A:1, A:2* and A*:3*.

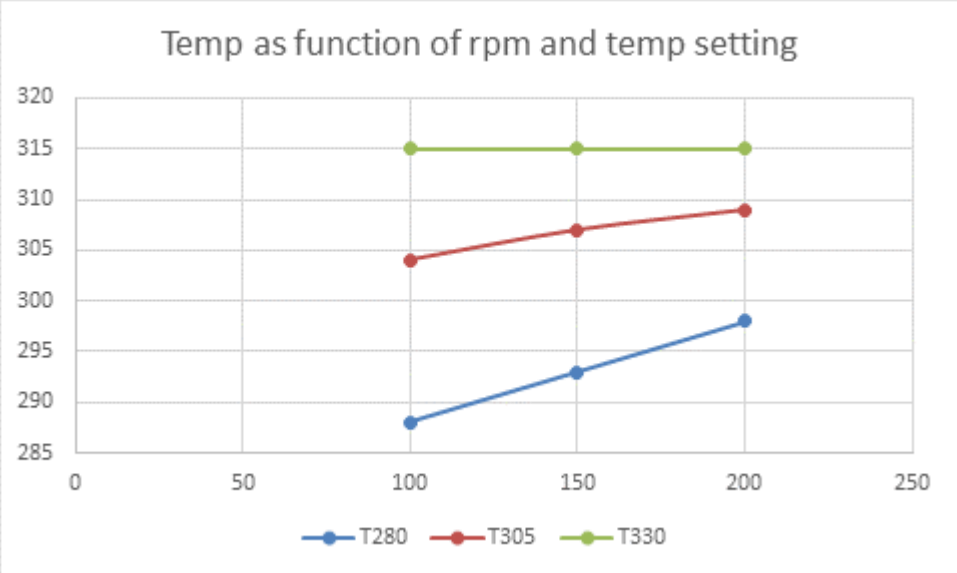


*Figure 6:2 The actual temperature on the molten film [°C] measured with Raytek as a function of extruder speed [rpm]. The blue line represents the lowest temperature, red line represents the middle temperature and the green line represents the highest temperature that could be obtained by the extruder.*

To obtain the desired temperatures on the molten film, correct temperature setting in the extruder had to be set. The extruder comprises six heating zones that contributes to the heating of the polymer. The temperature setting for the low, middle and high temperature on molten film can be found in Appendix A *table A:1*, *A:2* and *A:3* respectively.

Using a macro, calculations were made in order to investigate which parameters that had to be altered in order to obtain a uniform film thickness throughout all temperatures and line speeds. According to the software, to obtain a uniform film thickness of 20 µm, the coating width had to be changed when ramping up from 200 to 400 m/min and from 400 to 600 m/min. The coating width was in turn changed by altering the deckle settings. The deckle settings were adjusted manually by the operators in between each measurement meaning when line speed was ramped up from 200 to 400 the deckle settings were rapidly changed so when the next four tapes were to be coated, the coating line had adopted the correct settings. This was repeated when line speed was ramped up from 400 to 600 m/min, see the exact process settings in Appendix A, *table A:1, A:2 and A:3*.

## Results

The process settings were monitored in CDAS after the experiments were performed to check if the correct process settings had been obtained by the laminator. As can be seen in Appendix A, *figure A:1* and *A:2*, the laminator had applied correct settings on both days, there was no deviation. With line speed on the y-axis and date on x-axis one can monitor the process afterwards. Different variables from the extrusion coating process can be added in the

software such as line speed which is represented by the yellow line, see Appendix A *figure A:1* and *A:2*. The temperature of the six heating zones in the extruder was also looked in to in CDAS afterwards, those figures are however not attached to Appendix, but one interesting thing was detected. The operators had applied 315°C instead of 330°C in the last heating zone, which is in the feed block of the extruder. This mistake was only done when running at the highest temperature on the first day which could affect the results, but the probability is very low. The arrows in the images indicate where each sample was created. On the first day 12 materials were created with the test-ID 1-12 as indicated by the arrows in *figure A:1*. On the second day another 12 materials were created with the test-ID 13-24 as indicated by the arrows in *figure A:2*.

## 6.3 Mechanical Testing

### 6.3.1 Sample preparation

One coated tape per material was removed from the smaller test rolls, see *figure 6:1*, that had been cut out resulting in a total of 24 materials. From each material, four polymer sheets were cut out in machine direction, along the edge of the tape, and peeled off. Three of them were cut out using a template with the size 12 x 14 cm and a scalpel. The fourth film was a small strip that was cut out at the bottom of the material with the dimension 6 x 10 cm. Each polymer film was placed in a separate plastic folder and marked with correct test-ID. The three first sheets were to be used in tensile testing while the fourth sheet was to be used in thickness measurements. There was also room left on the material for possible samples to be cut out in cross direction for future investigation.

Four dog bone shaped samples see *figure 6:3*, were punched out from each polymer film for tensile testing which resulted in 12 replicates per material. Only eight dog bones were to be used for identifying the mechanical properties for each material, but 12 samples were prepared since some of the samples could contain defects due to the rollers in the laminator and dust from the floor.

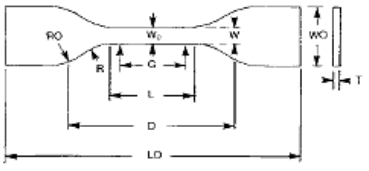


TYPE IV

Specimen Dimensions for Thickness, *T*, mm (in.)[A]

| Dimensions (see drawings) | 7 (0.28) or under | | Over 7 to 14 (0.28 to 0.55), incl | 4 (0.16) or under | | Tolerances |
|---|---|---|---|---|---|---|
| | Type I | Type II | Type III | Type IV[B] | Type V[C,D] | |
| *W*—Width of narrow section[E,F] | 13 (0.50) | 6 (0.25) | 19 (0.75) | 6 (0.25) | 3.18 (0.125) | ±0.5 (±0.02)[B,C] |
| *L*—Length of narrow section | 57 (2.25) | 57 (2.25) | 57 (2.25) | 33 (1.30) | 9.53 (0.375) | ±0.5 (±0.02)[C] |
| *WO*—Width overall, min[G] | 19 (0.75) | 19 (0.75) | 29 (1.13) | 19 (0.75) | ... | + 6.4 ( + 0.25) |
| *WO*—Width overall, min[G] | ... | ... | ... | ... | 9.53 (0.375) | + 3.18 ( + 0.125) |
| *LO*—Length overall, min[H] | 165 (6.5) | 183 (7.2) | 246 (9.7) | 115 (4.5) | 63.5 (2.5) | no max (no max) |
| *G*—Gage length[I] | 50 (2.00) | 50 (2.00) | 50 (2.00) | ... | 7.62 (0.300) | ±0.25 (±0.010)[C] |
| *G*—Gage length[I] | ... | ... | ... | 25 (1.00) | ... | ±0.13 (±0.005) |
| *D*—Distance between grips | 115 (4.5) | 135 (5.3) | 115 (4.5) | 65 (2.5)[J] | 25.4 (1.0) | ±5 (±0.2) |
| *R*—Radius of fillet | 76 (3.00) | 76 (3.00) | 76 (3.00) | 14 (0.56) | 12.7 (0.5) | ±1 (±0.04)[C] |
| *RO*—Outer radius (Type IV) | ... | ... | ... | 25 (1.00) | ... | ±1 (±0.04) |

*Figure 6:3 Illustration of a dog bone shaped polymer sample and its measurements.*

The dimensions of the test specimen are illustrated in *figure 6:3*. The red marking indicates the precise measurements of the dog bones used for the mechanical testing in this thesis.

### 6.3.2 Thickness measurement

Thickness measurements were made on small strips that were cut out from the materials. Each strip was assumed to represent the thickness variation for the entire material. The thickness was measured with Mitutoyo thickness gauge, see *figure 6:4*, which is a nondestructive test technique. Unlike a micrometer, the Mitutoyo only requires access to one side of the test sample.


*Figure 6:4 Mitutoyo thickness gauge ID-C112B.*

The thickness was measured on 20 different spots on the film, both in machine direction (MD) and cross direction (CD), to cover all the variations. The polymer film was placed on the base of the dial gage stand. After each measurement the film was slightly moved in order to measure another spot. When each spot was measured, the thickness was recorded in the Mitutoyo digimatic mini-processor. When all 20 spots had been measured the digimatic mini-processor calculated the average thickness which then was used as input in the software for tensile testing.

### 6.3.3 Tensile testing

Tensile testing was performed by testing 8 specimens in machine direction for each material. The shape of the specimen is illustrated in *figure 6:3*. The tensile tests were performed in the Instron 3365 with advanced video extensometer (Instron AVE). The tests were performed at room temperature with a 100 N load cell at a displacement rate of 500 mm/min. Two contrasting marks, white dots, were attached to each specimen to highlight the gage length, see *figure 6:3*. These marks were tracked using a high-resolution digital camera which then measured the strain. Real-time image processing algorithms located the centers of the two dots. This was done in order to prevent possible errors caused by stretching of the marks at high elongations, as seen in *figure 6:5* where the marks start to change shape due to the elongation. The specimen strain was then calculated from the mark separation at the start of the test and during elongation.

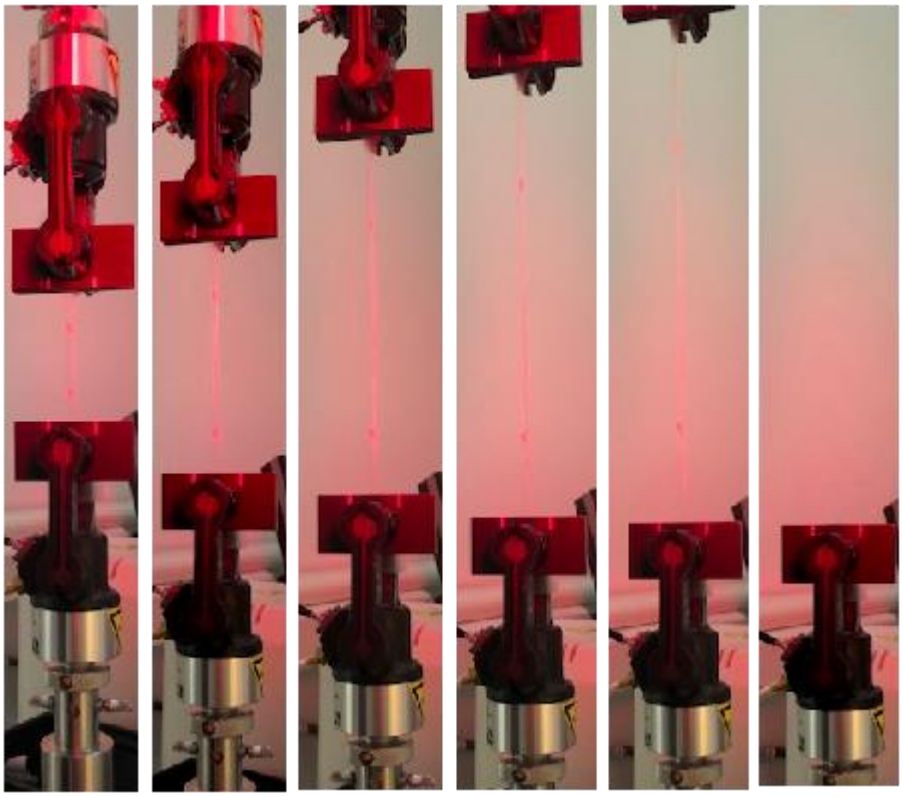

*Figure 6:5 The figure illustrates how a polymer sample from material 1 is being elongated as the tensile load increases. In the first image, to the left, the material is in its initial state and for each image the material is being further stretched until it breaks as seen in the last image, to the right.*

In *figure 6:5* above, a specimen from material 1 is being elongated. The sample is positioned between the two grips. The grip below is fixed while the grip above is pulling the sample. As the material is being pulled, it elongates even further until it breaks as seen in the last image, to the right.

## Results

Material was produced in the laminator with different process settings while trying to maintain the same film thickness in all materials, 20 µm. In order to do this some adjustments were made, as mentioned earlier in section 6.2.3. From the thickness measurements, the mean thickness was calculated, see *table 6:3*. Since thickness measurements were done in both MD and CD, a large variation in thickness was noted and therefore the standard deviation was calculated, see *table 6:3*.

*Table 6:3 Average thickness of the produced materials. One temperature per three line speeds (in the order 200, 400 & 600 m/min) producing three materials. Standard deviation in the thickness is also presented in the table.*

| **Test- ID** | **Mean thickness** [µm] **Mean ± SD** | **Line speed** [m/min] | **Melt temperature** [°C] |
|---|---|---|---|
| **1** | 29±0.92 | 200 | Low |
| **2** | 25±2.46 | 400 | |
| **3** | 21±2.16 | 600 | |
| **4** | 30±1.39 | 200 | Medium |
| **5** | 24±1.15 | 400 | |
| **6** | 22±1.29 | 600 | |
| **7** | 30±1.28 | 200 | High |
| **8** | 24±1.03 | 400 | |
| **9** | 25±3.33 | 600 | |
| **10** | 29±1.13 | 200 | Medium |
| **11** | 25±1.21 | 400 | |
| **12** | 21±2.53 | 600 | |
| **13** | 29±0.67 | 200 | Medium |
| **14** | 23±0.81 | 400 | |
| **15** | 21±2.75 | 600 | |
| **16** | 26±1.32 | 200 | High |
| **17** | 22±1.35 | 400 | |
| **18** | 19±2.56 | 600 | |
| **19** | 28±1-45 | 200 | Medium |
| **20** | 23±0.95 | 400 | |
| **21** | 21±2.99 | 600 | |
| **22** | 30±1.53 | 200 | Low |
| **23** | 25±0.89 | 400 | |
| **24** | 23±3.61 | 600 | |

Based on the results, it can be stated that the film is thicker when running at a lower coating speed, test – ID 1, 4, 7, 10, 13, 16, 19 and 22. When line speed is increased, the film thickness decreases in almost all cases. There is also a larger standard deviation in almost all materials produced at the highest line speed meaning that there is a larger thickness variation in those polymer films. There is also a difference in average thickness between materials produced under identical conditions. This can in turn result in differences among the mechanical properties among the replicates.

From the tensile testing, raw data was obtained. The raw data contained information regarding time of each measurement (sec), extension (mm), load (N), tensile stress (MPa), tensile strain (mm/mm) and axial strain (video) (mm/mm). Since tensile testing was performed on eight replicates per material, a standard deviation between the curves was expected due to some thickness variations and defects among the samples for each material. To make comparisons easier, a macro was used to create average stress – strain curves for each material using the raw data obtained from the dog bones. The average curves are a function of tensile stress (MPa) and axial strain (mm/mm), see *figure 6:6 – 6:9* below, with average film thickness used in the calculations of the curves. The figures illustrate the mechanical properties of the polymer films and how these are affected by an increasing line speed.

The mean curves for the samples, solid or dashed, are plotted up until the first break point (when first dog bone breaks). For each material, the mean break point is also plotted. The values for the mean break points are given in *table 6:4* below. The error bars on the mean break points show 95% confidence intervals for the mean break values in both x and y directions. A 95% confidence tells that from the available data, one can be 95% sure that the mean value for the material is within the limits of the confidence interval. A large spread in data results in a large confidence interval for the mean, compared to a small spread in data, and thus resulting longer error bars.

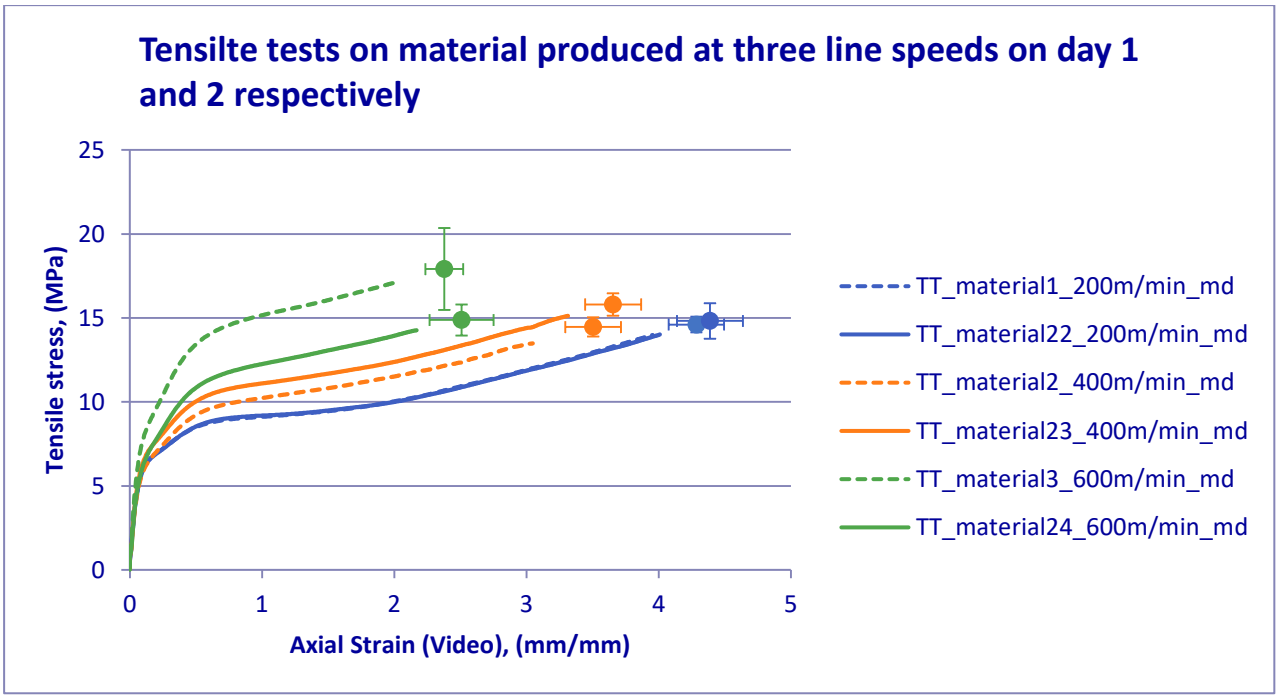


*Figure 6:6 The results from the tensile tests have been summarized in stress – strain curves. Average stress – strain curves have been calculated and summarized in the illustration for material 1 – 3, dashed lines, and 22 – 24, solid lines.*

Average stress – strain curves are illustrated in *figure 6:6*, for material 1 – 3 and 22 – 24. These materials have been produced at the lowest temperature setting in the extruder. The temperature that the polymer had in its molten state during extrusion coating is tabulated in *table 6:4*. Material 22 is a replicate of material 1, material 23 is a replicate of material 2 and material 24 is a replicate of material 3. Only difference is the time of production, material 1 – 3, indicated by the dashed lines, were produced on the first day at 12.37 pm and 22 – 24 on the second day at 1.51 pm, indicated by the solid lines.

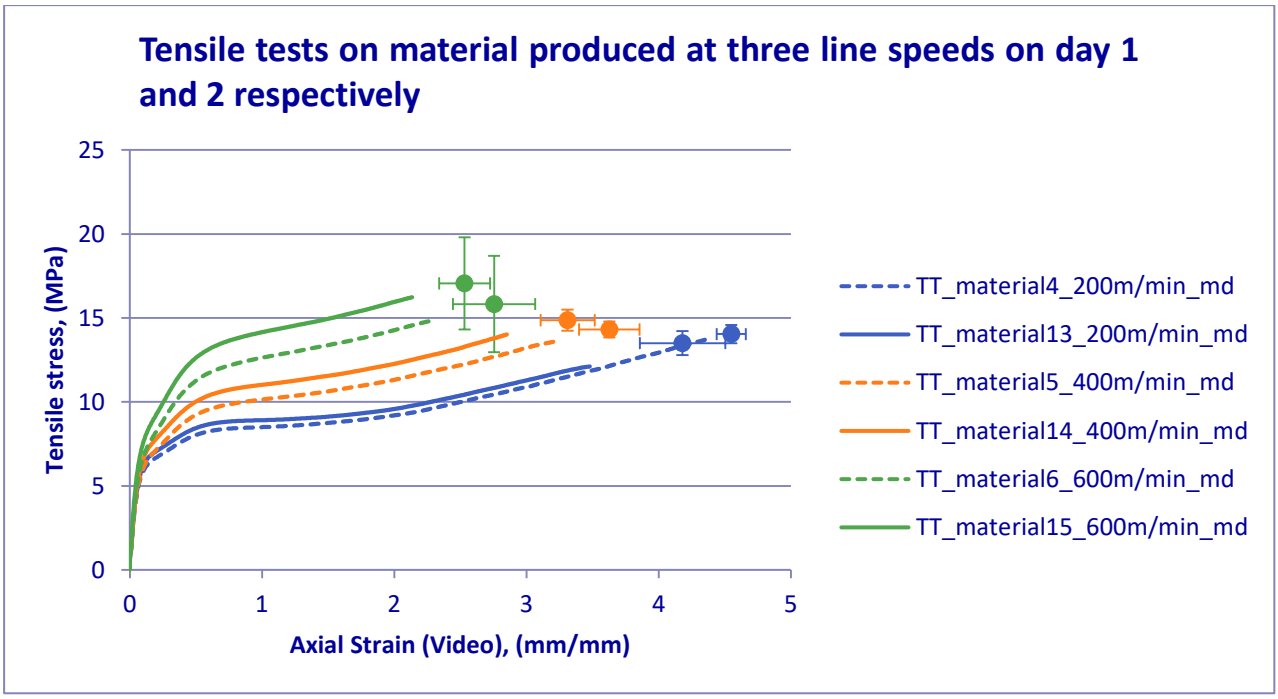


*Figure 6:7 The results from the tensile tests have been summarized in stress – strain curves. Average stress – strain curves have been calculated and summarized in the illustration for material 4 – 6, dashed lines, and 13 – 15, solid lines.*

Average stress – strain curves are illustrated in *figure 6:7*, for material 4 – 6 and 13 – 15. These materials have been produced at the medium temperature setting in the extruder and the temperature obtained on the molten film is tabulated in *table 6:4*. Material 13 is a replicate of material 4, material 14 is a replicate of material 5 and material 15 is a replicate of material 6. Only difference is the time of production, material 4 – 6, indicated by the dashed lines, were produced on the first day at 1.20 pm and 13 – 15 on the second day at 8.54 am, indicated by the solid lines.

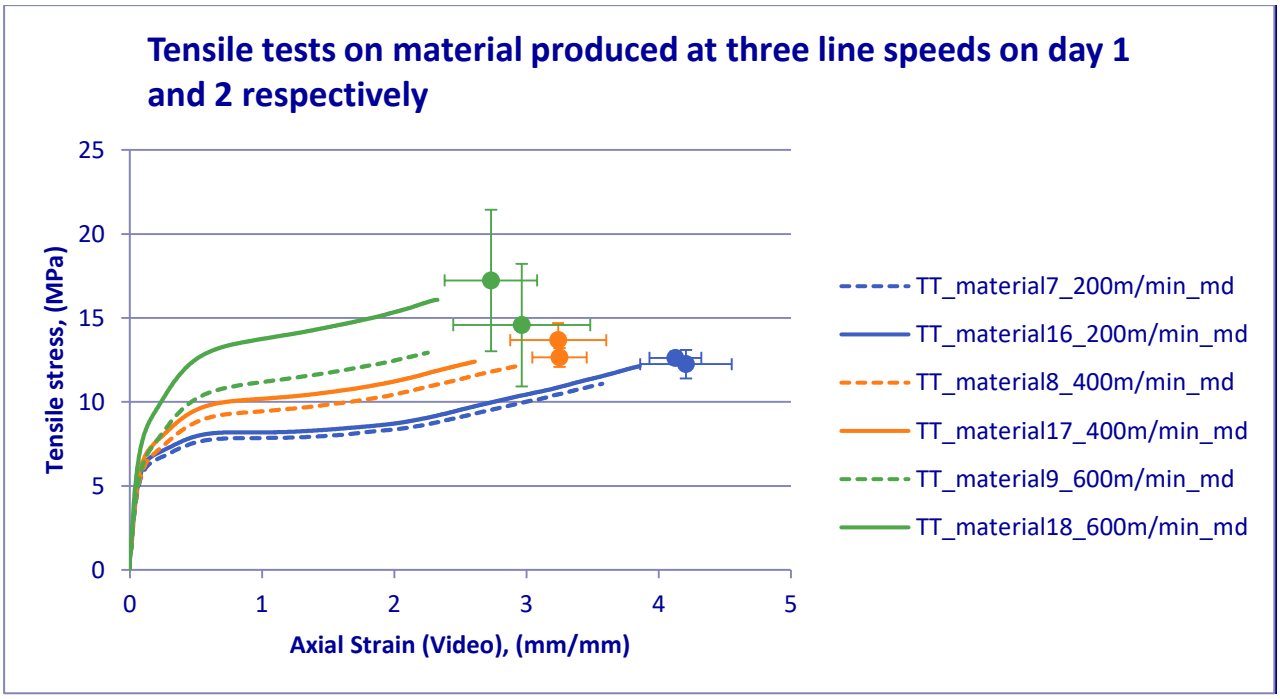


*Figure 6:8 The results from the tensile tests have been summarized in stress – strain curves. Average stress – strain curves have been calculated and summarized in the illustration for material 7 – 9, dashed lines, and 16 – 18, solid lines.*

Average stress – strain curves are illustrated in *figure 6:8*, for material 7 – 9 and 16 – 18. These materials have been produced at the highest temperature setting in the extruder and the temperature obtained by the molten film is tabulated in *table 6:4*. Material 16 is a replicate of material 7, material 17 is a replicate of material 8 and material 18 is a replicate of material 9. Only difference is the time of production, material 7 – 9, indicated by the dashed lines, were produced on the first day at 2.09 pm and 16 – 18 on the second day at 10.34 am, indicated by the solid lines.

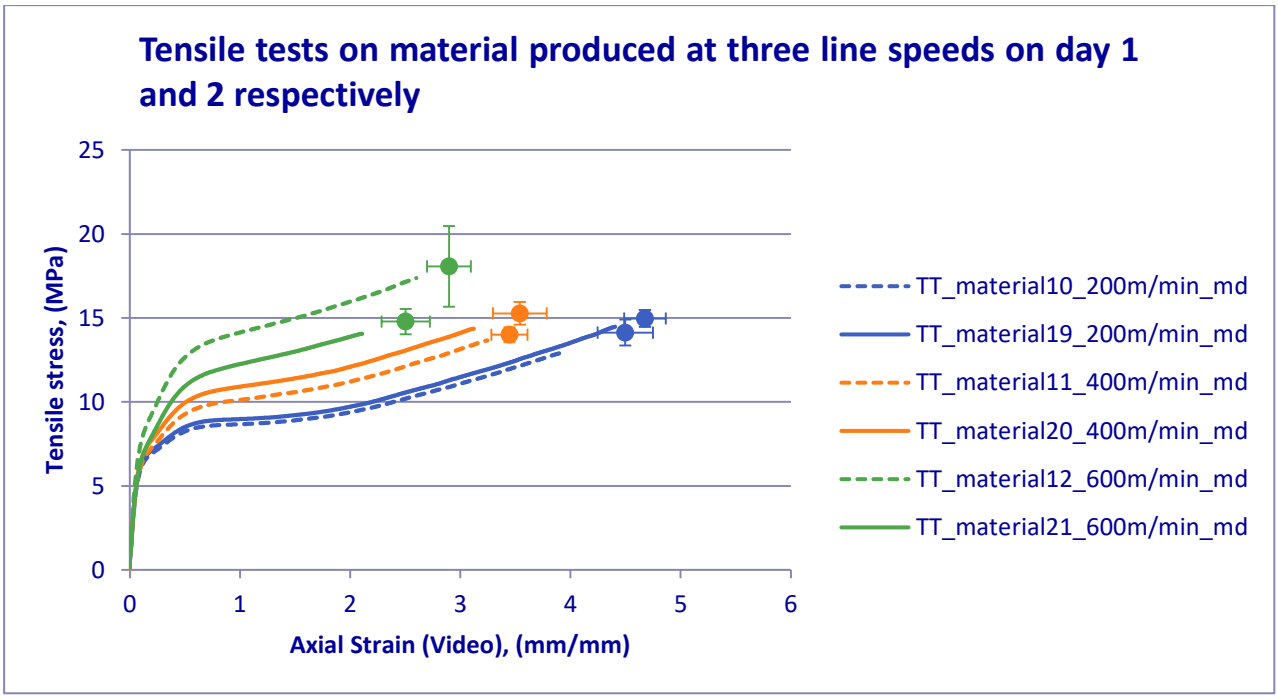


*Figure 6:9 The results from the tensile tests have been summarized in stress – strain curves. Average stress – strain curves have been calculated and summarized in the illustration for material 10 – 12, dashed lines, and 19 – 21, solid lines.*

Average stress – strain curves are illustrated in *figure 6:9*, for material 10 – 12 and 19 – 21. These materials have been produced at the medium temperature setting in the extruder and the temperature obtained on the molten film is tabulated in *table 6:4*. Materials 10 – 11 were produced on the first day as a replicate of the first materials, 4 – 6, produced at medium temperature. The materials 20 – 21 were produced on the second day as a replicate of the first materials, 13 – 15, produced at medium temperature.

Material 19 is a replicate of material 10, material 20 is a replicate of material 11 and material 21 is a replicate of material 12. Only difference is the time of production, material 10 – 12, indicated by the dashed lines, were produced on the first day at 3.13 pm and 19 – 21 on the second day at 12.25 pm, indicated by the solid lines.

The blue lines represent the materials that have been produced with the lowest line speed, 200 m/min. The replicates at this line speed are almost identical indicating that the materials have almost identical mechanical properties. The orange lines displays the materials produced at 400 m/min. The replicates at this line speed are very similar with some variations in between. It is however hard to state whether these differences depend on differences in mechanical properties or if it is just random variation which is why statistical analysis is needed to further understand what the variations mean.

The green lines represent the material produced at 600 m/min which is the highest line speed. The replicates are significantly different from each other despite being produced under the same conditions. These differences in mechanical properties can however be explained by their differences in film thickness, see *table 6:3*.

Overall, material produced at the lowest line speed, 200 m/min, can be stretched above 400 % according to *table 6:4* which displays the ultimate tensile properties. When increasing line speed to 400 m/min, the material can only be stretched to above 300 % and below 400 %. This indicates that the ductility of the material decreases, and the material becomes more brittle and thus tougher. When increasing line speed even further, up to 600 m/min, the ductility drops significantly to above 200 % but below 300 %.

*Table 6:4 The ultimate tensile properties are tabulated in the table below.*

| **Test-ID** | **Average tensile stress at break** [MPa] **Mean ± SD** | **Average axial strain (Video) at break** [mm/mm] **Mean ± SD** | **Temperature** [°C] |
|---|---|---|---|
| **1** | 14.61±0.56 | 4.29±0.25 | 290 |
| **2** | 14.46±0.68 | 3.51±0.25 | 297 |
| **3** | 17.91±2.92 | 2.38±0.17 | 297 |
| **4** | 14.04±0.65 | 4.55±0.13 | 305 |
| **5** | 14.31±0.56 | 3.63±0.27 | 308 |
| **6** | 15.83±3.43 | 2.76±0.37 | 308 |
| **7** | 12.24±1.02 | 4,21±0.41 | 315 |
| **8** | 12.65±0.68 | 3.25±0.25 | 315 |
| **9** | 14.57±4.37 | 2.97±0.62 | 315 |
| **10** | 14.12±0.92 | 4.50±0.30 | 305 |
| **11** | 13.99±0.53 | 3.45±0.20 | 308 |
| **12** | 18.07±2.88 | 2.90±0.24 | 308 |
| **13** | 13.50±0.85 | 4.18±0.39 | 305 |
| **14** | 14.87±0.76 | 3.31±0.24 | 308 |
| **15** | 17.05±3.28 | 2.53±0.23 | 308 |
| **16** | 12.61±0.45 | 4.13±0.23 | 315 |
| **17** | 13.68±1.20 | 3.24±0.43 | 315 |
| **18** | 17.24±5.48 | 2.73±0.46 | 315 |
| **19** | 14.97±0.61 | 4.68±0.23 | 305 |
| **20** | 15.27±0.81 | 3.54±0.29 | 308 |
| **21** | 14.78±0.89 | 2.50±0.26 | 308 |
| **22** | 14.82±1.26 | 4.39±0.30 | 290 |
| **23** | 15.80±0.80 | 3.66±0.25 | 297 |
| **24** | 14.88±1.11 | 2.51±0.29 | 297 |

Based on the results, it can be declared that the material properties are rate dependent. Line speed was however not the only process parameters that was intentionally altered. The influence from the temperature on the molten film was also examined. Averages curves were therefore made to show the temperature dependency, see *figure 6:10 – 6:12* below.

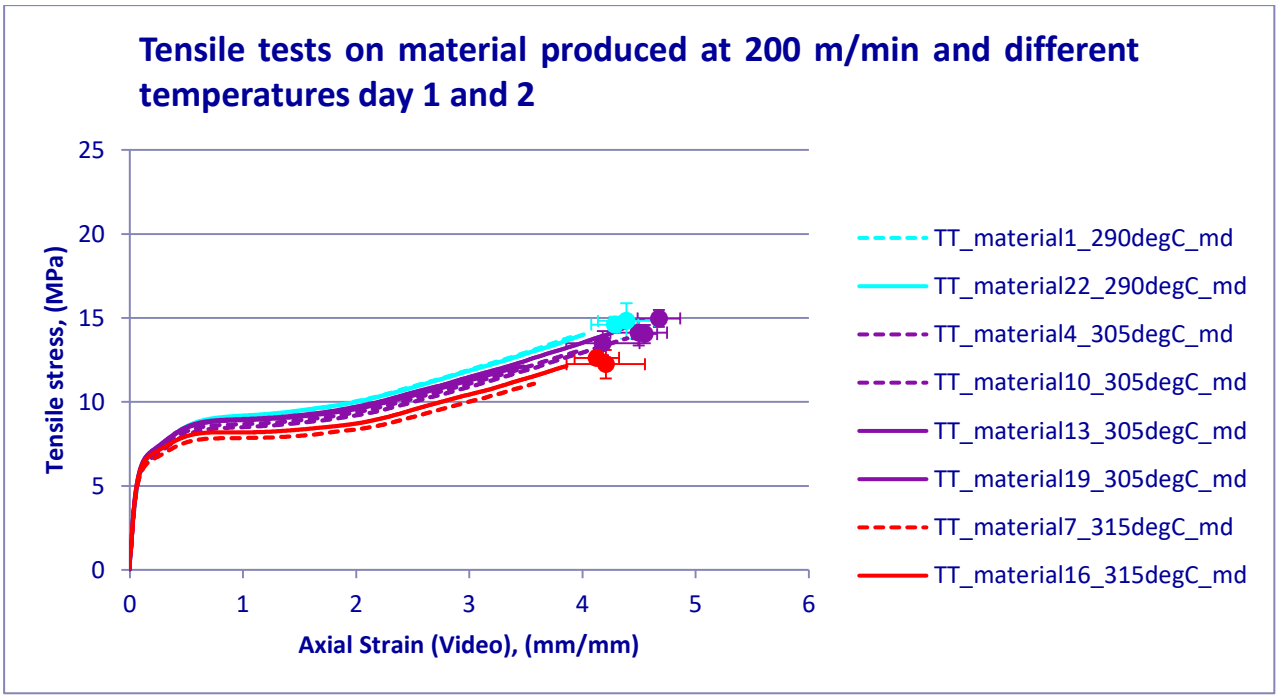


*Figure 6:10 Tensile stress is illustrated as a function of axial strain. The illustration shows eight graphs representing eight materials produced at different temperatures but at the same line speed. The red lines have been produced at 315°C, purple lines at 305°C and the turquoise at 290°C.*

The mechanical properties of all the materials produced at 200 m/min but at different temperatures are illustrated in *figure 6:10*. The red lines represent the material produced at 315°C where material 16, solid line, is a replicate of material 7, dashed line. Material produced at 305°C are displayed by the purple lines. Material 13, solid line, is a replicate of material 4, dashed line, and material 19, solid line, is a replicate of material 10, dashed line. The turquoise lines represent the material produced at 290 °C where material 22, solid line, is a replicate of material 1, dashed line.

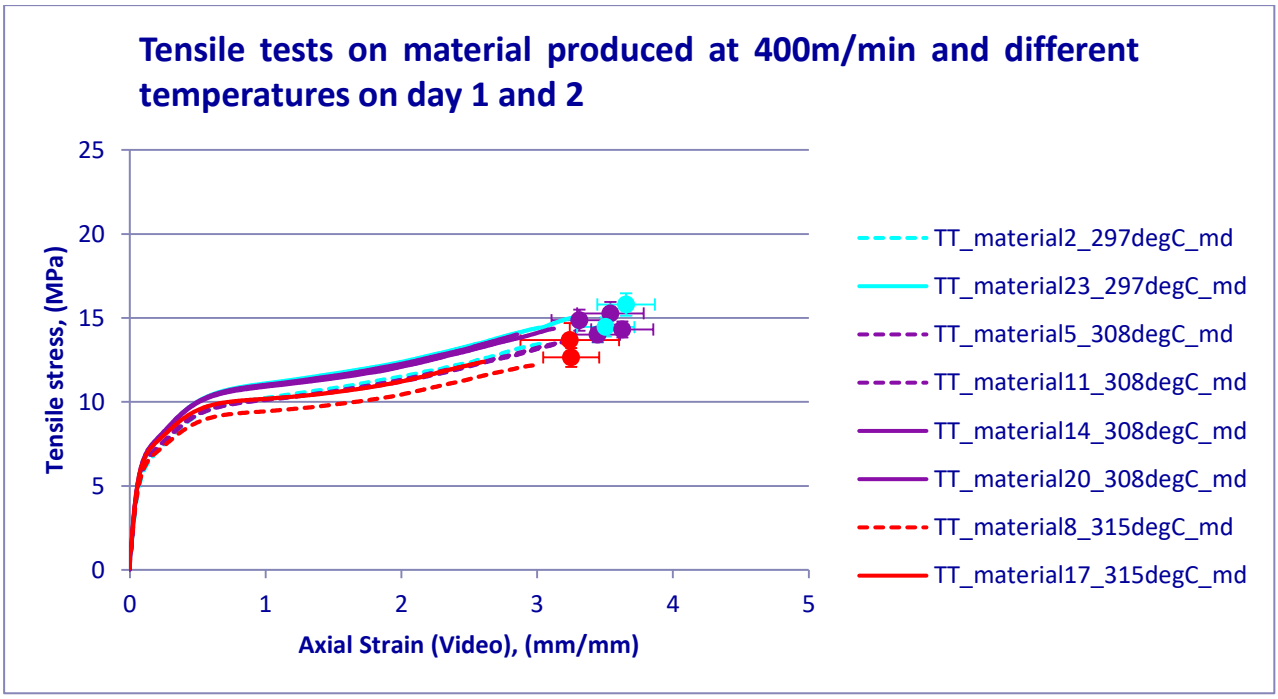


*Figure 6:11 Tensile stress is illustrated as a function of axial strain. The illustration shows eight graphs representing eight materials produced at different temperatures but at the same line speed. The red lines have been produced at 315°C, purple lines at 308°C and the turquoise at 297°C.*

The mechanical properties of all the materials produced at 400 m/min but at different temperatures are illustrated in *figure 6:11*. The red lines represent the material produced at 315°C where material 17, solid line, is a replicate of material 8, dashed line. Material produced at 308°C are illustrated by the purple lines. Material 14, solid line, is a replicate of material 5, dashed line, and material 20, solid line, is a replicate of material 11, dashed line. The turquoise lines represent the material produced at 297 °C where material 23, solid line, is a replicate of material 2, dashed line.

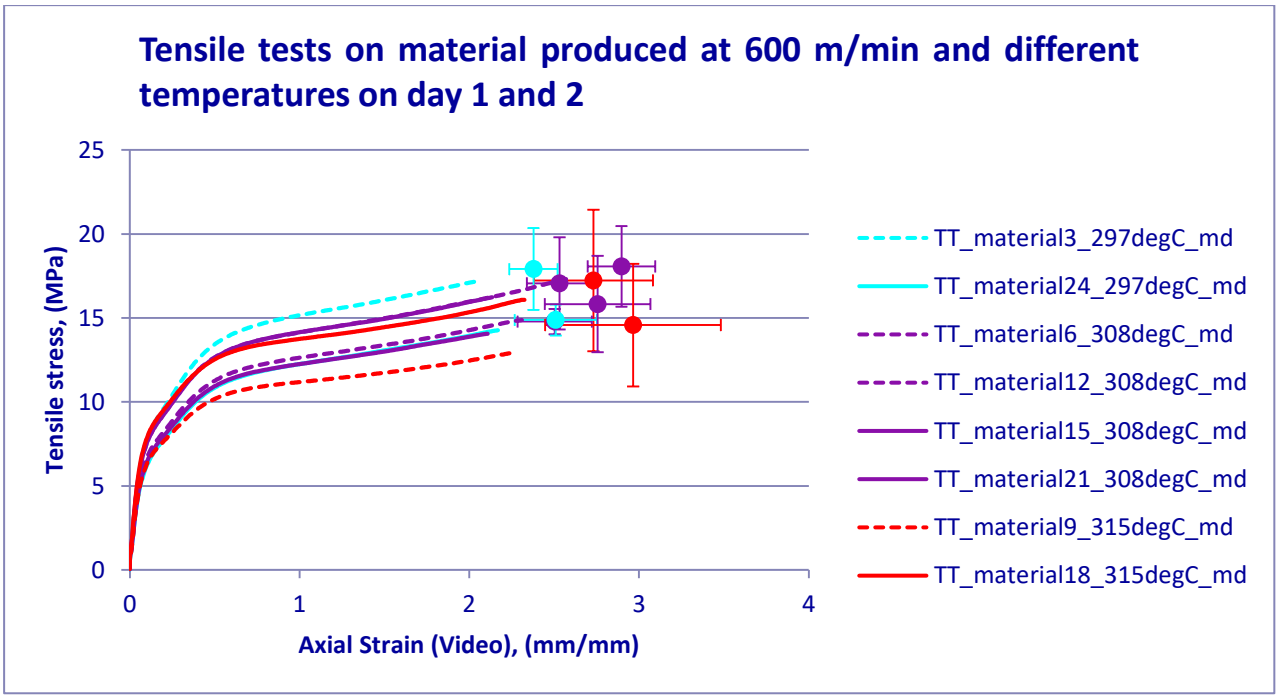


*Figure 6:12 Tensile stress is illustrated as a function of axial strain. The illustration shows eight graphs representing eight materials produced at different temperatures but at the same line speed. The red lines have been produced at 315°C, purple lines at 308°C and the turquoise at 297°C.*

The mechanical properties of all the materials produced at 600 m/min but at different temperatures are illustrated in *figure 6:12*. The red lines represent the material produced at 315°C where material 18, solid line, is a replicate of material 9, dashed line. Material produced at 308°C are illustrated by the purple lines. Material 15, solid line, is a replicate of material 6, dashed line, and material 21, solid line, is a replicate of material 12, dashed line. The turquoise lines represent the material produced at 297 °C where material 24, solid line, is a replicate of material 3, dashed line.

Based on *figure 6:10 – 6:12*, it is hard to draw any conclusions regarding the temperature dependency. Therefore, statistical analysis is needed to investigate if the temperature have an impact on the mechanical properties before any conclusions can be drawn.

## 6.4 Rheology

During the extrusion coating process, the extruder took pellets of unprocessed PE from a container. From this container, raw material was removed and put into plastic bags. The purpose was to perform rheology on the polymer to investigate the material ingredients such as storage modulus, zero shear viscosity and activation energy. Since the polymer only came from one batch, material was only taken at three different occasions during the experiment together on both days.

### 6.4.1 Sample preparation

To perform rheology, samples had to be prepared. Compression of pellets (raw material) was made at 150°C with a preheating for 60 seconds. The raw material was exposed to a linear increase of pressure up to 50 bar for 50 seconds. The pressure of 50 bar was remained on the polymer for further 40 seconds. The polymer was cooled for 30 seconds with a cooling cassette (cold water circulation). From the pressed specimen, five discs were stamped with a diameter of 25 mm and a thickness of 1.2 – 1.5 mm.

### 6.4.2 Procedure

A frequency sweep between 20 – 0.01 Hz divided into 18 steps respectively at 130°C, 150°C and 170°C in the linear viscoelastic region was performed. Three measurements with three specimens were made at each temperature to make sure there were no outliers. Loss modulus as a function of storage modulus was illustrated in the range of 200 – 700 Pa of the loss modulus. The plot showed a linear relation which enabled the determination of the storage modulus at a loss modulus of 500 Pa, see equation below.

$$Storage\ modulus = 10^{\frac{\log 500 - l}{m}} \qquad (2.6)$$

where $l$ is the intercept of the linear regression line and $m$ is the slope of the linear regression line.

The zero shear viscosity was defined by extrapolating the three parameters cross equation, see equation below.

$$\eta^* = \frac{\eta_0}{1 + \tau\omega^n} \qquad (2.7)$$

where $\eta^*$ is the complex viscosity (Pas), $\eta_0$ is the zero shear viscosity (Pas), $\tau$ is the characteristic relaxation time (s), $\omega$ is the frequency (rad/s) and $n$ is the power law index.

The activation energy for PE was calculated by performing a frequency sweep on 130°C, 150°C and 170°C. The horizontal, $a_T$, and vertical, $b_T$, shift factor was calculated and from those the horizontal and vertical activation energies were calculated using the equations below.

$$a_T = \exp\left[\frac{E_H}{R}\left(\frac{1}{T-273} - \frac{1}{T_0+273}\right)\right] \qquad (2.8)$$

$$b_T = \exp\left[\frac{E_V}{R}\left(\frac{1}{T-273} - \frac{1}{T_0+273}\right)\right] \qquad (2.9)$$

where $E_H$ is the horizontal activation energy, $E_V$ is the vertical activation energy, $T$ is the temperature and $R$ is the ideal gas constant. The equations above, *equation 2:8* and *2:9*, are based on the Arrhenius equation. The activation energy, $E_0$, is the sum of the horizontal and vertical activation energies which is of interest in this report.

### Results

In *table 6:5*, the raw material used for the rheology measurements is tabulated. In this thesis, the rheology measurements will only be used to show that the material ingredients of the

polymer used in the experiment falls within the material specifications. Three samples of raw material were removed from the container at different time slots. The purpose of this was to investigate if there were any differences in the material ingredients depending on when and were the samples were taken from the batch.

*Table 6:5 Polymer grade used for the rheology measurements and the date/time they were taken from the container.*

| Sample | Grade | Day | Time |
|---|---|---|---|
| 1 | PE | 2019-03-04 | 3.21 pm |
| 2 | PE | 2019-03-05 | 10.48 am |
| 3 | PE | 2019-03-05 | 1.14 pm |

Rheology was first performed at 170°C, see *figure 6:13*, to investigate if there were differences in rheology between the samples. The rheological differences are more enhanced at the highest temperature and so the measurements were first conducted at this.

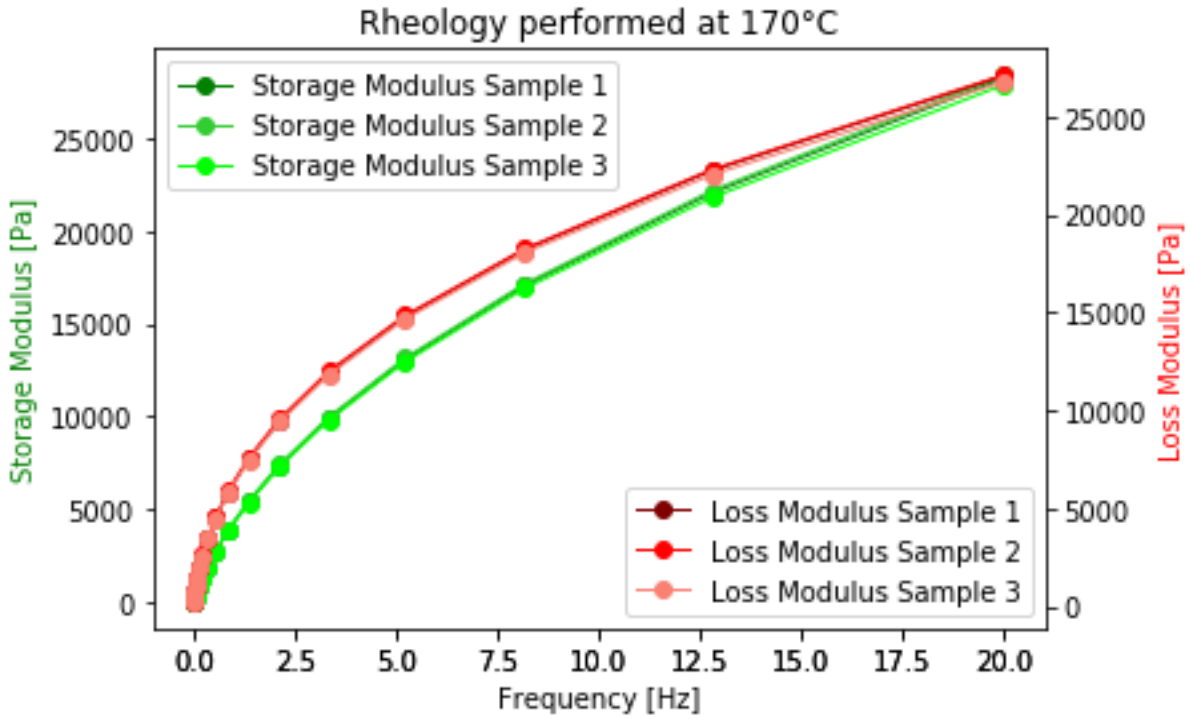


*Figure 6:13 Storage modulus and loss modulus at 170°C for sample 1, 2 and 3.*

According the figure above, no significant differences in storage modulus (green lines) and loss modulus (red lines) were detected meaning that the samples have similar elasticity. Differences in zero shear viscosity was not detected either meaning that the molecular weight is similar. This results in the conclusion that there are no sample variations. Therefore, only one of the samples, sample 3, needed to be measured at 150°C and 130°C. In *table 6:6*, the results from the rheology measurements have been tabulated.

*Table 6:6 The storage modulus and zero shear viscosity at the three temperature sweeps; 130°C, 150°C and 170°C.*

| Sample | Zero shear viscosity [Pa·s] | Storage modulus [Pa] | Zero shear viscosity [Pa·s] | Storage modulus [Pa] | Zero shear viscosity [Pa·s] | Storage modulus [Pa] |
|---|---|---|---|---|---|---|
| | 170°C | 170°C | 150°C | 150°C | 130°C | 130°C |
| 1 | 4793.0 | 117.5 | | | | |
| 2 | 4856.0 | 117.4 | | | | |
| 3 | 4759.0 | 117.9 | 9298.0 | 122.9 | 18605.0 | 125.3 |

In *figure 6:14*, the storage modulus (green lines) and loss modulus (red lines) have been displayed for sample 3 at the three temperature sweeps; 130, 150 and 170°C. According to the figure, the viscoelastic properties of the polymer change with temperature during the measurements as expected. Storage modulus increases with decreasing temperature and so does the zero shear viscosity, see *table 6:6*.

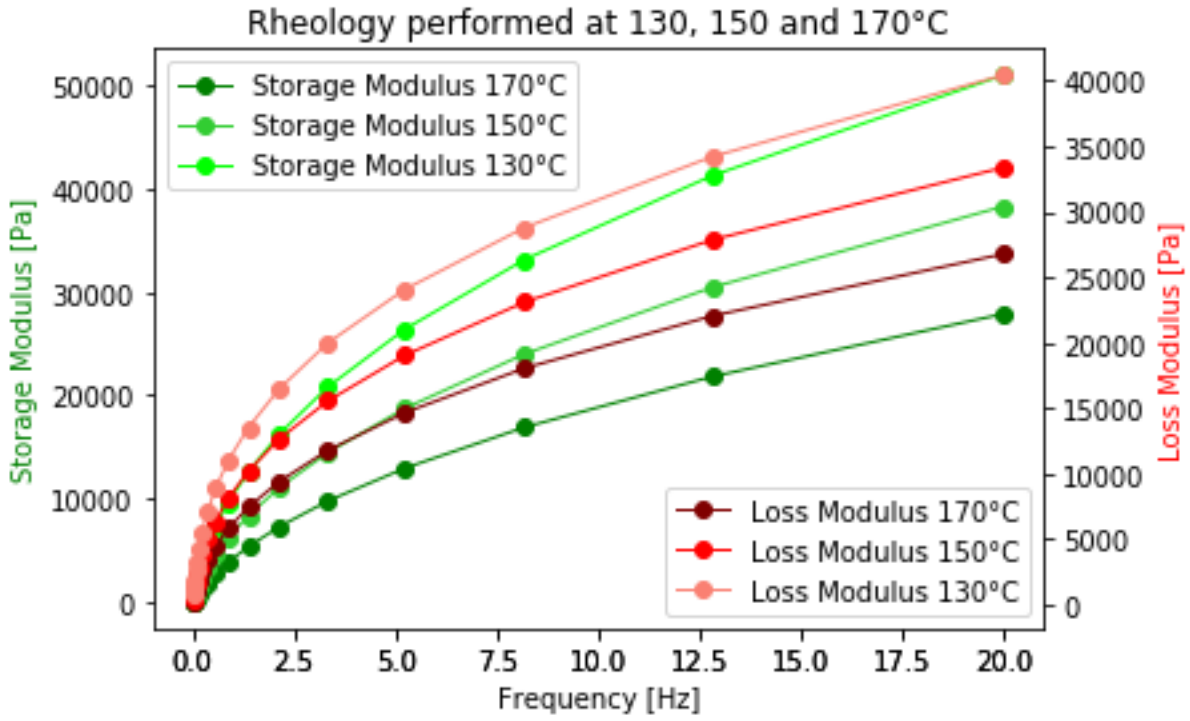


*Figure 6:14 Storage modulus and loss modulus at 130 ,150 and 170°C for sample 3.*

The activation energy was calculated using the equations listed in section 6.4.2 and is displayed in *table 6:7*. The values obtained from the rheology measurements correspond to the values in the material specification for this specific PE grade.

*Table 6:7 Activation Energy*

| **Activation Energy** [kJ/mol] | | | |
|---|---|---|---|
| **Grade name** | EH | EV | EH+EV |
| PE | 62.2 | 8.5 | 70.7 |

## 6.5 Differential Scanning Calorimetry

For DSC measurements, samples from the polymer films used for thickness measurement were used. From each material, circular samples, with a diameter of 4 mm, were pushed out and weighed. The sample weight in a DSC needs to be in the range of 2 mg – 9 mg. In order to maximize the contact area between the sample and the pan, a weight closer to 9 mg was used. When the weight was inserted into the DSC software, the sample was placed inside the pan and sealed with the lid using a press and afterwards, positioned in a sample cell in the instrument.

Polymer films produced at low temperature and high temperature on both days respectively were analysed in order to investigate if there were any clear differences in the degree of crystallinity.

### Results

First heating cycle was of interest since it contains the thermal history of the sample and so it describes the impact made from the process (laminator). Below, the DSC results are displayed in six figures. Each figure contains the result of two samples that have been produced under identical processing conditions but on two different days. This was made in order to investigate if the process affects the polymer differently on different days even though the settings in the extruder are the same.

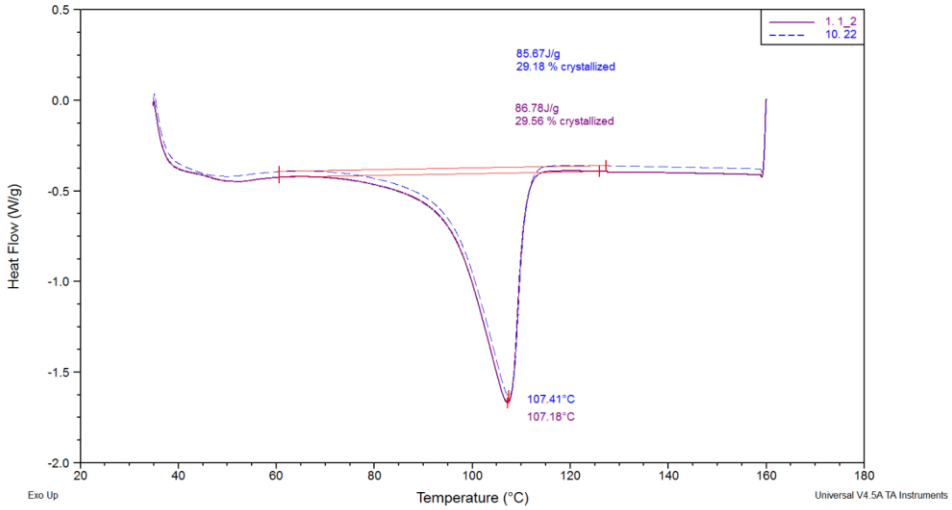


*Figure 6:15 The results from the DSC measurements showing the first heating cycle. Two samples are illustrated in the figure, both produced at a low melt temperature in the process and at a low line speed.*

Material 1 and 22 are illustrated above in *figure 6:15*, both produced at low melt temperature and low line speed. The figure shows that the heating cycles are not entirely identical on the first and second day for material 1 and 22. The melt temperature for which the largest crystals melt is slightly different. The smaller crystals do not start to melt at the same time which indicates why there is a difference in the degree of crystallinity (amount of crystals).

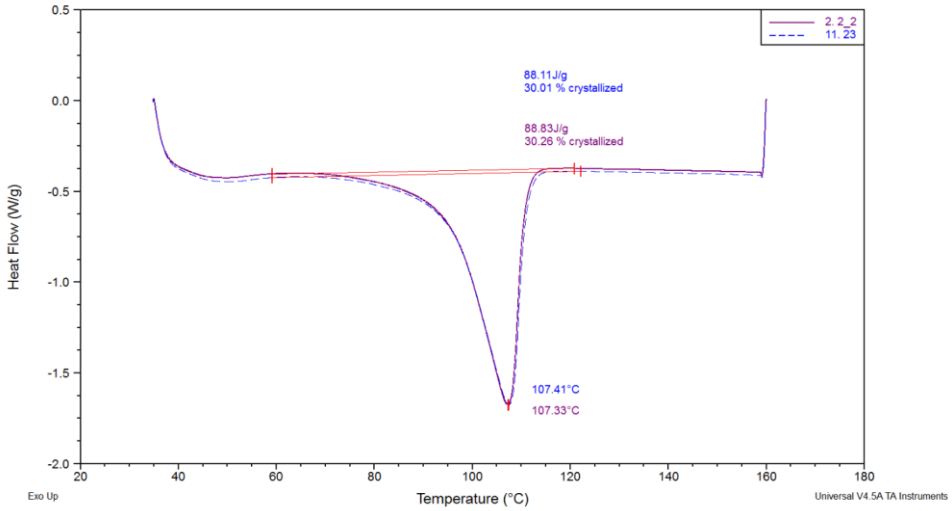


*Figure 6:16 The results from the DSC measurements showing the first heating cycle. Two samples are illustrated in the figure, both produced at a low melt temperature in the process and at a medium line speed.*

Material 2 and 23 are illustrated in *figure 6:16*, both produced at a low melt temperature and at a medium line speed. A slight difference between the heating cycles can be detected for material 2 and 23. The smaller crystals do not start to melt simultaneously and so there is a difference in the amount of crystals which is also demonstrated in the difference in degree of crystallinity. The melt temperature for which the largest crystals melt is also different which can be a result of the difference in amount of crystals.

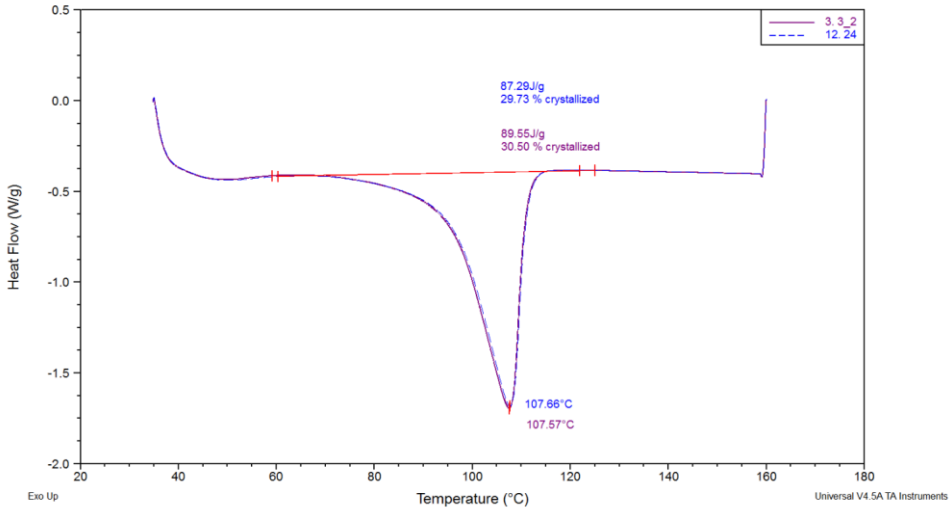


*Figure 6:17 The results from the DSC measurements showing the first heating cycle. Two samples are illustrated in the figure, both produced at a low melt temperature in the process and at a high speed.*

Material 3 and 24 are illustrated in *figure 6:17*, both produced at low melt temperature and high line speed. The first heating cycle is almost identical on the first and second day. The melt temperature for which the largest crystals melt is however slightly different which could depend on slightly larger crystals in material 24. The smaller crystals start to melt at approximately the same time. There is also a slight difference in the degree of crystallinity.

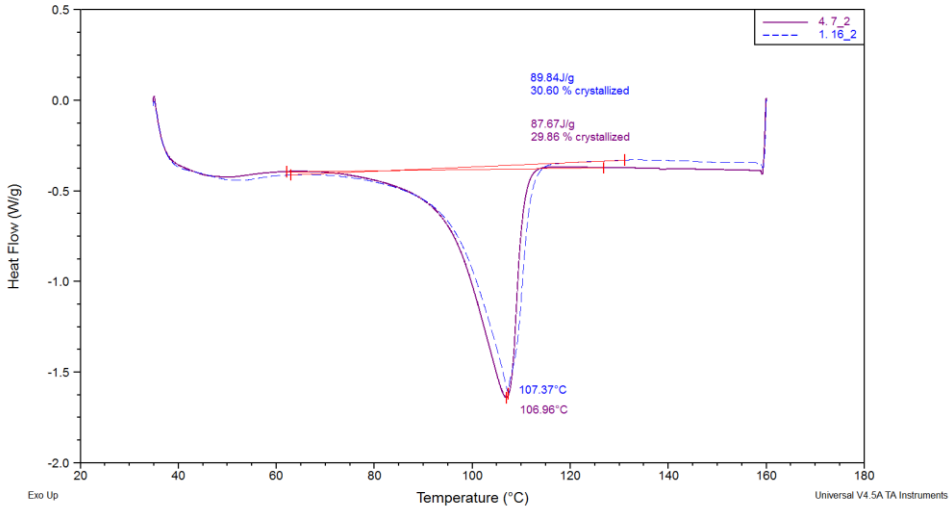


*Figure 6:18 The results from the DSC measurements showing the first heating cycle. Two samples are illustrated in the figure, both produced at a high melt temperature in the process and at a low line speed.*

Material 7 and 16 are illustrated in *figure 6:18*, both produced at a high melt temperature in the process and at a low line speed. A slight difference between the heating cycles can be detected. The smaller crystals do not start to melt simultaneously. The melt temperature for which the largest crystals melt is also different which can be a result of the difference in amount of crystals.

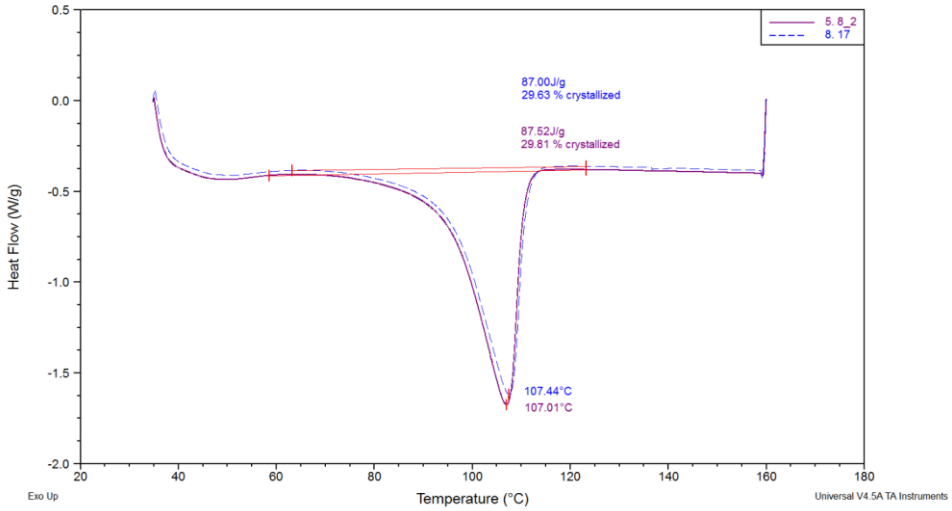


*Figure 6:19 The results from the DSC measurements showing the first heating cycle. Two samples are illustrated in the figure, both produced at a high melt temperature in the process and at a medium line speed.*

Material 8 and 17 are illustrated in *figure 6:19*, both produced at a high melt temperature and at a medium line speed. There is a difference between the heating cycles and therefore a difference in degree of crystallinity and melt temperature. This is due to the fact that there is a difference in amount of crystals between the samples and also a difference in size of the largest crystals since the melt temperature where the largest crystals melt is different.

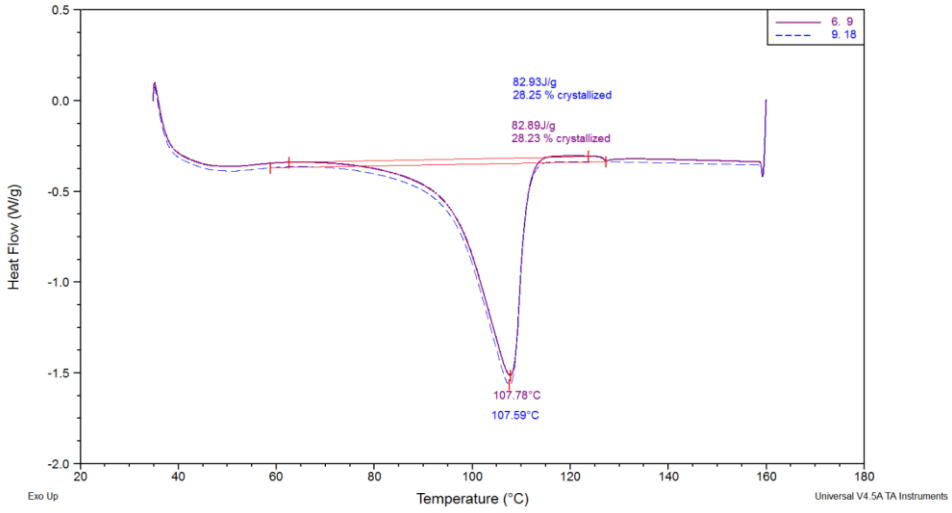


*Figure 6:20 The results from the DSC measurements showing the first heating cycle. Two samples are illustrated in the figure, both produced at a high melt temperature in the process and at a high line speed.*

Material 9 and 18 are illustrated in *figure 6:20*, both produced at a high melt temperature and high line speed. When comparing the first heating cycle between these materials, it can be detected that there is a difference in when the smallest crystals start to melt. There is also a difference in when the largest crystals melt by looking at the melt temperature on the peak. This results in a difference in amount of crystals and hence degree of crystallinity.

The degree of crystallinity was calculated using the DSC software. As can be seen in *table 6:8,* there is no clear pattern regarding how the process impacts the degree of crystallinity.

*Table 6:8 The degree of crystallinity for the material produced at the lowest and highest temperatures on both days respectively. The temperature where the largest crystals melt is also illustrated in the table for each material.*

| Test- ID | Degree of crystallinity [%] | Melt temperature [°C] |
|---|---|---|
| 1 | 29.56 | 107.18 |
| 2 | 30.26 | 107.33 |
| 3 | 30.50 | 107.57 |
| 7 | 29.86 | 106.96 |
| 8 | 29.81 | 107.01 |
| 9 | 28.23 | 107.78 |

| Test-ID | Degree of crystallinity [%] | Melt temperature [°C] |
|---|---|---|
| 16 | 30.60 | 107.37 |
| 17 | 29.63 | 107.44 |
| 18 | 28.25 | 107.59 |
| 22 | 29.18 | 107.41 |
| 23 | 30.01 | 107.41 |
| 24 | 29.73 | 107.66 |

The temperature at the tip of the peak, in *figure 6:15* to *6:20,* can be related to the stability of the crystals. This temperature increases slightly with increasing line speed according to the data which has been summarized in *table 6:8*. It can be assumed that when increasing line speed, the crystals grow larger and become more stable.

# 7. Model building and Machine Learning

During the modelling part, the interest is to create a model that can predict the mechanical properties of a PE film only by knowing how it has been processed. The mechanical properties were studied with tensile tests that provided stress – strain curves. To start with, the stress – strain curves were divided into different sections. Since Young's modulus increases with increasing degree of crystallinity this area would be interesting to model using machine learning. However, since there was no difference in degree of crystallinity among the materials, according to the DSC measurements, indicating that the process had not made an impact on the degree of crystallinity, this area was no longer of interest. Focus was instead shifted to the ultimate tensile properties were the effect from the process was clear according to the results from tensile testing.

The ultimate tensile properties were divided in stress and axial strain at break, and the relation to line speed and temperature of the molten film was investigated separately for each outcome using the 24 observations. Classical statistical analysis such as ANOVA was performed to detect interactions between the input parameters (features) and the output

parameters (target). Predictive models were built using linear regression and random forest regression which is a supervised machine learning algorithm.

## 7.1 Analysis of Variance – ANOVA

### 7.1.1 Axial strain at break

The data was first examined by using classical methods to investigate the relationship between the features and the target. The influence from line speed and melt temperature on axial strain at break. In *figure* 7:1 below, axial strain at break is plotted as a function of line speed with a color based on a third variable, temperature on molten film.

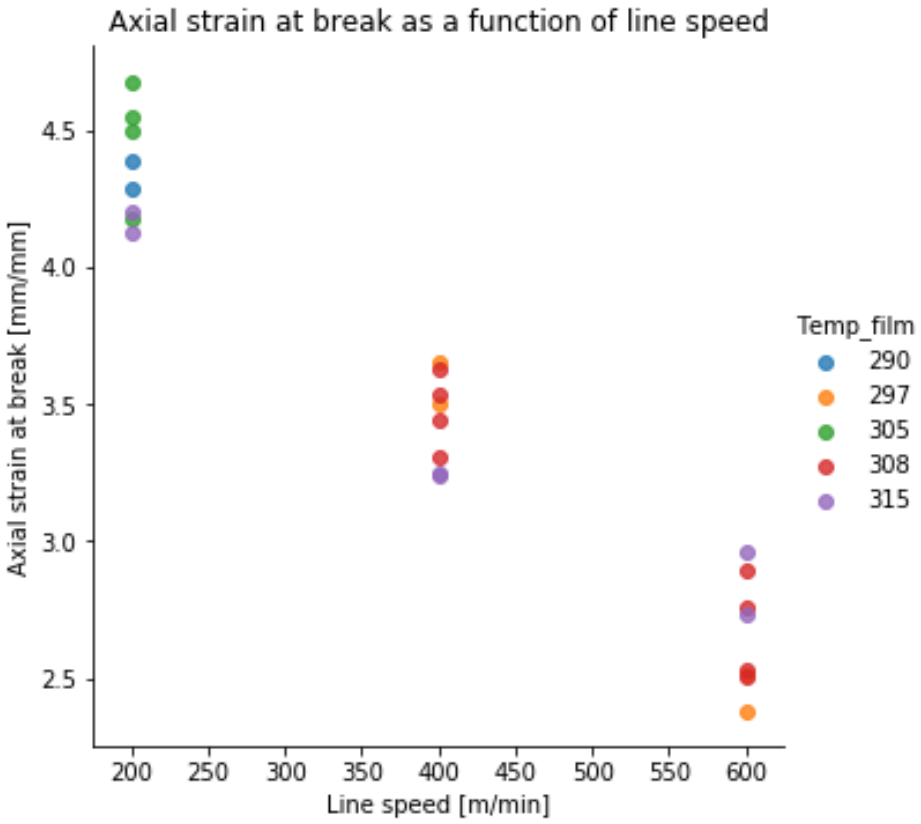


*Figure 7:1 Scatter plot of axial strain at break vs line speed, color separated for temperature on molten film.*

There is a clear trend between decreasing axial strain at break and increasing line speed in *figure 7:1*. The effect of temperature is less clear, as is also seen in *figure 7:2*, displaying axial strain at break vs temperature on molten film.

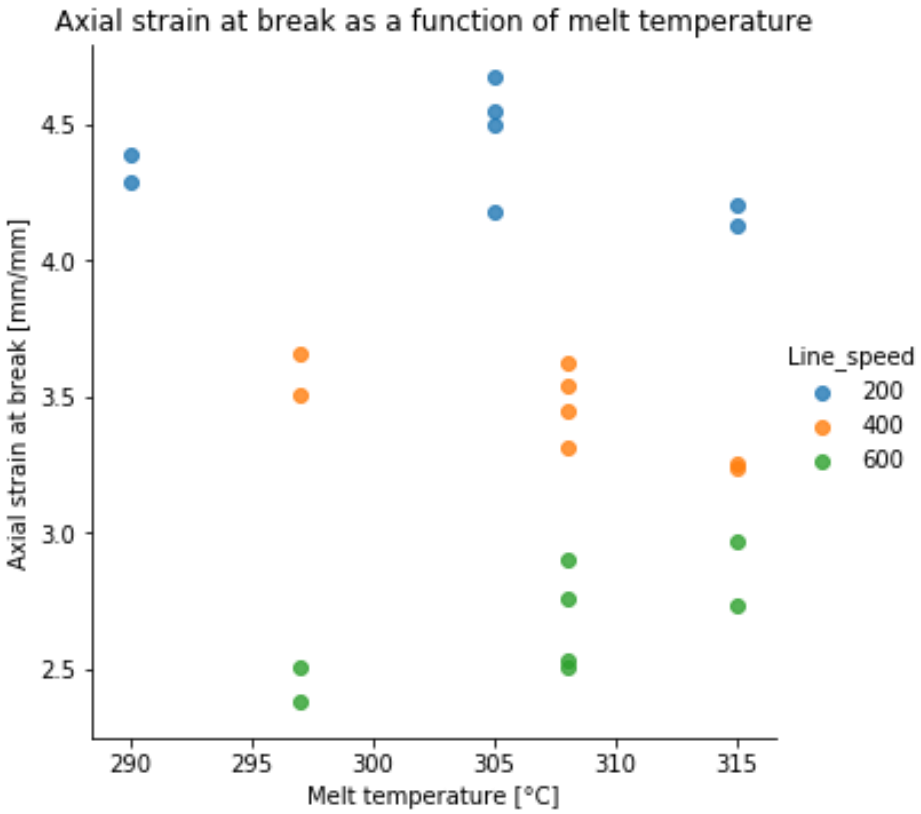


*Figure 7:2 Scatter plot axial strain at break vs temperature on molten film, color separated for line speed.*

When increasing temperature at 200 m/min compared to when increasing temperature at 600 m/min, two different trends are shown. A higher temperature does not affect the sample strain at break at low speed, while strain at break decreases at medium speed and increases at high speed. Thus, the effect of temperature is not physically intuitive and might be attributed to random sampling error.

To gain further understanding in how the mechanical properties are influenced by melt temperature and line speed, statistical analysis were used. In *table 7:1*, results from a 2 way ANOVA is shown where main effects from line speed and melt temperature are described. The interaction between the main effects were also investigated but no interaction was detected.

*Table 7:1 Results from 2 way ANOVA showing main effects from line speed and melt temperature on axial strain at break.*

| Parameter | Sum of Squares | Degrees of freedom | F - value | PR(>F) |
|---|---|---|---|---|
| Line speed [m/min] | 11 | 1 | 3.0e+2 | 6.50e-14 |
| Melt temperature | 3.2e-3 | 1 | 0.09 | 0.8 |
| Residual | 0.78 | 21 | | |

Thus, there is evidence of an effect of line speed on axial strain at break ($p<0.0001$), but no evidence of a simultaneous effect of melt temperature ($p=0.8$).

The resulting model when using line speed solely as feature can be seen in *table 7:2* below.

*Table 7:2 Results from ANOVA showing effect line speed on axial strain at break.*

| Parameter | Coef | Std err | t | P > \|t\| | [0.025 | 0.975] |
|---|---|---|---|---|---|---|
| Intercept | 3.5 | 0.039 | 90 | 0.00 | 3.4 | 3.6 |
| Line speed per 100 m/min | -0.43 | 0.024 | -18 | 0.00 | -0.48 | -0.38 |

The above analysis includes melt temperature as a linear covariate. To allow for a more complex relation between axial strain at break and melt temperature, a more flexible model was fitted where a quadratic term in the melt temperature and an interaction term between line speed and melt temperature was also added to the analysis. Line speed and melt temperature were also scaled by 100, so the effect estimates amounts to a change of 100 m/min or 100°C respectively, see *table 7:3*.

*Table 7:3 Results from ANOVA showing effect from interaction between line speed and melt temperature on axial strain at break. Model was also fitted by applying a quadratic term in melt temperature.*

| Parameter | Coef | Std err | t | P > \|t\| | [0.025 | 0.975] |
|---|---|---|---|---|---|---|
| Intercept | 3.6 | 0.047 | 76 | 0.00 | 3.5 | 3.7 |
| Line speed per 100 m/min | -0.43 | 0.024 | -21 | 0.00 | -0.48 | -0.39 |
| Melt temp per 100°C | -0.38 | 0.51 | -0.74 | 0.47 | -1.5 | 0.69 |
| Quadratic melt temp | -14.7 | 6.14 | -2.4 | 0.027 | -28 | -1.9 |
| Line speed : Melt temp | 0.88 | 0.30 | 3.0 | 0.008 | 0.25 | 1.5 |

From this model an interaction effect between line speed and melt temperature can be detected ($p=0.008$), and possibly an effect of quadratic melt temperature can also be detected from the table ($p=0.027$).

This model is overly complex compared to the amount of data that it is fitted from. We will use machine learning techniques to compare the prediction ability between the simpler and more flexible linear regression models.

### 7.1.2 Stress at break

The data was then examined by using classical methods to investigate the influence from line speed and melt temperature on stress at break. In *figure* 7:3 below, axial strain at break is plotted as a function of line speed with a color based on a third variable, temperature on molten film.

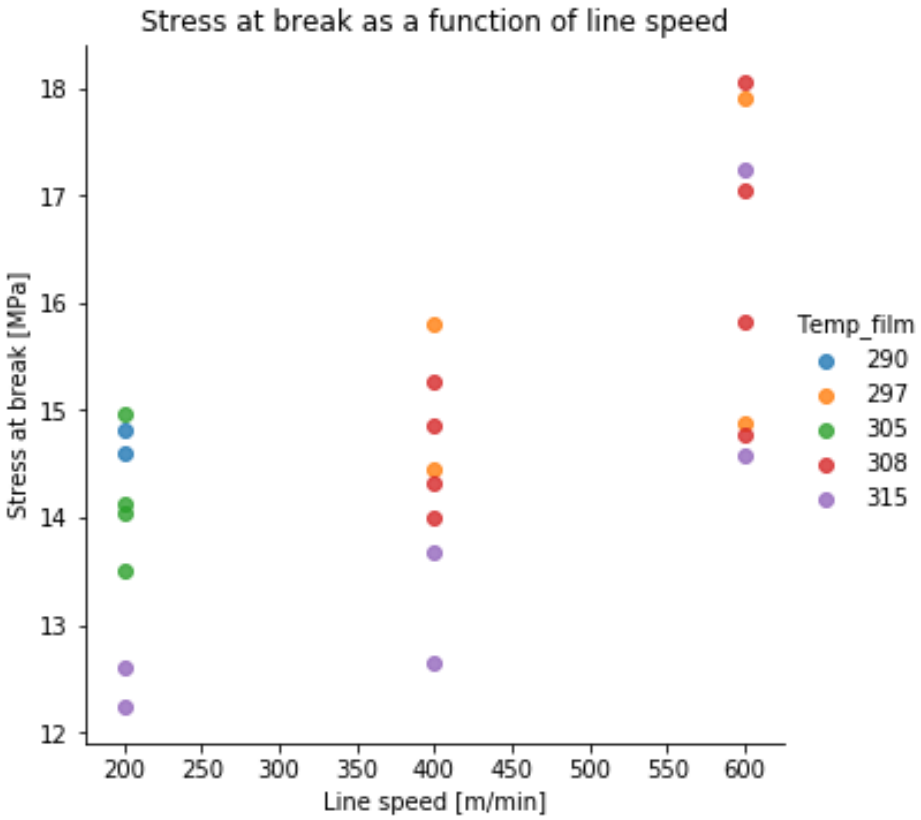


*Figure 7:3 Scatter plot of stress at break vs line speed, color separated for temperature on molten film.*

There is a trend between increasing stress at break and increasing line speed in *figure 7:3*. The effect of temperature is however less clear, as is also seen in Figure 7:4, displaying stress at break vs temperature on molten film.

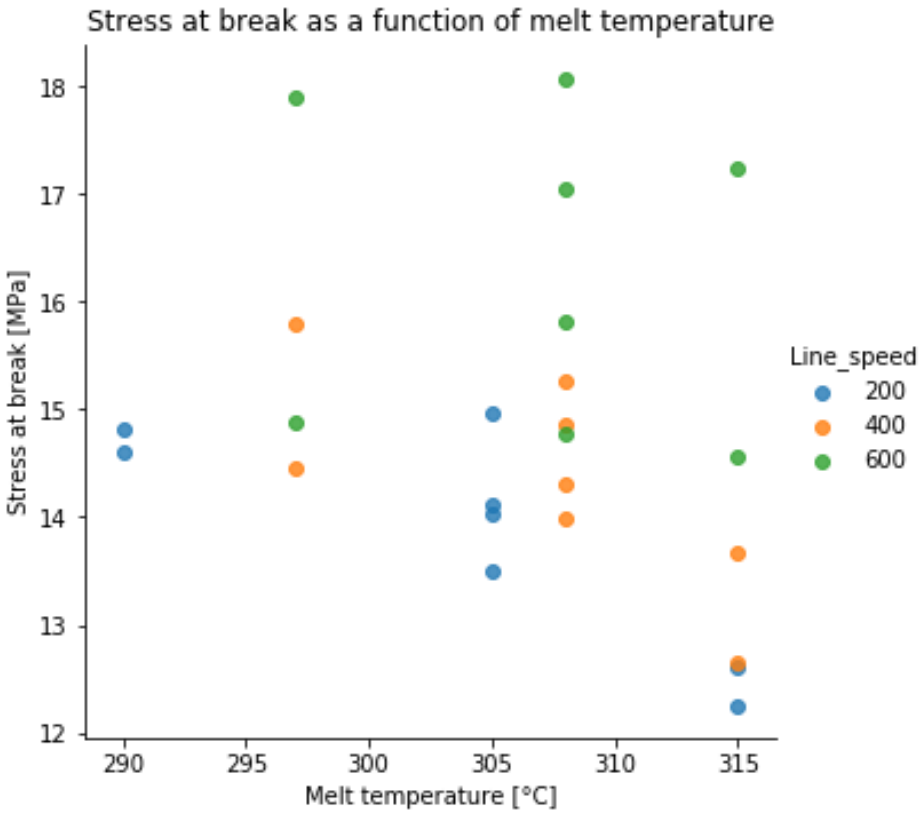


*Figure 7:4 Scatter plot stress of at break vs temperature on molten film, color separated for line speed.*

In *figure 7:4*, line speed at 200 m/min is indicated by the blue color, line speed at 400 m/min is indicated by the orange color and line speed at 600 m/min is indicated by the green color. The temperature dependency is harder to interpret since no clear trends are demonstrated but when increasing temperature at 200 m/min one can detect a linear decrease in the stress at break values. Similar trend is detected at 400 m/min. At 600 m/min it is somewhat harder to interpret the results since a large spread in the data points is detected.

To gain further understanding in how the mechanical properties are influenced by melt temperature and line speed, statistical analysis were used. In *table 7:4*, results from a 2 way ANOVA is shown where main effects from line speed and melt temperature are described. The interaction between the main effects were also investigated but no interaction was detected.

*Table 7:4 Results from 2 way ANOVA showing main effects from line speed and melt temperature on stress at break.*

| Parameter | Sum of Squares | Degrees of freedom | F - value | PR(>F) |
|---|---|---|---|---|
| Line speed [m/min] | 27 | 1 | 25 | 0.000059 |
| Melt temperature | 7.8 | 1 | 7.05 | 0.015 |
| Residual | 23 | 21 | | |

Thus, there is evidence of an effect of line speed on axial strain at break ($p<0.0001$), but no evidence of a simultaneous effect of melt temperature ($p=0.015$).

## 7.2 Evaluating the Predictive Ability of Linear Models (ANOVA) and Machine Learning Models

According to *table 6:1*, there is a significant variation in the thickness of the film. Since strain at break is not as thickness dependent as stress at break, there is a larger uncertainty in the results for stress at break hence the large standard deviation in stress at break displayed by the error bars in *figure 6:6 – 6:9*. Therefore, strain at break was the main focus for the model evaluation.

Linear Regression is a supervised machine learning algorithm that observes continuous features and predicts an outcome. It can run a single variable called linear regression, or many features called multiple linear regression. Linear Regression assigns optimal weights to variables to create a line of the form $y = ax + b$, that is used to predict the output. The regression line fits a relationship between independent and dependent variables. Quadratic terms and interaction terms can also be included in the linear regression model.

A decision tree is constructed of branches and leaves. With the branches representing the observations and the leaves representing the target values, the predicted values, see *figure 7:5*.

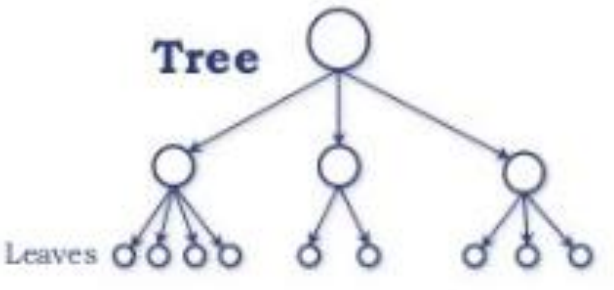


*Figure 7:5 Decision Tree [41]*

Random Forest Regression is a supervised machine learning algorithm that is constructed of a multitude of such decision trees for regression, 100 trees in this thesis. The results from the decision trees are aggregated into one final prediction, see illustration in *figure 7:6*. The algorithm has the ability to limit overfitting without increasing error due to bias which makes it better than when using one single decision tree.

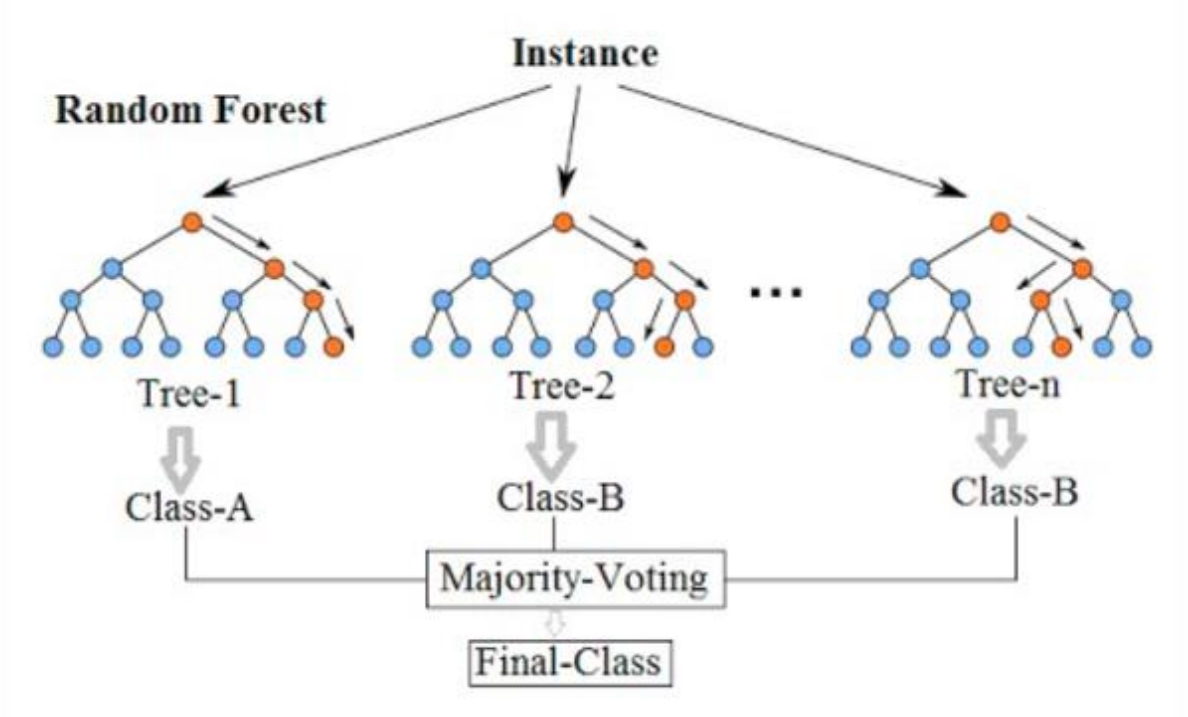


*Figure 7:6 Random Forest Regression – a simplified model. [42]*

Random forests train on random sampling of data points when trees are built which reduces variance. It also reduce variance by using a random subset of features in each model. It is however important to use many trees in the forest to ensure that all features have been included. Random forest regression will together with linear regression be used for the modelling in this thesis.

Four models were compared by means of the ability to predict strain at break:

1. Linear regression using only line speed as a feature (LinReg 1).
2. Linear regression using line speed, melt temperature, quadratic melt temperature and the interaction term between line speed and melt temperature as features (LinReg 2).
3. Random forest using only line speed and melt temperature as features (RF 1)
4. Random forest using all the process parameters (13 in total) as features (RF 2).

The process parameters used in RF 2 were line speed, coating width, deckle settings, heating zone 1, heating zone 2, heating zone 3, heating zone 4, heating zone 5, heating zone 6, temperature on molten film, air gap, cooling and offset.

To evaluate the predictive ability of each of the 4 models, training and testing matrices were built for the features and the output respectively. In the first part each training set consisted of 20 randomly selected samples and the testing set of the remaining 4, see *figure 7:7* for an example of such a split, together with the predicted values from linear regression (LinReg1) with the present training set.

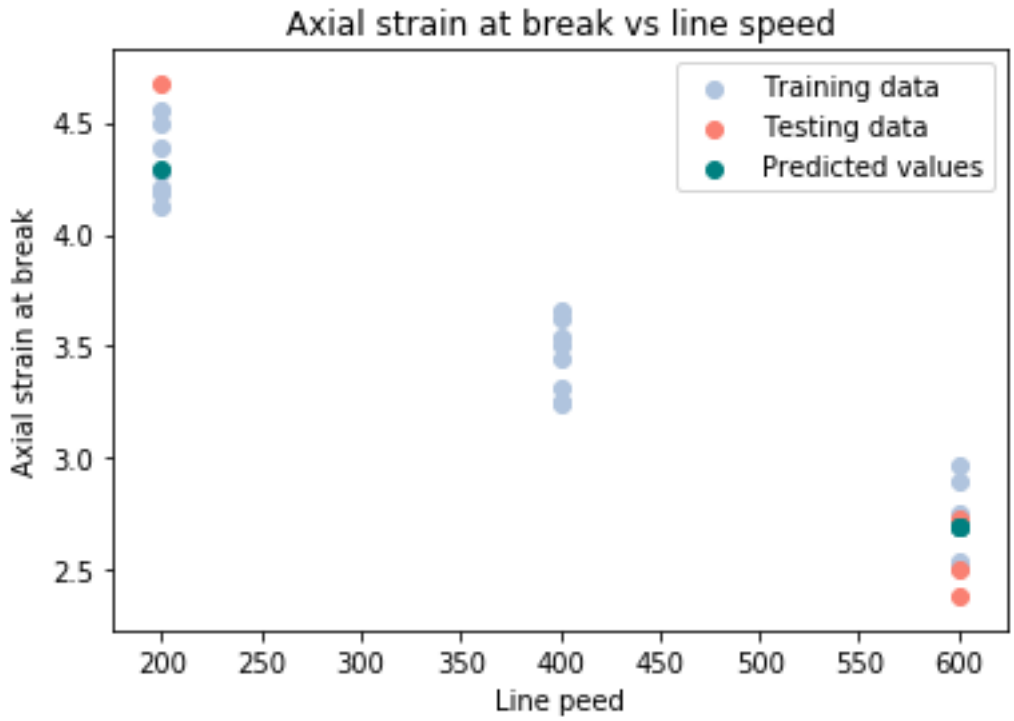


*Figure 7:7 Training (blue data points) and testing matrices (pink data points) used in the first set of training and testing of the model LinReg 1. The predicted values (green data points) have also been illustrated in the image.*

In a first step ten different random splits were used for each model, to investigate if similar accuracy was obtained, between models and between different splits, and a table of results was generated for the 10 splits. Root Mean Squared Error (RMSE) and Coefficient of Determination for the predicted (R – squared) are presented as a measures of prediction ability in the tables below.

Root Mean Squared Error is a measure of the magnitude of prediction errors; it is the square root of the average of squared prediction errors. In *table 7:5*, the RMSE have been summarized for all the four models.

*Table 7:5 Root mean squared error (RMSE).*

| | Root Mean Squared Error | | | | | | | | | |
|---|---|---|---|---|---|---|---|---|---|---|
| **Model** | M1 | M2 | M3 | M4 | M5 | M6 | M7 | M8 | M9 | M10 |
| LinReg 1 | 0.193 | 0.225 | 0.190 | 0.229 | 0.234 | 0.252 | 0.117 | 0.250 | 0.264 | 0.267 |
| LinReg 2 | 0.151 | 0.224 | 0.159 | 0.158 | 0.201 | 0.231 | 0.419 | 0.218 | 0.235 | 0.207 |
| RF 1 | 0.158 | 0.234 | 0.237 | 0.161 | 0.173 | 0.220 | 0.120 | 0.188 | 0.192 | 0.230 |
| RF 2 | 0.192 | 0.223 | 0.247 | 0.161 | 0.168 | 0.259 | 0.128 | 0.188 | 0.195 | 0.284 |

To better visualize the root mean square error values, a bar plot is displayed in *figure 7:8*. As expected from the small dataset with only 20 observations in the training set and 4 in the test

set, the variability in RMSE is large between splits (which is the reason why several splits must be investigated). Comparing the linear regression models, one can see that the simplest model, LinReg 1 performs worst in most (but not all) splits, but on the other side it is more robust whereas the more complicated linear regression model, LinReg 2, is a bit more sensitive to the data in the training and testing matrices.

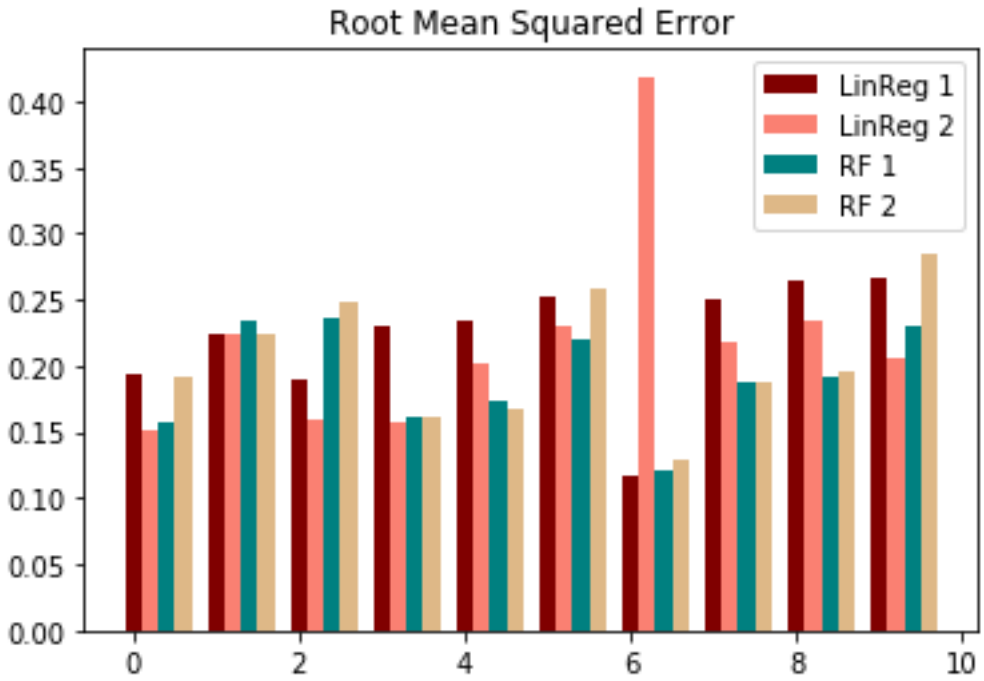


*Figure 7:8 Prediction model results – root mean squared error for each model respectively for the ten different splits of data into training and testing set.*

Another measure of the prediction ability is the coefficient of determination, also called R squared. It can be viewed as the proportion of variance in the dependent variable that is predictable from the model. The coefficient of determination should be between 0 and 1. However, a negative value may appear which indicates that the variance is higher for the prediction errors than the outcome values themselves, i.e. a rather useless model. A coefficient of determination close to 0, means that the dependent variable cannot be predicted from the model. If the value is close to 1, then that means that the dependent variable can be well predicted using the model. If for example, the coefficient of determination is 0.30 then that means that only 30 percent of the original variance Y is explained by the model. In *table 7:6*, the coefficient of determination is displayed for all the four models and their ten combinations of training and testing matrices.

*Table 7:6 Coefficient of Determination (r squared).*

| Model | Coefficient of Determination | | | | | | | | | |
|---|---|---|---|---|---|---|---|---|---|---|
| | M1 | M2 | M3 | M4 | M5 | M6 | M7 | M8 | M9 | M10 |
| LinReg 1 | 0.912 | 0.468 | 0.605 | 0.773 | 0.802 | 0.881 | 0.830 | 0.241 | 0.560 | 0.919 |
| LinReg 2 | 0.946 | 0.470 | 0.723 | 0.892 | 0.853 | 0.900 | -1.18 | 0.422 | 0.652 | 0.951 |
| RF 1 | 0.942 | 0.423 | 0.388 | 0.889 | 0.892 | 0.909 | 0.821 | 0.572 | 0.767 | 0.939 |
| RF 2 | 0.913 | 0.475 | 0.333 | 0.889 | 0.898 | 0.874 | 0.796 | 0.569 | 0.760 | 0.908 |

To easer visualize the coefficient of determination, a bar plot was created displayed in *figure 7:9*. It shows the same pattern as for RMSE, a variability between splits and that the more complicated linear regression model, LinReg 2, predicts poorly on the sixth split in training and testing matrices.

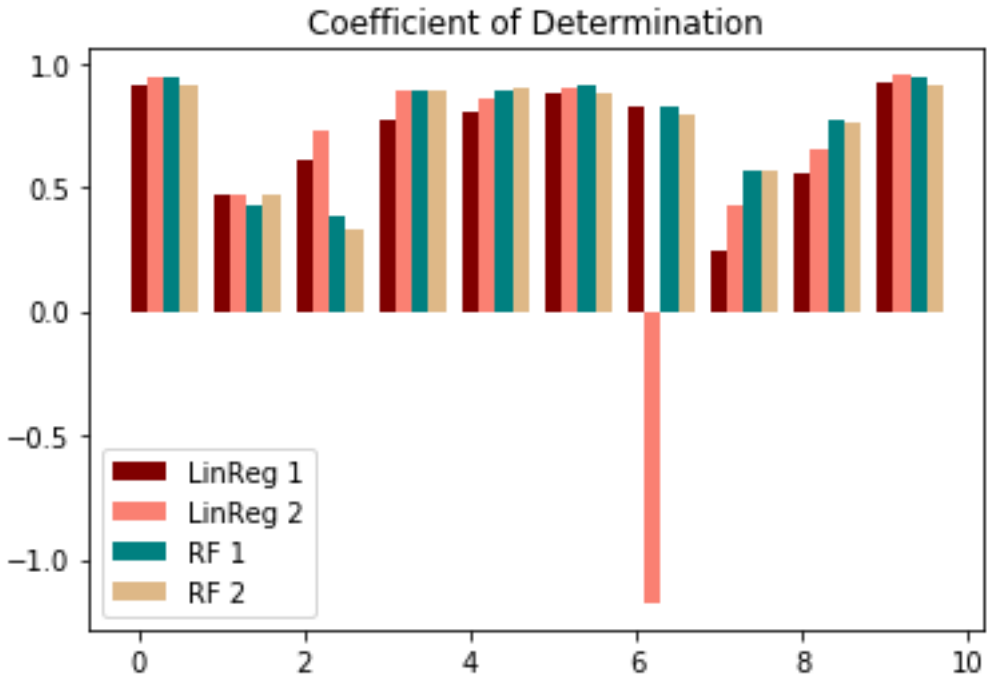


*Figure 7:9 Prediction model results – coefficient of determination for each model respectively for the ten different splits of data into training and testing set.*

Since the performance of the model prediction ability depend on the data used in the training and testing matrices, a thousand training and testing matrices were created to make sure that proper conclusions are drawn regarding the predictive performance of all of the models. In *figure 7:10* below, the distribution of the root mean square error values for all the four models have been displayed. The shape of the distribution gives information regarding how well the models predict. As noted, LinReg 2 is more sensitive and therefore a less reliable model since it responds with high root mean squared error on several sets of training and testing matrices. The prediction ability is on average slightly better for the Random Forests (RF1 and RF2) than

the simplest model (LinReg1) but compared to the variability between splits the difference is negligible.

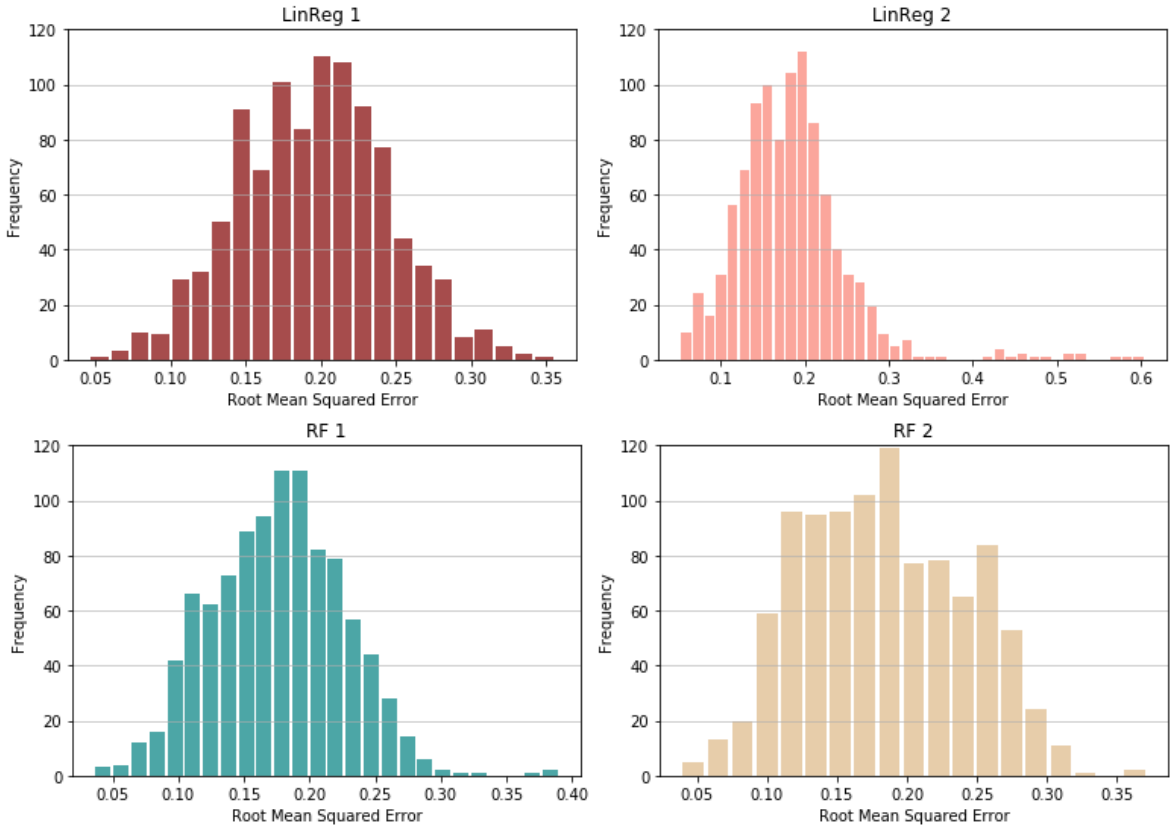


*Figure 7:10 Prediction model results – root mean squared error for a thousand training and testing matrices for each model respectively.*

To visualize how the predictions of each model depend on line speed alone, a new set of values for the explanatory variables was constructed and used with the different models to obtain the corresponding predicted values for axial strain at break. For LinReg1, a new matrix was created where the line speed was set to a range between 100 and 700 with ten steps in between. This matrix was then inserted into the model, to predict values on axial strain at break for each line speed. Ten lines were created since ten training and testing matrices were created. These predicted values, created by the model LinReg 1, are illustrated in *figure 7:11* by the red lines.

For LinReg 2, line speed was set to range between 100 and 700. Melt temperature was added as a second explanatory variable with temperature fixed at three different levels; 315°C, 305°C and 290°C. The explanatory variables quadratic melt temperature and interaction (line speed times melt temperature) term were also added. The predicted values, created by model LinReg 2, are illustrated in *figure 7:9* by the pink (305°C), purple (315°C) and grey lines (290°C).

For RF1, line speed was set to range between 100 and 700. Melt temperature was added as a second explanatory column with a fixed value of 305 °C. The predicted values are displayed in *figure 7:11* by the green lines.

Since the values follow a perfectly linear trend as seen in section 7.1, the performance of RF1 turns out as expected. Random forest would be better suited if there were non-linear relationships in either temperature or line speed. Here, the data points were gathered at three different line speeds resulting in three distinct groups indicated by each step in the green lines. If the line speeds were to be more continuous, the model would have a better predictive capacity.

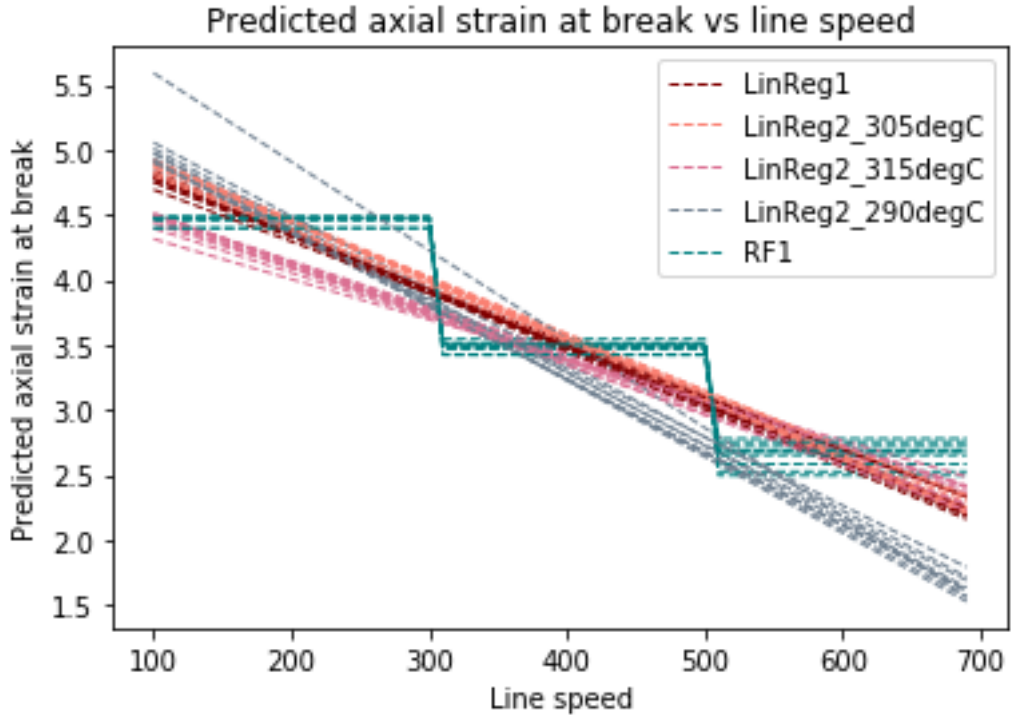


*Figure 7:11 Predicted axial strain at break vs line speed using the models.*

How predictions from RF2 vary with line speed is not easily captured in the type of graph above, as all the process parameters were used as features and could not easily be set to fixed values separate to line speed.

The models were also evaluated with leave one out cross validation. With leave one out, the model is trained on all the data except for one point which the prediction is made upon. This procedure is then repeated for each of the available observations. Since all data except one observation is used for each estimated model, there is risk for overfitting. On the other hand, the model gets more data points to train on which helps in provide more accurate predictions. In *figure 7:12*, the first training matrix and test matrix is illustrated for LinReg 1 and the predicted value as well to illustrate how leave one out functions.

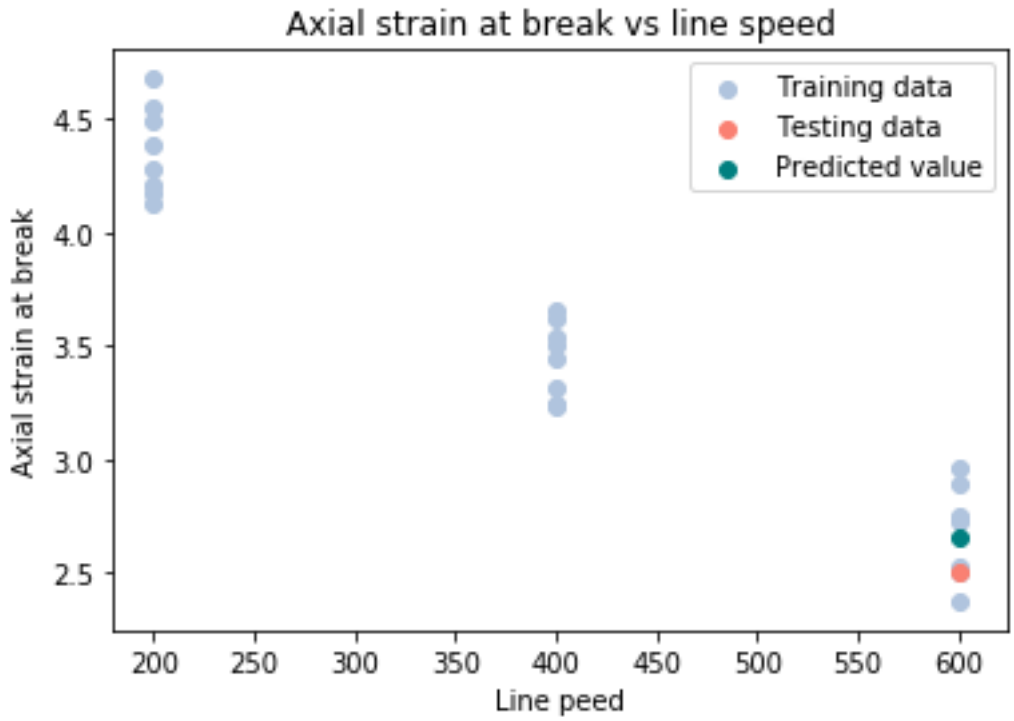


*Figure 7:12 Training matrix (blue data points) and testing matrix (pink data point) used in the first set of training and testing of the model LinReg 1. The predicted values (green data points) have also been illustrated in the image.*

In *table 7:6*, the coefficient of determination and root mean squared error have been displayed when using leave one out cross validation.

*Table 7:6 Leave one out cross validation*

| | Coefficient of Determination | Root Mean Squared Error |
|---|---|---|
| **LinReg1** | 0.924 | 0.199 |
| **LinReg2** | 0.938 | 0.180 |
| **RF1** | 0.942 | 0.173 |
| **RF2** | 0.934 | 0.184 |

All methods above still run the risk of giving an impression of too good prediction ability, since the data for test and training set was collected simultaneously. Therefore prediction ability should optimally be tested from a separate set of validation data. Unfortunately, no external validation set was available. As a way to mimic the models' ability to predict a new set of data, a whole group of data was selected as a test set (and not included in the training set).

In *figure 7:13*, the training and testing matrix used to evaluate LinReg 1 is illustrated. One group of line speed, 400 m/min, have been removed and used as testing matrix instead as displayed in the figure. The green data point in the illustration represents the predicted value.

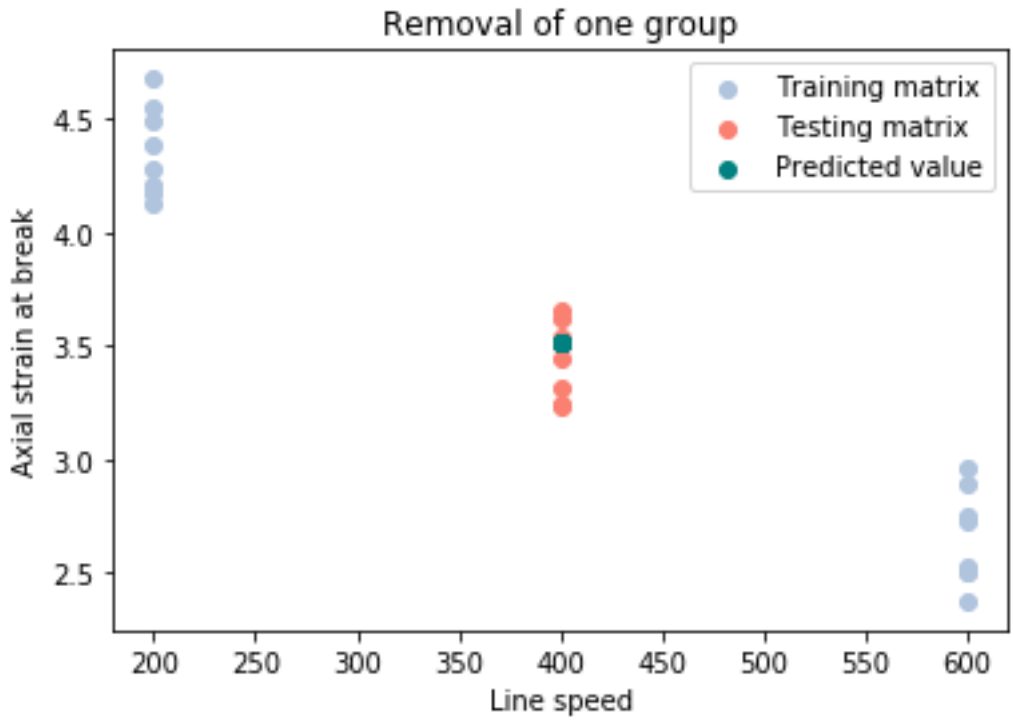


*Figure 7:13 Training matrix (blue data points) and testing matrix (pink data point) used in the first set of training and testing of the model LinReg 1. The predicted values (green data points) have also been illustrated in the image.*

In *table 7:7*, the root mean squared error is displayed for all the four models showing how far off the regression line the predicted value is. Now, the simplest model, LinReg1, has the best performance, followed by LinReg2. The poor performance of RF1 and RF2 illustrate that these models do not generalize well to a line speed not included in the model. The reason for this is however not mainly overfitting, but an artefact of random forest working with categorizations of data. Thus, a completely new category is difficult for such models to predict.

*Table 7:7 Recreation of the models using one line speed, 400 m/min, as testing matrix.*

| | Root Mean Squared Error |
|---|---|
| **LinReg1** | 0.166 |
| **LinReg2** | 0.179 |
| **RF1** | 0.928 |
| **RF2** | 0.704 |

# 8. Discussion

## 8.1 Experimental

During the production of materials, one of the goals was to maintain a constant temperature on the molten film. Experiments were conducted in order to see if the temperature could be held constant while increasing the line speed from 200 to 400 m/min and from 400 to 600 m/min. According to the results, see *figure 6:2*, it was harder to maintain a low film temperature compared to a high film temperature in the process while increasing the line speed. The processing settings seemed to be more stable at a higher temperature. The low temperature was supposed to be 280°C but the extruder could not provide a film with that temperature and so the temperature on the molten film was instead 290°C when running at 200 m/min. When line speed was increased to 400 m/min, the extruder speed was increased from 130 to 204 rpm, Appendix A *table A:1*, which resulted in an increase in melt temperature from 290 to 297°C, see *figure 6:2* blue line. When line speed was further increased to 600 m/min the extruder speed and melt temperature was still 204 rpm. The high temperature was supposed to be 330°C but the extruder could not provide a polymer film with that temperature. The temperature on the molten film could only go up to a maximum of 315°C when running at 200 m/min. When the line speed was increased to 400 and 600, the extruder speed was increased to 204 rpm for both cases, see Appendix A *table A:3*. When running at these two line speeds, the temperature on the molten film was still 315°C as seen in *figure 6:2*, green line.

The middle temperature was first set to be 310°C. However, since the high temperature was 315°C and the low temperature around 290°C, the mid temperature was decreased to 305°C. When running at low line speed, 200 m/min, the temperature on the molten film was 305°C, see *figure 6:2*. When line speed was further increased to 400 and 600 m/min, the extruder speed was increased to 204 rpm in both cases, see Appendix A *table A:2*, and the temperature was increased from 305 to 308°C, see *figure 6:2* red line. A higher temperature thus fluctuates less and is more stable throughout changes in the process while the low temperature is harder to maintain when changes in the process are made.

These experiments were conducted a few days before the extrusion coating process. Ideally, the temperature on the molten film should have been measured with the Raytek during the experiment to ensure that right temperature had been obtained. This could therefore be a possible error source.

## 8.2 Effect from Film Thickness on Mechanical Properties

The principle layers in a typical carton package have been illustrated in *figure 1:1*. In this thesis, the décor was investigated. Usually the layer thickness of the décor is very thin. Performing mechanical tests on the décor layer is quite complicated since the number of defects in the material increases with decreasing thickness. The results from tensile tests on thin films will also provide with a larger standard deviation in the stress – strain curves since some samples will contain more defects than others. This will make it harder to interpret the results. It will also be harder to find proper and accurate correlations in these kind of results with the supervised machine learning algorithm. Therefore, the thickness on the décor layer was increased to 20 µm which is still very thin.

When comparing results from mechanical testing among samples, it is important that they have similar film thickness. Similar film thickness for all the materials could only be obtained by altering the coating width. The deckle settings were therefore varied in the extruder, to obtain a uniform film thickness of 20 µm.

Normally, samples for tensile testing are cut out in the middle of the board since there is a larger thickness variation along the sides as a result from neck-in. The samples in this thesis were cut out from the coated tapes along the edges. The coating width varied depending on line speed used. The materials produced at 200 m/min had a coating width of 0.47 m meaning that the entire board was coated, see *figure 8:*1. The large thickness variation (edge effect) as a result from neck-in therefore occurred outside of the area where material for tensile testing was removed. Materials produced at 400 m/min had a coating width of 0.40 m meaning that almost the entire board was coated, see *figure 8:1*. The samples used for tensile testing from these materials where therefore also not affected by the large thickness variation due to neck-in. However, material produced at 600 m/min had a coating width of 0.28 m, see *figure 8:1*. The entire tape was therefore not coated. The neck-in area was thus set within the area where samples where cut out, resulting in a larger thickness variation within those samples which will be explained later in the text.

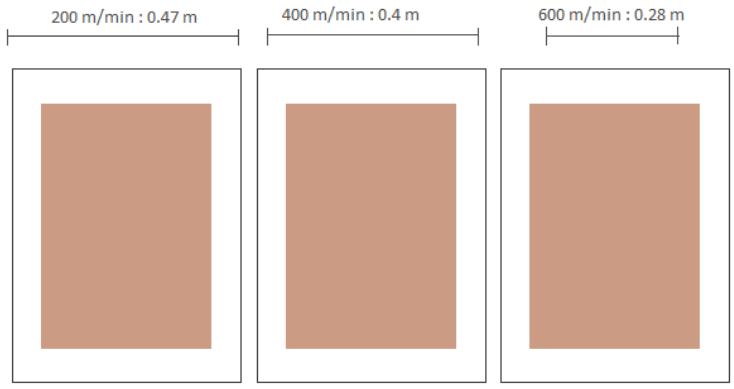


*Figure 8:1 The illustration shows how much of the board that was coated with polymer during the experiment. The brown markings in the image illustrate the tape.*

The samples used for tensile testing had the shape of a dog bone. Eight dog bones per material resulting in eight stress – strain diagrams for each material. These were then summarized in a mean stress – strain curve that represented the mechanical properties of that specific material. There was a larger thickness variation in cross direction (CD) compared to machine direction (MD) which will result in a greater variation in stress – strain diagrams for CD samples When calculating a mean curve for samples pulled in CD direction there is a greater uncertainty in the results since there is a greater thickness variation in each dog bone compared to MD samples which have a more uniform thickness in each dog bone. A large variation in the dog bones will result in inaccurate stress – strain diagrams. Since the results were to be used in creating a model, the results needed to be as reliable as possible and therefore MD samples were chosen for this thesis, to minimize the large thickness variation caused by CD samples. However, to understand why and how the material behaves in a certain way one has to look into the orientation of the polymer chains. This is most easily done by comparing mechanical data of MD and CD. However, due to lack of time, mechanical testing on CD samples could not be performed. This is a very important step in order to understand why a change in mechanical properties appear instead of only stating that a change has occurred, but the reason is unknown.

From the thickness measurements it was also clear that when coating speed (line speed) was increased, the film thickness overall decreased, see *table 6:3.* A thin film will contain more defects compared to a thick film. If the sample contains more defects, then this will affect the ultimate tensile properties of that sample. Since the films were overall thinner at 600 m/min, the number of defects could be more present and thus contribute to the ultimate tensile properties of those films. The film thickness thus has a strong influence on the mechanical properties and ideally the film thickness should be thick when performing tensile tests. Some samples did however contain visible defects such as scratches as a result from the rollers in the coating line. Those samples were therefore eliminated from the results and new samples were cut out and used instead. Some defects were also visible as shiny spots or grains in the film structure. Other samples that had no visible defects but resulted in abnormal stress – strain diagrams were also removed since the probability of defects being present was very high.

The thickness of the film also affects the residence time inside the extruder and thereby the time for chemical reaction to occur such as degradation and polymerization of the polymer chains. Also the chemical change of the polymers in the airgap due to oxidation. The degradation can also be affected by extruder speed. In the ideal case, the extruder speed would be kept constant throughout all measurements to make sure that the polymer has been treated the same way through the production. A constant extruder speed could however not be obtained throughout the measurements because when line speed is increased, extruder speed automatically increases.

The average film thickness was used during tensile testing, as mentioned earlier in section 6.3.2. In the results from tensile testing, a large standard deviation for the materials produced at 600 m/min was noted indicated by the error bars especially for stress at break, see *figure 6:6 – 6:9*, green bars. This can be explained by the large thickness variation, see *table 6:3*, that most likely appeared due to neck-in. Stress at break is more thickness dependent compared to axial strain at break which explains the larger error bars in y direction. The blue, 200 m/min, and orange, 400 m/min, error bars are much smaller indicating a smaller thickness variation in those materials which can be explained by the wider coating width thus eliminating neck-in. The usage of an average film thickness is therefore wrong in the case of materials produced at 600 m/min. To gain accurate mechanical data from those materials, the individual film thickness should have been used instead of the average film thickness.

To highlight the importance of using the individual film thickness when a large thickness variation is present, material 18 produced at 600 m/min was tested again, see *figure B:1* in Appendix B. A comparison between tensile tests on material 18 was made to visualize the difference in mechanical properties when using the average film thickness and individual film thickness. Comparing *figure B:1* and *B:2* in Appendix B, one can see that there is a larger standard deviation in the curves when the average film thickness is used, *figure B:1*. When the individual film thickness is used, *figure B:*2, the standard deviation decreases significantly and thus a more accurate result is provided. The ultimate tensile properties for each dog bone using the average film thickness has been tabulated in Appendix B, *table B:1.* The ultimate tensile properties for each dog bone using the individual film thickness has been tabulated in Appendix B, *table B:2*. From the tables it is apparent that a smaller standard deviation in stress at break is obtained when using the individual film thickness as input in the software for tensile testing. It will provide with more accurate results. In Appendix B *table B:2*, the film thickness for each dog bone has been tabulated showing how much the thickness varies in the material. In *figure 8:2* a comparison between the mean stress – strain curves for material 18 using average film thickness and individual film thickness is made. The error bars in the illustration show how large the standard deviation around the mean value is.

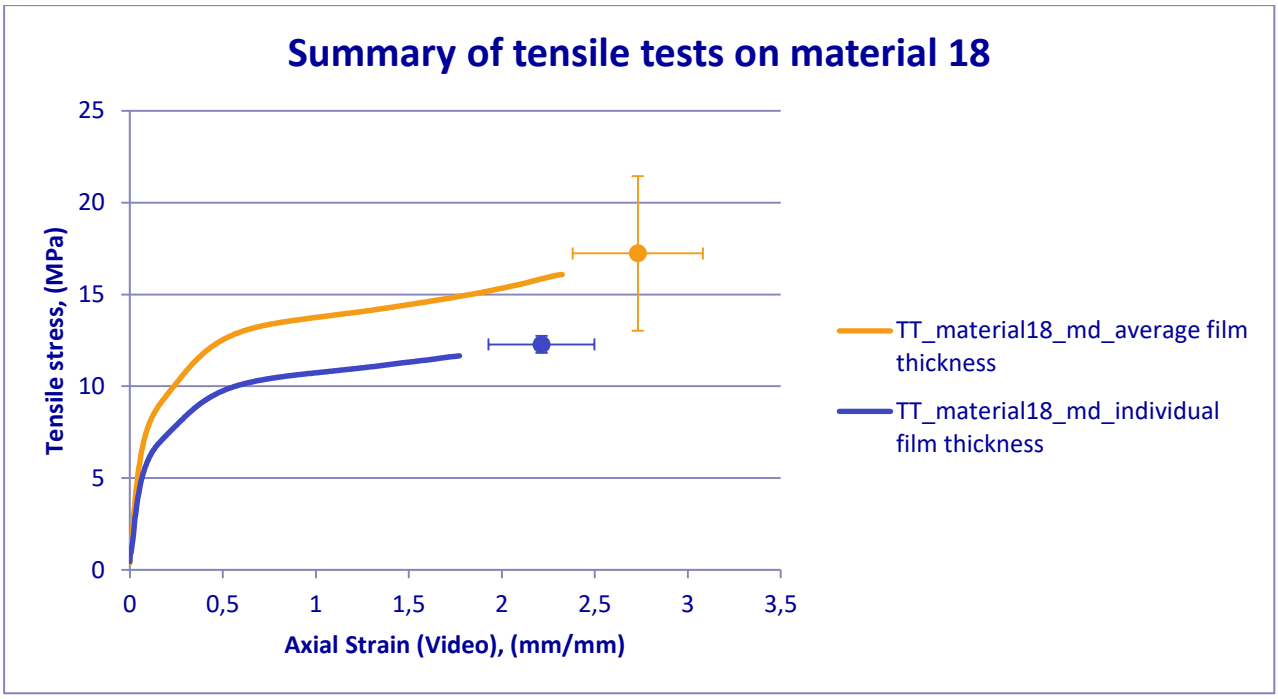


*Figure 8:2* Illustration of the mean stress – strain curves for material 18. Orange curve represents the mean curve when average film thickness has been used. Blue curve represents the mean curve when individual film thickness has been used.

As can be seen in *figure 8:2*, strain at break is not as affected by the film thickness as stress at break however one can see that even the mean value for strain at break is decreased when using the individual film thickness. The standard deviation in strain at break is however more dependent on the number of defects present in the material rather than the thickness. From this it can be concluded that the stress at break values obtained from the materials produced at 600 m/min are inaccurate. The blue line shows that the stress strain – curve for material 18 should be much lower with a correspondingly lower stress at break, 12.28 MPa instead of 17.24 MPa, see Appendix B *table B:1* and *B:2*. When calculating the stress – strain curves, the software uses the film thickness and divides the force with it. When a material contains a film thickness variation between 18 and 31 µm, the average film thickness cannot be used. If average film thickness is used, then the force for the thinner samples will be divided with a thicker film thickness resulting in a sample that will break at a lower stress. When using the same thickness for the thicker sample, this will break at a much higher stress than it would do if the real film thickness was to be used instead. This will result in a large spread in data between each material where a film thickness variation is significant, and the results obtained will be similar to the orange curve in *figure 8:1*. This will provide with inaccurate data. Due to this, axial strain at break was solely chosen for the modeling.

This highlights the importance of using the individual film thickness for each dog bone. This is especially important when the process window is narrow which the temperature window is. The usage of average film thickness in this thesis may therefore be the cause to why some correlations were not found and why the effect from melt temperature was not as clear. The

process window for line speed was however large. The effect from line speed on the mechanical properties was therefore much clearer.

In *figure 7:1*, strain at break is illustrated as a function of line speed with temperature as a third color variable. From the figure it is clear that a higher line speed leads to lower strain at break. This is because a higher line speed results in a higher draw ratio and thus the time for relaxation of the polymer chains is short. The polymer chains do not have time to relax and will remain stretched when solidifying. The polymer chains will be more oriented, resulting in a lower strain at break. In *figure 7:3*, stress at break is illustrated as a function of line speed with temperature as a third color variable. According to the figure, a higher line speed leads to a tougher material that can withstand a higher stress which is due to the fact that the polymer chains are oriented. A lower line speed thus results in a more ductile material which and a higher line speed results in a more brittle material.

It can also be concluded that line speed has an impact on the mechanical properties from *figure 6:6 – 6:9.* The slope of the curves are different depending on what line speed they have been produced at. Material produced at the highest line speed have a steeper slope. The slope of the curves turns flatter when line speed is decreased. The temperature dependency is however harder to interpret. In *figure 6:10*, material produced at 200 m/min and at different temperatures are illustrated. From the figure some temperature dependency can be detected since the mechanical properties are different at the different temperatures. Material produced at the highest temperature has the lowest ultimate tensile properties. When temperature is decreased to 305°C the ultimate tensile properties increase. When decreasing the temperature even further to 290°C it is apparent that stress at break increases, indicating a higher degree of orientation and is therefore a more brittle material. In *figure 6:11,* the line speed is increased to 400 m/min, and a somewhat similar temperature dependency is detected. When line speed is increased even further up to 600 m/min, see *figure 6:12*, this temperature dependency gets harder to interpret. If the individual thickness was to be instead, a clearer temperature dependency could be detected even at higher line speeds since more accurate results would be obtained and outliers would be limited to some degree.

In *figure 7:2*, strain at break is illustrated as a function of melt temperature with line speed as a color variable. From the figure a slight temperature dependency can be suspected but how it affects strain at break is not clear. In *figure 7:3*, stress at break is illustrated as a function of melt temperature with line speed as a third color variable. A slight temperature dependency can also be suspected from the image but how it affects stress at break is not clear. Therefore, statistical analysis was conducted to investigate how and if the temperature has an effect on the ultimate tensile properties.

According to the ANOVA *table 7:1*, there is only an effect from line speed (6.5e-14) on axial strain at break. However, in a more flexible model (allowing for quadratic terms for temperature and interaction with line speed) a possible influence of temperature is found, see *table 7:3*. Considering the small sample size, the model is too complex to believe in, but thus well suited to use machine learning methods to investigate the model prediction ability.

According to ANOVA *table 7:3*, there is a significant effect from line speed (<0.0001) and a small effect from melt temperature (0.015) on stress at break. Further analysis was however not conducted since it was apparent that the values on stress at break from the tensile testing were not representative for the materials produced at 600 m/min due to the noise from the thickness variation.

According to ANOVA *table 7:4*, there is a significant effect from line speed (0.000059) and a small effect from melt temperature (0.0148) on stress at break. Further analysis was however not conducted since it was apparent that the values on stress at break from the tensile testing were not representative for the materials produced at 600 m/min due to the noise from the thickness variation.

Comparing the results from the tensile testing made on the materials produced on the two individual days, one can say that the experiment can be reproduced even though differences have occurred. These differences are only clear at 600 m/min and those are believed to depend on the film thickness variation rather than on the measurement day.

The deckle settings were not the same on the two days even though the process settings were identical. At the low and middle temperature, the deckle settings were different at 200 m/min, see Appendix A *table A:1* and *A:2*. From *figure 6:6*, no difference in the stress – strain curves obtained at 200 m/min on both days at the lowest temperature (290°C) was detected indicating that the varying deckle settings have not influenced the mechanical properties. According to *figure 6:7* and *6:9*¸ no difference in stress – strain curves obtained at 200 m/min on both days at the middle temperature (305°C) was noted meaning that the deckle settings have little or no impact on the mechanical properties. At 400 m/min and 600 m/min the deckle settings were identical on both days and so the differences that appeared in the mechanical properties cannot be explained by the deckle settings.

When comparing the replicates produced at the high temperature, the deckle settings were different throughout all line speeds. However, there was a very small difference among the replicates produced at 200 m/min and 400 m/min indicating that the deckle settings do not have a large impact on the mechanical properties. The difference is greater at 600 m/min but is probably due to the large thickness variation as earlier explained. This gives an even greater support that the film thickness is the cause to the differences among the replicates and not the deckle settings (process). The conclusion would be that the experiment can be reproduced.

## 8.3 Effect from Processing on Degree of Crystallization

Differential scanning calorimetry was performed in order to investigate if different processing conditions affects the degree of crystallinity. According to the results, there is no significant change. Any differences in mechanical properties does therefore not depend on the degree of crystallinity since there is no difference in the amount of crystals between the materials. However, this does not exclude the fact that there may be a difference in the size of the crystals and how these are distributed in the material which then could affect the mechanical properties. This has not been evaluated in the thesis since it was not a part of the scope to study the morphology of the polymer films. It should however be a part of further studies if interest is in understanding why the mechanical properties turned out in a certain way.

Based on the DSC results an increase in temperature of the melt peak can be detected when increasing line speed, see *table 6:8*. This can be related to the size and stability of the crystals. When line speed is increased, the crystals grow larger and more stable and thus require a higher temperature in order to melt. This increase is quite marginal and involves only a few decimals but since there is a clear pattern, this conclusion can be drawn.

When comparing the DSC results between materials produced under identical conditions one can detect a slight difference in the appearance of the first heating cycle. Between material 1 and 22, there is a slight difference in melting temperature where the largest crystals melt and also a difference when the smaller crystals start to melt. Even though the processing conditions have been identical on both days the deckle settings were slightly different, 680 mm and 670 mm on the first and second day respectively. Material 1 had an average thickness of 29.00 µm and material 22 had an average thickness of 30.35 µm. The difference in thickness may be the result to why the melting temperatures and degree of crystallinity is not identical.

Material 2 and 23 also show a difference in the melt temperature for which the largest crystals melt. There is also a slight difference in amount of crystals. The processing conditions have been identical and also the deckle settings (621 mm) on both days, see Appendix A *table A:1*. The average thickness is 25.50 µm for material 2 and 24.80 µm for material 23 which can be the reason to why there is a difference in the melt temperatures.

Between material 3 and 24, there is a slight difference in melting temperature where the largest crystals melt. The processing conditions have been identical and also the deckle settings (500 mm on both days), see Appendix A *table A:1*. The thickness between these two materials were however slightly different, see *table 6:3*, where material 3 had an average thickness of 21.50 µm and material 24 had an average thickness of 22.75 µm. This can in turn be the reason to why there is a small difference in the heating cycles.

A minor difference in the amount of crystals between material 7 and 16 was noted. The melt temperature where the largest crystals melt is therefore not identical, see *table 6:8*. The processing conditions have not been identical as mentioned earlier due to a mistake when inserting the temperature setting in the extruder on the first day. The deckle settings were also different, 680 mm and 700 mm on the first and second day respectively, see Appendix A

*table A:3*. A difference in thickness between these two materials was also noted, see *table 6:3*. Material 7 had an average thickness of 30.55 µm and material 16 had an average thickness of 26.45 µm which may be the reason to why there is a difference in the heating cycles.

Material 8 and 17 show a difference in melt temperature which indicates that there is a small difference in the size and stability of the largest crystal in the samples respectively. This difference does however only concern a few decimals and may not be as significant, but it still exists, see *table 6:8*. The processing conditions were the same. The deckle settings were however different, 621 mm and 640 mm on the first and second day respectively, see Appendix A *table A:3*. Material 8 had an average thickness of 24.30 µm and material 17 had an average thickness of 21.65 µm which could be the reason to why there is a difference when comparing the heating cycles.

Between material 9 and 18 there is a difference in the heating cycles which can also be seen when comparing the degree of crystallinity and melt temperature where the largest crystals melt, see *table 6:8*. These differ from each other indicating that there is a difference in amount of crystals. The processing conditions were the same. The deckle settings were however different, 500 mm and 530 mm on the first and second day respectively, see Appendix A *table A:3*. The average thickness is 25.45 µm for material 9 and 18.60 µm for material 18 which is a large difference. This may be the reason to why there is a difference in the heating cycles.

Another factor that could affect the results from the DSC when comparing material produced under identical conditions could be that they were produced at a different time and sequence during the day. This means that the performance of the laminator could be affected by which time during the day it is running the material which in turn could result in a difference in the results, but this is only a thought rather than a statement. Since the DSC result did not show a significant difference in degree of crystallinity, the midpoints were not analyzed.

## 8.4 Monitoring of the Process Settings in CDAS

When monitoring the process settings in CDAS after the experiment had been conducted it was noted that the last heating zone in the extruder was only set to reach 315°C instead of 330°C. That is 15°C lower than the temperature settings. The first thought was that since the last heating zone is situated in the feed block, this should not affect the results too much. The results from the DSC did not show a big difference in the degree of crystallinity. It is therefore hard to draw any conclusions regarding if and how these 15°C affects the results.

The sequence on the measurements were different on the second day compared to the first day which could have an impact on the results. The extruder had for instance 50 minutes longer to reach 330°C on the second day and so all the heating zones had enough time to reach the desired temperature before the tests were conducted. The time between each measurement was significantly longer on the second day. On the first day, the intervals between the measurements were much smaller and so the extruder had much less time for heating and cooling before the experiments were performed. During heating to 330°C on the

first day, two of the heaters did not have enough time to stabilize. However, there is no apparent evidence that suggests that having longer intervals will have any significance on the how stabilized the temperature is.

## 8.5 Usage of Machine Learning in Material Science

Building predictive models like the ones in this thesis are always an issue regarding quality of data. Ideally the amount of data should be large and not small as the one used in this thesis. The main gain of machine learning algorithms is for data collected under a non-controlled environment which was not the case in this thesis. Here, the data was collected from a designed experiment, and is thus suited to analyse with standard ANOVA. The influence from line speed on mechanical properties was already known, and the only unknown factor was the influence from melt temperature.

From the results in the section Modelling with Machine Learning, the predictive models that were built in this thesis can predict axial strain at break with fairly good precision given the current data. In *figure 7:10*, a thousand training and testing matrices were created for each model to make sure that all the possible predictive outcomes have been covered. According to the histograms, the models predict quite good with a corresponding low RMSE. The model LinReg 1 has a RMSE around 0.20 and LinReg 2 has a RMSE around 0.18 but this complex model is less reliable since it is more sensitive to small changes in training and testing matrices hence the high RMSE scores that appear in the histogram. The model RF 1 has a RMSE around 0.18 and RF 2 has a RMSE around 0.20. The conclusion based on the results is that LinReg 1, RF 1 and RF 2 are the more stable models with low RMSE scores which means that they provide with good predictions. To choose a complex model it has to be significantly better than the simple model and, in this case, the simple linear regression performs better than the complex linear regression model where melt temperature, quadratic melt temperature and the interaction term was considered. The random forest regression also provided with two fairly good and stable predictive models, however such models trained with categorical data generalizes badly when the model is used for prediction in categories of explanatory variables not used in the training, see *table 7:7*.

To visualize how the predictions of each model depend on line speed alone, a new set of values for the explanatory variables was constructed and used with the different models to obtain the corresponding predicted values for axial strain. According to *figure 7:11*, it is clearly shown that the simplest models, LinReg 1 and RF 1, manage to show the effect from line speed better than the more complex models. The simplest models are less sensitive and thus the lines for each of the ten training and testing matrices used are very well assembled which does not apply to the more complex model, LinReg 2, as expected.

To evaluate the performance of the models even further, leave one out cross validation was performed. As seen in *table 7:6*, the coefficient of determination is high (close to 1) which indicates a good predictive capacity whereas the root mean square error is low (closer to 0) which also indicates a good predictive performance. However, since one value is removed and

used as testing matrix, all data except one observation is used for the prediction of each point, thus the good results may be due to overfitting. The better predictive performance compared to when a smaller training set was used indicates that overfitting is present. However, the better predictions may also partly be explained by a larger training matrix used when the model is estimated

The predictive performance of the models was also evaluated by removing an entire line speed (400 m/min) and using it as the testing matrix and the other two as a training matrix. According to *table 7:7*, the linear regression models predicted quite well but the models based on random forest regression predicted quite poorly. This can however be explained by the fact that the random forest is ideally built on approximating a function from continuous values. In this thesis, the line speed is categorized in three groups rather than being continuous. The algorithm can therefore not generalize among the data when one entire group is removed and therefore predicts poorly.

The expectations were not that the complex models would perform better than the simple model since this was a planned experiment with small amount of data which makes the complex models more sensitive. If a larger amount of random data points would have been available, then the complex models would probably perform better. For the present data however, the conclusion is that the simple linear regression model performs better.

The values obtained from the rheology measurements correspond to the values in the material specification for this specific PE grade. In this thesis, the rheology was merely used as a control to check that correct polymer had been used. In the future, the thought is however to use the rheology as input in the model to try to understand how different polymers responds to the processing.

# 9. Conclusion

In this thesis, the influence from extrusion coating on the mechanical properties of PE was investigated. The creation of a model for predicting the mechanical properties of extruded polymer film was also a part of the scope. The thesis has included a variation of experimental techniques and highlighted the importance of accuracy when measuring the mechanical properties of a polymer film containing significant thickness variations. From tensile testing, it can be concluded that the material behavior is dependent on the process conditions. Most significant effect on the mechanical properties was from line speed. A lower line speed results in a more ductile material which provides with more desirable properties in the packaging material and a higher line speed results in a more brittle material. A higher line speed is however preferred in the industries due to economic reasons, but the polymer properties provided by a fast line speed is less desirable in the packaging material. Ideally, a morphology similar to a material processed at low line speed is wanted but the process should be performed at a high line speed. To be able to reach this goal, further investigation is required regarding how the processing has affected the morphology of the polymer such as analyzing the orientation of the polymer chains.

Effect from melt temperature was unfortunately not distinguishable in the material produced in this thesis. Main reason to this is believed to depend on the noise from the large thickness variations which was not included in the calculations during tensile testing, combined with a small sample size. Ideally the material should have been remeasured to see if the effect from melt temperature could be captured, but due to lack of time this could not be done. Instead, one material was remeasured to point out that the values are indeed wrong as seen in *figure 8:2*.

The effect from processing on the degree of crystallization was also investigated by performing DSC. No effect on degree of crystallization was detected which excluded this to be the reason to why differences in mechanical properties appeared. However, a slight increase in temperature of the peak in the DSC curve was detected when increasing line speed which can be related to the size and stability of the crystals. Increasing line speed thus results in larger growing crystals that become more stable and hence require a higher temperature in order to melt. The temperature is however increased with only a few decimals but since there is a pattern, this conclusion can be stated.

The purpose of this master thesis was to understand to what extent the process influenced the mechanical properties of polyethylene. Some of the process influence was captured but not all which was mainly due to narrow process window used for melt temperature. The purpose was also to investigate if supervised machine learning algorithms could be applied in material science. Even though the models need to be further improved, they showed a fairly good predictive performance meaning that it can be used in this area of application. The amount of data must be expanded in order to take full advantage of the more complex machine learning algorithms. In this thesis, the simpler linear regression model was found to be the best predictor. The more complex random forest models were also found to be good predictors, but more data is required before further conclusions can be drawn regarding these models.

# 10. Future work

This master thesis is a first step in applying machine learning into material science. Therefore, the possibilities for further studies are great. First of all, mechanical testing should be performed on cross direction since this will give information regarding the sample orientation. The sample orientation plays a big part in determining how much a sample can be elongated and to understand the results provided from the tensile tests, the morphology of the materials must be examined. The strain induced crystallization occurs due to the orientation of the molecular chains which is a result from the processing. This phenomenon is important to understand when investigating the morphology of the polymer since it gives information regarding how the crystals have crystallized. This can be measured using Wide Angle X-ray Scattering (WAXS) or Small Angle X-ray Scattering (SAXS). However, since morphological studies was not a part of the scope, these studies were not made but could be of great importance to do for further understanding especially if one wants to optimize and change

the morphology of the polymer and make them more ductile despite running at high line speeds.

To make most possible use of machine learning, more data points should be collected. This would increase the validity of the model. When performing machine learning on a small dataset, it is extremely important that the data is correct and represent accurate relationships. In this thesis, mechanical testing was performed on the polymer films to collect data points for the algorithm. From the stress – strain curves a large standard deviation was detected in stress at break among each material produced at 600 m/min. The large standard deviation was the result from using average film thickness instead of individual film thickness in the software for tensile testing. If the individual film thickness was used instead for each dog bone, then that would minimize the noise and more accurate data could be obtained. It would also enable modeling of stress at break. Due to this, only strain at break was modelled. In the future, it is important to first perform a sensitivity analysis in order to ensure proper test method is being used. Since more material is available from the test run, the tensile testing should be performed again on the materials produced at 600 m/min using the individual film thickness for each dog bone. Measuring the mechanical properties of the polymer films again would conclude in more accurate results and perhaps a clearer temperature dependency could be detected. The effect from melt temperature was assumed in this thesis to behave more non-linear rather than linear as line speed. If this dependency could be captured by adding more data, then machine learning could be more advantageous. When more data has been collected, an alternative is to try to predict in two dimensions rather than one meaning that the output would be both stress and axial strain at break.

The existing predictive model can be tweaked endlessly, but that will not matter if the model is not fed with more data. Since the gathering of data is quite complex and time consuming, the focus can be shifted to an area that already has a huge amount of existing data within material such as adhesion. Also, to be really successful in creating a model, a real validation matrix is needed to evaluate the performance of the model.

Further studies should also be made on other grades of polyethylene to investigate if this has any effect on the mechanical properties. Studies on additional polyolefins should be performed as well to investigate if the response to the processing is different compared to the PE grade used in this thesis. This is also of interest when investigating how the mechanical properties are affected by different material ingredients combined with different process settings. Other process variables could be varied in the future to for instance investigate how air gap affects the mechanical properties. If possible, a wider temperature range should be investigated since there are some indications that the melt temperature affects the mechanical properties.

# 11. References


1. Tetra Pak, *About Tetra Pak*. Retrieved from https://www.tetrapak.com/about [Accessed 2019-02-11]
2. Tetra Pak, *Packaging material for Tetra Pak carton packages*. Retrieved from https://www.tetrapak.com/packaging/materials [Accessed 2019-02-11]
3. M. Buggy. (2016). Polymeric Materials. In *Materials Science and Materials Engineering.* Retrieved from https://www.sciencedirect.com/science/article/pii/B9780128035818041047 [Accessed 2019-01-24]
4. *Polymeric Materials* (University of Warwick). (June 27 2012) Retrieved from https://warwick.ac.uk/fac/sci/wmg/globalcontent/courses/ebm/mant/materials/polymeric_materials/ [Accessed 2019-01-24]
5. Cowie, J.M.G., & Arrighi, V. (2007). The Crystalline State and Partially Ordered Structures. In *Polymers: Chemistry and Physics of Modern Materials* (3rd ed. pp 291-293). [Accessed 2019-01-28]
6. Harris, L. (September 2011). *A Study of the Crystallisation Kinetics in PEEK and PEEK composites* (University of Birmingham) Retrieved from https://core.ac.uk/download/pdf/1631655.pdf [Accessed 2019-01-28]
7. Sondalini, M. (2017). *Polyethylene: Its Properties and Uses.* Retrieved from https://accendoreliability.com/polyethylene-properties-uses/#comments [Accessed 2019-01-24]
8. Cowie, J.M.G., & Arrighi, V. (2007). The Crystalline State and Partially Ordered Structures. In *Polymers: Chemistry and Physics of Modern Materials* (3rd ed. pp 432-434). [Accessed 2019-01-28]
9. Styles, S. (September 24, 2015). *LDPE – The First Polyethylene*. Retrieved from https://www.paxonplastic.com/ldpe-the-first-polyethylene/ [Accessed 2019-01-24]
10. Bhatnagar, P. (October 25, 2017). *Which type of plastic is good for food packaging (LDPE or HDPE)?* Retrieved from *https://www.quora.com/Which-type-of-plastic-is-good-for-food-packaging-LDPE-or-HDPE* [Accessed 2019-01-28]
11. Morris, B.A. (2017). Rheology of Polymer melts. In *The Science and Technology of Flexible Packaging* (pp 121-147). Retrieved from https://www.sciencedirect.com/science/article/pii/B9780323242738000058 [Accessed 2019-01-28]
12. TA Instruments. *Application of Rheology of Polymers*. Retrieved from http://www.tainstruments.com/pdf/literature/AAN009e_Application_of_Rheology_to_Polymers.pdf [Accessed 2019-01-25]
13. Campo, E.A. (2008). Mechanical Properties of Polymeric Materials. In *Selection of Polymeric Material* (pp 41-101). Retrieved from https://www.sciencedirect.com/science/article/pii/B9780815515517500048 [Accessed 2019-01-25]

14. Editors of Encyclopaedia Britannica. (January 10, 2019). *Young's Modulus*. Retrieved from https://www.britannica.com/science/Youngs-modulus [Accessed 2019-01-25]
15. Balani, K., Verma, V., Agarwal, A., & Narayan, R. (2015) Physical, Thermal and Mechanical Properties of Polymers. In *Biosurfaces: A Materials Science and Engineering Perspective* (1st ed.). Retrieved from https://onlinelibrary.wiley.com/doi/pdf/10.1002/9781118950623.app1 [Accessed 2019-01-25]
16. Ashby, M.F., & Jones H.R.D. (1986). Mechanical Behavior of Polymers. In *Engineering Materials 2* (3rd ed. p. 274). Retrieved from http://www.nanotech.unn.ru/sites/default/files/m.a._ashby_-_engeneerig_matherials_elseiver_2006_vol2.pdf [Accessed 2019-01-25]
17. Leonov, A.I. *A Theory of Necking in Semi-Crystalline Polymers*. Retrieved from https://arxiv.org/ftp/cond-mat/papers/0203/0203254.pdf [Accessed 2019-01-29]
18. Sepe, M. (July 29, 2016). *Materials: Understanding Strain-Rate Sensitivity in Polymers*. Retrieved from https://www.ptonline.com/columns/materials-understanding-strain-rate-sensitivity-in-polymers [Accessed 2019-01-25]
19. Callister W.D. (2000). *Materials Science and Engineering* (5th ed.). Retrieved from https://www.chegg.com/homework-help/stress-strain-data-poly-methyl-methacrylate-shown-figure-153-chapter-16-problem-1qp-solution-9780471320135-exc [Accessed 2019-01-28]
20. Iggesund Paperboard. *Extrusion Coating and Lamination.* Retrieved from https://www.iggesund.com/globalassets/iggesund-documents/rm-pdfer/1.-from-forest-to-market/extrusion_coating_and_lamination_en.pdf [Accessed 2019-01-30]
21. Morikawa, M., & Masutani, Y. (2009). *Development and Simulation of Extrusion Lamination Process with Polyethylene.* Retrieved from https://www.sumitomo-chem.co.jp/english/rd/report/files/docs/20090100_2su.pdf [Accessed 2019-01-30]
22. Mount III, E.M. (2011). Extrusion Processes. In *Applied Plastics Engineering Handbook* (pp 227-266). Retrieved from https://www.sciencedirect.com/science/article/pii/B9781437735147100157 [Accessed 2019-01-30]
23. Plastics Technology. *The Extrusion Process.* Retrieved from https://www.ptonline.com/knowledgecenter/Profile-Extrusion/profile-extrusion-fundamentals/History-and-fundamentals-of-extrusion [Accessed 2019-01-30]
24. PTFE Machinery. (February 22, 2017). *Polymer Screw Extrusion Introduction.* Retrieved from https://ptfemachineryblog.wordpress.com/2017/02/22/polymer-screw-extrusion-introduction/ [Accessed 2019-01-30]
25. Toft, N. (2002). *Rheological Behavior and Extrusion Coating of Polyethylene.* Department of Materials Science and Engineering, Chalmers University of Technology. [Accessed 2019-01-31]
26. Oveby, C., & Clevenhag, P.Å. *Rheological Indicators to Predict the Extrusion Coating Performance of LDPE*. Retrieved from

http://www.tappi.org/content/enewsletters/eplace/2004/03-4Clevenhag.pdf [Accessed 2019-01-39]
27. Griffin, F. (2017). *Short Introduction into Rheology*. Retrieved from https://slideplayer.com/slide/10472893/ [Accessed 2019-01-31]
28. Wyss, H.M., Larsen R.J., & Weitz, D.A. (2007). *Oscillatory Rheology: Measuring the Viscoelastic Behaviour of Soft Materials*. Retrieved from http://www.mate.tue.nl/~wyss/home/resources/publications/2007/Wyss_GIT_Lab_J_2007.pdf [Accessed 2019-01-31]
29. Instron. (2017). *Tensile Testing: What is Tensile Testing?* Retrieved from http://www.instron.us/en-us/our-company/library/test-types/tensile-test [Accessed 2019-01-29]
30. Department of Materials Science and Engineering. (2019). *Tensile Test Experiment.* Retrieved from https://www.mtu.edu/materials/k12/experiments/tensile/ [Accessed 2019-01-29]
31. Total Materia. (2001). *True Stress – True Strain Curve: Part two*. Retrieved from https://www.totalmateria.com/page.aspx?ID=CheckArticle&site=kts&NM=42 [2019-01-29]
32. Groenewoud, W.M. (2001). Differential Scanning Calorimetry. In *Characterization of Polymers by Thermal Analysis* (pp 10-60). Retrieved from https://www.sciencedirect.com/science/article/pii/B9780444506047500029 [Accessed 2019-01-31]
33. Pham, T.H. (2018). *DSC – Differential Scanning Calorimetry*. Retrieved from https://liveatlund.lu.se/departments/CAS/KASN20/KASN20_2018VT_100_1_NML__1281/CourseDocuments/Instructions%20DSC%20Lab.pdf [Accessed 2019-01-31]
34. Hitachi. (2019). *Principle of Differential Scanning Calorimetry*. Retrieved from https://www.hitachi-hightech.com/global/products/science/tech/ana/thermal/descriptions/dsc.html [Accessed 2019-01-31]
35. Imarticus. (September 7, 2017). *What is Machine Learning and Does it Matter?* Retrieved from https://imarticus.org/what-is-machine-learning-and-does-it-matter/ [Accessed 2019-02-01]
36. SAS. (2019). *Machine Learning: What it is and why it matters.* Retrieved from https://www.sas.com/en_ae/insights/analytics/machine-learning.html [Accessed 2019-02-01]
37. Brownlee, J. (March 16, 2016). *Supervised and Unsupervised Machine Learning Algorithms*. Retrieved from https://machinelearningmastery.com/supervised-and-unsupervised-machine-learning-algorithms/ [Accessed 2019-02-01]
38. Alhindawi, F., & Altarazi, S., (2018). *Predicting the Tensile Strength of Extrusion-blown High Density Polyethylene Film Using Machine Learning Algorithms*. Retrieved from http://resolver.ebscohost.com.ludwig.lub.lu.se/openurl?sid=EBSCO%3aedseee&genre=chapter&issn=2157362X&isbn=9781538667866&volume=&issue=&date=2018120

1&spage=715&pages=715-719&title=2018+IEEE+International+Conference+on+Industrial+Engineering+and+Engineering+Management+(IEEM)%2c+Industrial+Engineering+and+Engineering+Management+(IEEM)%2c+2018+IEEE+International+Conference+on&atitle=Predicting+the+Tensile+Strength+of+Extrusion-blown+High+Density+Polyethylene+Film+Using+Machine+Learning+Algorithms&btitle=2018+IEEE+International+Conference+on+Industrial+Engineering+and+Engineering+Management+(IEEM)%2c+Industrial+Engineering+and+Engineering+Management+(IEEM)%2c+2018+IEEE+International+Conference+on&jtitle=2018+IEEE+International+Conference+on+Industrial+Engineering+and+Engineering+Management+(IEEM)%2c+Industrial+Engineering+and+Engineering+Management+(IEEM)%2c+2018+IEEE+International+Conference+on&series=&aulast=Alhindawi%2c+F.&id=DOI%3a10.1109%2fIEEM.2018.8607816&site=ftf-live [Accessed 2019-02-13]

39. Kopal, I., Labaj, I., Harničárová, M., Valíček, J., & Hrubý, D. (2018). *Prediction of the Tensile Response of Carbon Black Filled Rubber Blends by Artificial Neural Network*. Retrieved from https://www.mdpi.com/2073-4360/10/6/644/htm [Accessed 2019-02-01]
40. Srinivasu, G., Rao, R.N., Nandy, T.K., & Bhattacharjee, A. (2012). *Artificial Neural Network Approach for Prediction of Titanium Alloy Stress – Strain Curve*. Retrieved from https://www-sciencedirect-com.ludwig.lub.lu.se/science/article/pii/S1877705812023399 [Accessed 2019-02-01]
41. Ignatov, D. Yu., Ignatov, A. D. (2017). Decision Stream: *Cultivating Deep Decision Trees* https://www.researchgate.net/figure/Decision-Stream-complexity-reduction-by-merging-similar-nodes_fig3_320934707 [Accessed 2019-05-15]
42. Koehrsen, W. (2017). *Random Forest Simple Explanation* https://medium.com/@williamkoehrsen/random-forest-simple-explanation-377895a60d2d [Accessed 2019-05-14]

# Appendix

## Appendix A

*Table A:1 The process settings of the experiments conducted at the lowest temperature.*

| **Test no.** | **Setup** | | **1 roll** | |
|---|---|---|---|---|
| Laminator | Lab line Pilot Plant Lund | Lab line Pilot Plant Lund | Lab line Pilot Plant Lund | Lab line Pilot Plant Lund |
| Raw paper | 80 mN | 80mN | 80mN | 80mN |
| Web width | 430 mm | 430 mm | 430 mm | 430 mm |
| Line speed | 200 m/min | 200 m/min | 400 m/min | 600 m/min |
| | | | | |
| **Décor layer** | Décor layer | Décor layer | Décor layer | Décor layer |
| Polymer | Ineos 19N730 | Ineos 19N730 | Ineos 19N730 | Ineos 19N730 |
| Desired polymer thickness | 20 µm | 20 µm | 20 µm | 20 µm |
| Extruder speed | 130 rpm | 130 rpm | 204 rpm | 204 rpm |
| Coating width | 0.47 m | 0.47 m | 0.4 m | 0.28 m |
| Deckle setting day 1 | 680 mm | 680 mm | 621 mm | 500 mm |
| Deckle setting day 2 | 670 mm | 670 mm | 621 mm | 500 mm |
| Temperature setting | 220, 240, 280, 280, 280, 280°C | 220, 240, 280, 280, 280, 280°C | 220, 240, 280, 280, 280, 280°C | 220, 240, 280, 280, 280, 280°C |
| Temperature on molten film | 290°C | 290°C | 297°C | 297°C |
| Airgap | 277 mm | 277 mm | 277 mm | 277 mm |
| Offset | 25 mm | 25 mm | 25 mm | 25 mm |
| Cooling water temp, in | 15°C | 15°C | 15°C | 15°C |

*Table A:2 The process settings of the experiments conducted at the middle temperature.*

| **Test no.** | **Setup** | | **1 roll** | |
|---|---|---|---|---|
| Laminator | Lab line Pilot Plant Lund | Lab line Pilot Plant Lund | Lab line Pilot Plant Lund | Lab line Pilot Plant Lund |
| Raw paper | 80 mN | 80mN | 80mN | 80mN |
| Web width | 430 mm | 430 mm | 430 mm | 430 mm |
| Line speed | 200 m/min | 200 m/min | 400 m/min | 600 m/min |
| | | | | |
| **Décor layer** | Décor layer | Décor layer | Décor layer | Décor layer |
| Polymer | Ineos 19N730 | Ineos 19N730 | Ineos 19N730 | Ineos 19N730 |
| Desired polymer thickness | 20 µm | 20 µm | 20 µm | 20 µm |
| Extruder speed | 130 rpm | 130 rpm | 204 rpm | 204 rpm |
| Coating width | 0.47 m | 0.47 m | 0.4 m | 0.28 m |
| Deckle setting day 1 | 675 mm | 675 mm | 621 mm | 500 mm |
| Deckle setting day 2 | 680 mm | 680 mm | 621 mm | 500 mm |
| Temperature setting | 220, 240, 280, 300, 300, 300°C | 220, 240, 280, 300, 300, 300°C | 220, 240, 280, 300, 300, 300°C | 220, 240, 280, 300, 300, 300°C |
| Temperature on molten film | 305°C | 305°C | 308°C | 308°C |
| Airgap | 277 mm | 277 mm | 277 mm | 277 mm |
| Offset | 25 mm | 25 mm | 25 mm | 25 mm |
| Cooling water temp, in | 15°C | 15°C | 15°C | 15°C |

*Table A:3 The process settings of the experiments conducted at the highest temperature.*

| **Test no.** | **Setup** | | **1 roll** | |
|---|---|---|---|---|
| Laminator | Lab line Pilot Plant Lund | Lab line Pilot Plant Lund | Lab line Pilot Plant Lund | Lab line Pilot Plant Lund |
| Raw paper | 80 mN | 80mN | 80mN | 80mN |
| Web width | 430 mm | 430 mm | 430 mm | 430 mm |
| Line speed | 200 m/min | 200 m/min | 400 m/min | 600 m/min |
| | | | | |
| **Décor layer** | Décor layer | Décor layer | Décor layer | Décor layer |
| Polymer | Ineos 19N730 | Ineos 19N730 | Ineos 19N730 | Ineos 19N730 |
| Desired polymer thickness | 20 µm | 20 µm | 20 µm | 20 µm |
| Extruder speed | 130 rpm | 130 rpm | 204 rpm | 204 rpm |
| Coating width | 0.47 m | 0.47 m | 0.4 m | 0.28 m |
| Deckle setting day 1 | 680 mm | 680 mm | 621 mm | 500 mm |
| Deckle setting day 2 | 700 mm | 700 mm | 640 mm | 530 mm |
| Temperature setting | 220, 240, 280, 310, 330, 330°C | 220, 240, 280, 310, 330, 330°C | 220, 240, 280, 310, 330, 330°C | 220, 240, 280, 310, 330, 330°C |
| Temperature on molten film | 315°C | 315°C | 315°C | 315°C |
| Airgap | 277 mm | 277 mm | 277 mm | 277 mm |
| Offset | 25 mm | 25 mm | 25 mm | 25 mm |
| Cooling water temp, in | 15°C | 15°C | 15°C | 15°C |

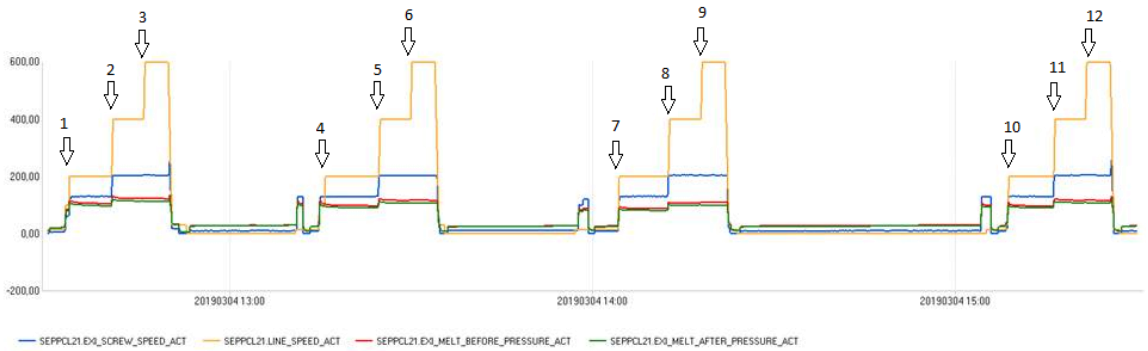


*Figure A:1 Datasheet collected from CDAS which can be used to check if the process was run under the right conditions the first day. The coating speed on the y-axis and date on x-axis.*

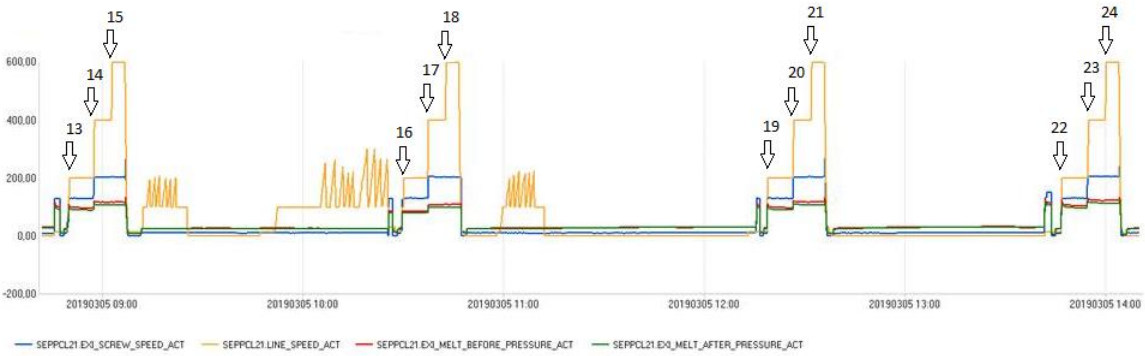


*Figure A:2 Datasheet collected from CDAS which can be used to check if the process was run under the right conditions the second day. The coating speed on the y-axis and date on x-axis.*

# Appendix B

*Table B:1 The ultimate tensile properties for material 18 when the average film thickness was used is tabulated in the table below.*

| **MD** | **Tensile stress at break** [MPa] | **Axial strain (Video) at break** [mm/mm] | **Thickness** [µm] |
|---|---|---|---|
| **1** | 23.6 | 3.15 | 19 |
| **2** | 13.8 | 2.46 | 19 |
| **3** | 12.8 | 2.33 | 19 |
| **4** | 14.4 | 2.49 | 19 |
| **5** | 12.9 | 2.33 | 19 |
| **6** | 22.8 | 3.09 | 19 |
| **7** | 12.9 | 2.44 | 19 |
| **8** | 15.3 | 2.68 | 19 |
| **9** | 26.6 | 3.63 | |
| **Average** | 17.3 | 2.73 | |
| **Std** | 5.48 | 0.46 | |

*Table B:2 The ultimate tensile properties for retested material 18 is tabulated in the table below. The individual thickness of each dog bone is also tabulated.*

| MD | Tensile stress at break [MPa] | Axial strain (Video) at break [mm/mm] | Thickness [µm] |
|---|---|---|---|
| 1 | 11.6 | 1.95 | 20 |
| 2 | 13.5 | 2.65 | 21 |
| 3 | 12.4 | 2.52 | 26 |
| 4 | 12.1 | 2.34 | 22 |
| 5 | 12.1 | 2.50 | 31 |
| 6 | 12.2 | 1.81 | 22 |
| 7 | 12.2 | 1.77 | 20 |
| 8 | 12.3 | 2.17 | 21 |
| | 12.3 | 2.21 | |
| Std | 0.55 | 0.34 | |

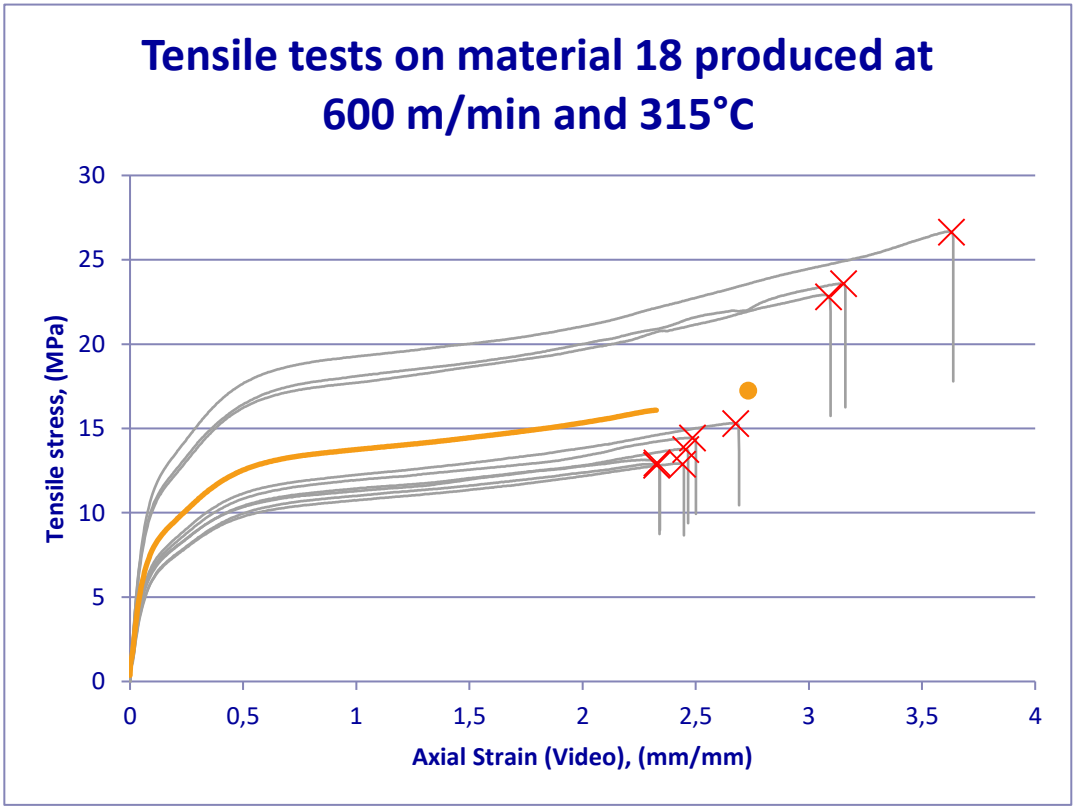


*Figure B:1 Stress – strain curves for material 18. All the dog bones have been illustrated in the figure to show how the data is distributed when using average film thickness as input in the software for tensile testing. The orange line is a summary of the mean stress – strain curve obtained from the results.*

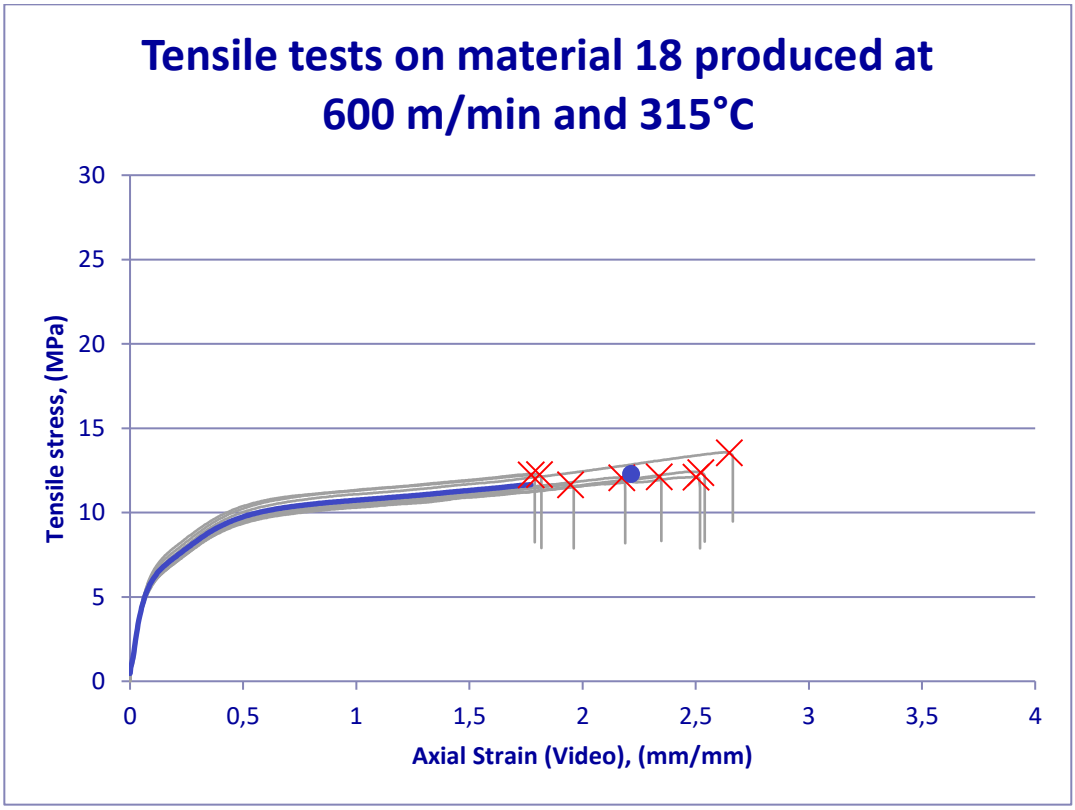


*Figure B:2 Stress – strain curves for material 18. All the dog bones have been illustrated in the figure to show how the data is distributed when using the individual film thickness as input in the software for tensile testing. The blue line represents is a summary of the mean stress – strain curve obtained from the results.*